ENDOPLASMIC RETICULUM HOMEOSTASIS IN THE MOUSE MAMMARY EPITHELIUM DURING LACTATION

A Dissertation

Presented to the Faculty of the Graduate School

of Cornell University

In Partial Fulfillment of the Requirements for the Degree of

Doctor of Philosophy

by

Kristen Ross Davis

May 2015

ENDOPLASMIC RETICULUM HOMEOSTASIS IN THE MOUSE MAMMARY EPITHELIUM DURING LACTATION

Kristen Ross Davis, Ph. D.
Cornell University 2015

Lactation is an essential stage of mammalian life. Milk is a complex fluid that provides complete nutrition for neonates in the early stages of postnatal life. The organic components of milk, such as milk proteins and lipids, are synthesized and secreted by mammary epithelial cells (MEC). A key differentiation event in MEC is the development of an extensive endoplasmic reticulum (ER) network. At the onset of lactation, copious amount of lipid and protein synthesis could perturb the ER luminal environment. However, little is known about ER function in the context of lactation. Professional secretory cells rely on adaptive mechanisms to maintain ER homeostasis including the Unfolded Protein Response (UPR) and elimination of misfolded and improperly modified proteins via the Endoplasmic Reticulum Associated Degradation (ERAD). Two components of the UPR and ERAD, XBP1 and Sel1L respectively, have been implicated in maintaining ER function in secretory cells. However, the roles of XBP1 and Sel1L during lactation have not been investigated. To this end, we specifically ablated XBP1 and Sel1L in MEC during lactation. Our findings indicate that XBP1 is required for sustaining pup

growth during lactation. Absence of XBP1 resulted in a severe reduction of the ER compartment and substantially smaller mammary epithelial compartment during lactation. Notably, our findings are the first to directly demonstrate that XBP1 is absolutely necessary for the development and expansion of an extensive ER network in the MEC. In the case of Sel1L, its absence had little impact on lactation, even though the morphology of the ER was abnormal and markers of ER stress were elevated. More importantly, our findings are the first to suggest that Sel1L is dispensable for MEC function. Taken together, our findings provide novel insight of the contribution of the two ER homeostatic systems during the dynamic and metabolically demanding stage of lactation.

BIOGRAPHICAL SKETCH

Kristen Davis was born in Raleigh, North Carolina on July 22nd of 1987 to parents John and Siobhan Davis. She grew up on sweet tea and grits with her younger brother, Dylan Davis. She always loved animals and her dream was to join the Wolfpack. After graduating salutatorian from high school in 2005, she was accepted to North Carolina State University. Her enthusiasm for animal science research originated from her experiences assisting in various piglet research experiments led by her academic advisor Dr. Jack Odle. In 2006, she worked with a team under the guidance of Dr. Sarah Ash to bring locally produced pork to the dining halls. This experience inspired her to learn more about sustainable agriculture and she interned at the Center for Environmental Farming Systems. In 2007, she executed an honors research project examining the effects of cross fostering piglets in an alternative production system under the direction of Dr. Steve Washburn. In 2008, she joined Dr. Laura Reed's research group and gained invaluable research experience by assisting in a large experiment utilizing the fruit fly to examine the genetic and environmental factors contributing to the Metabolic Syndrome. She graduated magna cum laude in 2009 with a Bachelors degree in Animal Science. Then she began her doctoral studies at Cornell University under the mentorship of Dr. Yves Boisclair with the objective of understanding ER homeostatic systems during lactation by utilizing transgenic mouse models.

To all who supported me on this journey and

to my everything, for everything.

ACKNOWLEDGMENTS

I offer my sincerest gratitude to the mentorship and guidance of my academic advisor, Dr. Yves Boisclair. Not only did you fortify my confidence as a scientist, but you also challenged me to be a better person. I enjoyed our impromptu science conversations in the Morrison hallways and your infamous life anecdotes. I am forever grateful for the life changing opportunity to work and learn from you. I wish you all the best.

I would also like to thank my committee members, Dr. Qiaomong Long, Dr. Ling Qi, and Dr. Robert Weiss for their guidance and insightful suggestions throughout my degree program.

A special thank you is for my lab guardian angel, Dr. Sarah Giesy. None of this work would have been completed without your meticulous planning, organization, and scientific vigor. You are my scientific role model. You are able to contribute and guide every one of the projects being conducted in the Boisclair Lab. You are kind, thoughtful, and loyal to the ones you love. Thank you for being my lab guardian angel and my friend.

Another special thank you goes to my graduate school ‘BARN CALL’ partner turned fellow lab associate turned dissertation doula, Dr. Kate Schoenberg.

Your kind encouraging words were instrumental for me completing my degree. I could have never completed this journey without your friendship.

Also thank you to the rest of the Dr. Boisclair lab for your assistance throughout my degree program: Dr. Jose Manuel Ramos-Nieves, Luciano Caixeta, Brittany Moore, and Christopher Krumm.

The entirety of my PhD degree program can be summarized by the LOTR. My dissertation was as daunting, overwhelming, intimidating, and practically impossible as it was for Frodo to destroy the ring in the fires of Mordor. The next part of my acknowledgements is for all the Samwise Gamgees in my life that carried me through this journey.

To my Wolfpack and North Carolina family, especially Samantha Stover, Molly Preston, Santos Menjares, Samantha Shintay, Mandy Womble, Dr. Nadia Hassounah, Stephanie Williams, and Allison Evan Welch. Thank you for listening during my endless graduate school frustration fueled rants and showing me that there is more to life than lab work.

A special thank you goes to my Wolfpack mentors, Dr. Laura Reed, Dr. Steve Washburn, and Dr. Sarah Ash. Thank you for your continued support and

guidance.

Thank you to all the instructors and mentors at Cornell University I have had the pleasure of meeting along the way, especially Dr. Debbie Cherney, and Dana Palmer. Your unwavering faith in my abilities reminded me of my passion for science and teaching. And for that I will always be grateful.

Thank you to the wonderful support staffs that is the backbone to the Animal Science Department: Terry Haines, Joanne Parsons, Aubrey Whitaker, and Deloris Bevins. Thank you for putting up with my last minute requests and giving me a break during experimental run times.

A special thank you goes to Amy. Thank you for reminding me when I lost all perspective. I could not have done this without you.

To my Big Red Barn family, especially Kris Corda, thank you for being so welcoming and granting me reprieve during a time where I felt abandoned.

To my Morrison Crew and the rest of my Cornell family: Claire and Will Stephens, Dr. Julie Huzzey, Dr. Elizabeth Ann Staiger, Dr. Xi Yan, Jeremy Allen, Natasha Pettifor, Katherine Churchill, Dr. Fernando Migone, Maris McCarthy, Dr. Keenan McRobert, Dr. Jacqueline Benson, Dr. Jay and Sarah

Giesy, Dillan, Ashton, and Colton Giesy, Dr. Jon and Kate Schoenberg, Marie and Whitney Schoenberg, Dr. Karen Chiang Leineweber, Dr. Matthew Leineweber, Dr. Benjamin Hasseldine, Dr. Rodrigo Zeledon, Abigail Hart, Sarah Dinger, Danielle Matt and Callie Morgan, Dr. Li Jiang, Rebecca Rozek, Mike Meller, Erik Huber, Annika Kreye, and Doug and Bev Moore. Our times together represent all of the wonderful, unforgettable moments of graduate school that I will always cherish.

To my Morrison wife and my dandelion, Claire Stephens. Thank you for unconditional support and love. I will miss our impromptu talks in your office, BRB Friday night runs, dinner dates, and lazy TV marathons with the dogs. Our friendship is one of the most beautiful things to come out of that building and I cannot wait to see what life looks like after Morrison with you.

To my dearest Granddad and Grandma Barb. Way before I entered graduate school, before I started college, or even high school you believed in me and showed me that the sky is the limit. This piece of work would never exist without your unconditional love and support. I am eternally grateful and could never thank you enough.

To my Mom and Dad, how do I even begin? You two are the first loves of my life. You taught me life's most important lessons: how to laugh, how to be kind to

others, how to feel confident, how to dream and how to love myself. Everything you have done for me and continue to do for me and our family is awe-inspiring. I am the luckiest person in the world to have you as my parents. I love you best in the west.

A special thank you goes to my favorite person in the world, my little brother, my lil TP, Dylan. You are my role model. I am always in awe of your passion and enthusiasm for life. I admire that you have never been afraid to live life on your own terms. Your smile and laughter is contagious. I'm so proud of you and can't wait to watch you start the next chapter of your life on the West Coast! I love you, Dylan!

Last, but not least, thank you to the love of my life, Alex. From the moment I met you, you have been my partner and supported me through this crazy journey. All those crazy rants you endured, keeping me company late at night in Morrison while I ran experiments, spending date nights in Mann library, and every moment you kept a smile on my face. Cornell will always hold a special place in my heart because that is where we met, fell in love, and started a new life together. I cannot wait to begin the next adventure with you as your wife. Alex, I love you with an all consuming, crazy fierceness.

TABLE OF CONTENTS

LIST OF FIGURES

LIST OF ABBREVIATIONS

MEC	Mammary epithelial cell
ER	Endoplasmic reticulum
UPR	Unfolded protein response
ERAD	Endoplasmic reticulum associated degradation
TAG	Triacylglycerides
TEB	Terminal end buds
SLC	Mitochondrial citrate transporter
ACLY	ATP citrate lyase
ACC	Acetyl-CoA carboxylase
FASN	Fatty acid synthase
SCD1	Stearoyl-CoA desaturase 1
VLDL	Very low density lipoproteins
LPL	Lipoprotein lipase
ACSL	Acyl-CoA synthase
GPAT	Glycerol-3-phosphate O-acyltransferase
AGPAT	1-acylglycerol-3-phosphate O-acyltransferase
PAP	Phosphatidic acid phosphatase

DAG	Diacylglycerol
DGAT	Diacylglycerol O-acyltransferase
CLD	Cytoplasmic lipid droplet
MFGM	Milk fat globule membrane
ADPH	Adipophilin
XO	Xanthine oxidoreductase
WAP	Whey acidic protein
GALE	UDP-galactose-4-epimerase
N-linked	Asparagine linked
EDEM1	ER degradation enhancing α-mannosidase like protein 1
PC	Phosphatidylcholine
PE	Phosphatiylethanolamine
CHK	Choline kinase
PCYT1	Choline cytidyltransferase
CHPT1	Choline phosphotransferase
PEMT	Phosphatidylethanolamine N-methyltransferase
PERK	Double stranded RNA-activated protein kinase PKR-like ER kinase
ATF6	Activating transcription factor 6
IRE1	Inositol requiring enzyme 1

bZIP	Basic leucine zipper domain
uORF	Untranslated open reading frame
CHOP	C/EBP homologous protein
GADD34	Growth arrest and DNA damage inducible 34
XBP1	X-box binding protein 1
sXBP1, uXBP1	Spliced or unspliced X-box binding protein 1
RIDD	Regulated IRE1 dependent decay of mRNA
JNK	JUN N-terminal kinase
PDI	Protein disulfide isomerase
MTP	Microsomal TAG transfer protein
HRD1	Hydroxymethyglutaryl reductase degradation 1
SEL1L	Suppressor/enhancer of lin-12-like 1
OS9	Osteosarcoma 9
XTP3B	Endoplasmic reticulum lectin 1
L0, L1, L5, L14	Lactation day 0, 1, 5, 14
PBS	Phosphate buffered saline
β2M	Beta-2 microglobulin

MG	Mammary gland
E	Efficiency
EDTA	Ethylenediaminetetraacetic acid
TBS-T	Tri-buffered saline with tween
WT	Wild type
P14, P18	Pregnancy day 14, 18
β-CSN	Beta-Casein
SE	Standard error
Lf	Lactoferrin
SA	Serum albumin
α-CSN	Alpha-casein
BTN	Butyrophilin
CIDEA	Cell death inducing DNA fragmentation factor
α-LALBA	Alpha-lactalbumin
B4Galt1	UDP-Gal:Beta GlcNAc Beta1,4-galactosyltransferase
H&E	Hematoxylin and eosin
N	Nucleus
LD	Lipid droplet
M	Mitochondria
PCYT2	Phosphate cytidylyltransferase 2

	ethanolamine
WFS	Wolfram syndrome 1 homolog
ERDJ3	DnaJ HSP40 homolog
TEM	Transmission electron microscopy
BIP	Heat shock protein

CHAPTER 1

INTRODUCTION

The physiological period of lactation represents a dynamic and metabolically demanding stage in mammalian life. The mammary gland has evolved for the sole purpose of supporting neonatal growth. Milk is the only source of nourishment for most mammalian neonates in the early stages of life. As a result, milk is a complex fluid that provides complete nutrition (1, 2). Our overall objective of this work is to contribute new knowledge of the mechanisms that initiate and sustain lactation.

Most of humanity relies on lactation for nutritional and economic reasons. Exclusive breastfeeding is recommended as the optimal feeding strategy for infants (3). In addition, the production and consumption of dairy products is intimately linked to societies around the world. Dairy commodities are a daily staple as well as a source of income for many people (4).

In order to support sudden and intense demand for milk production, the mammary gland differentiates from a gland with little secretory capacity to a metabolically active gland. The organic components of milk are synthesized and secreted by the mammary lobulo-alveolar system. This system develops within a short twenty-day gestation period in the mouse. The mammary gland undergoes a series of morphological changes in order to prepare for copious

milk production during lactation with the majority of essential developmental events driven by hormonal signals. Furthermore, the mammary gland is regarded as a remarkably adaptable organ because it can cycle through these developmental stages multiple times over the lifespan. For example, mammary gland tissue remodeling is initiated with the cessation of milk withdrawal at the end of lactation. This developmental event returns the gland to a state with little secretory capacity and allows the gland to initiate another round of differentiation upon a subsequent pregnancy (5, 6).

MEC are responsible for synthesis and secretion of organic milk components and are characterized by an extensive ER (7). Specifically, the ER in MEC is the site of synthesis of proteins, lipids, and phospholipids. The assembly of lipids and phospholipids occur in regions of the ER devoid of ribosomes whereas proteins destined for secretion are synthesized within regions of the ER studded with ribosomes (8). In order to support pup growth, the synthesis of these milk components within the ER must be efficient.

In order to sustain the fidelity of these pathways, ER homeostasis must be preserved. ER homeostasis is sensitive to chronic or acute disruptions. Roughly 75% of all proteins destined for secretion are synthesized within the ER illustrating the importance of preserving ER homeostasis in secretory cells (9). The biosynthetic capacity of the ER must match its export demands to maintain ER homeostasis. Secretory cells rely on an adaptive increase in ER abundance in order to cope with periods of heightened synthesis demands. In

the event of a perturbed ER luminal environment, the cell has two homeostatic systems devoted to the restoration of ER homeostasis: UPR and ERAD. Both are highly conserved pathways that initiate adaptations aimed at promoting cell survival and eliminating misfolded and aggregated proteins (10–12).

Data from yeast, *C. elegans*, and mammalian cell culture were the first to suggest that XBP1 and Sel1L, two vital components of the UPR and ERAD pathways, were essential for maintain ER function (13–15). Ablation of these components *in vivo* has confirmed their pivotal roles in maintaining ER function in secretory cells (16–21). In comparison to other professional secretory cells, the MEC is unparalleled in its ability to secrete not only copious amounts of milk proteins but also large quantities of triacylglycerides (TAG) and lactose. For example, the mouse mammary gland is capable of secreting its own body weight in milk lipids alone (7). However the roles of XBP1 and Sel1L in the MEC during lactation has not been investigated.

In the first part of this thesis, I will review the literature pertaining to XBP1 and Sel1L function and focus primarily on their roles in secretory cells. I will then report on the effect on lactation of ablating either XBP1 (Chapter 3) or Sel1L (Chapter 4) in the mammary epithelial cell compartment.

References

1. Capuco, A. V, and Akers, R. M. (2009) The origin and evolution of lactation. *J. Biol.* **8**, 37

2. Neville, M. C. (1990) The physiological basis of milk secretion. *Ann. N. Y. Acad. Sci.* **586**, 1–11

3. Imdad, A., Yakoob, M. Y., and Bhutta, Z. A. (2011) Effect of breastfeeding promotion interventions on breastfeeding rates, with special focus on developing countries. *BMC Public Health* **11**, S24

4. Haug, A., Høstmark, A. T., and Harstad, O. M. (2007) Bovine milk in human nutrition--a review. *Lipids Health Dis.* **6**, 1–16

5. Hennighausen, L., and Robinson, G. W. (2005) Information networks in the mammary gland. *Nat. Rev. Mol. Cell Biol.* **6**, 715–25

6. Richert, M. M., Schwertfeger, K. L., Ryder, J. W., and Anderson, S. M. (2000) An atlas of mouse mammary gland development. *J. Mammary Gland Biol. Neoplasia* **5**, 227–41

7. Anderson, S. M., Rudolph, M. C., McManaman, J. L., and Neville, M. C. (2007) Secretory activation in the mammary gland: it's not just about milk protein synthesis! *Breast Cancer Res.* **9**, 204

8. Fagone, P., and Jackowski, S. (2009) Membrane phospholipid synthesis and endoplasmic reticulum function. *J. Lipid Res.* **50 Suppl**, S311–6

9. Fu, S., Watkins, S. M., and Hotamisligil, G. S. (2012) The role of endoplasmic reticulum in hepatic lipid homeostasis and stress signaling. *Cell Metab.* **15**, 623–34

10. Ron, D., and Walter, P. (2007) Signal integration in the endoplasmic reticulum unfolded protein response. *Nat. Rev. Mol. Cell Biol.* **8**, 519–29

11. Cao, S. S., and Kaufman, R. J. (2012) Unfolded protein response. *Curr. Biol.* **22**, R622–R626

12. Olzmann, J. A., Kopito, R. R., and Christianson, J. C. (2013) The Mammalian Endoplasmic Reticulum-Associated Degradation System. *Cold Spring Harb. Perspect. Biol.* **5**, 1–17

13. Lee, K., Tirasophon, W., Shen, X., Michalak, M., Prywes, R., Okada, T., Yoshida, H., Mori, K., and Kaufman, R. J. (2002) IRE1-mediated unconventional mRNA splicing and S2P-mediated ATF6 cleavage merge to regulate XBP1 in signaling the unfolded protein response. *Genes Dev.* **16**, 452–66

14. Calfon, M., Zeng, H., Urano, F., Till, J. H., Hubbard, S. R., Harding, H. P., Clark, S. G., and Ron, D. (2002) IRE1 couples endoplasmic reticulum load to secretory capacity by processing the XBP-1 mRNA. *Nature* **415**, 92–6

15. Francisco, A. B., Singh, R., Li, S., Vani, A. K., Yang, L., Munroe, R. J., Diaferia, G., Cardano, M., Biunno, I., Qi, L., Schimenti, J. C., and Long, Q. (2010) Deficiency of suppressor enhancer Lin12 1 like (SEL1L) in mice leads to systemic endoplasmic reticulum stress and embryonic lethality. *J. Biol. Chem.* **285**, 13694–703

16. Moore, K., and Hollien, J. (2012) The unfolded protein response in secretory cell function. *Annu. Rev. Genet.* **46**, 165–83

17. Lee, A.-H., Scapa, E. F., Cohen, D. E., and Glimcher, L. H. (2008) Regulation of hepatic lipogenesis by the transcription factor XBP1. *Science* **320**, 1492–6

18. Wang, S., Chen, Z., Lam, V., Han, J., Hassler, J., Finck, B. N., Davidson, N. O., and Kaufman, R. J. (2012) IRE1α-XBP1s Induces PDI Expression to Increase MTP Activity for Hepatic VLDL Assembly and Lipid Homeostasis. *Cell Metab.* **16**, 473–86

19. Gregor, M. F., Misch, E. S., Yang, L., Hummasti, S., Inouye, K. E., Lee, A.-H., Bierie, B., and Hotamisligil, G. S. (2013) The Role of Adipocyte XBP1 in Metabolic Regulation during Lactation. *Cell Rep.* **3**, 1430–9

20. Sha, H., Sun, S., Francisco, A. B., Ehrhardt, N., Xue, Z., Liu, L., Lawrence, P., Mattijssen, F., Guber, R. D., Panhwar, M. S., Brenna, J. T., Shi, H., Xue, B., Kersten, S., Bensadoun, A., Péterfy, M., Long, Q., and Qi, L. (2014) The ER-associated degradation adaptor protein Sel1L regulates LPL secretion and lipid metabolism. *Cell Metab.* **20**, 458–70

21. Sun, S., Shi, G., Han, X., Francisco, A. B., Ji, Y., Mendonça, N., Liu, X., Locasale, J. W., Simpson, K. W., Duhamel, G. E., Kersten, S., Iii, J. R. Y., Long, Q., and Qi, L. (2014) Sel1L is indispensable for mammalian endoplasmic reticulum-associated degradation, endoplasmic reticulum homeostasis, and survival. *Proc. Natl. Acad. Sci. U. S. A.* **111**, 6115

CHAPTER 2

LITERATURE REVIEW

Introduction

The mammary gland undergoes a number of developmental and metabolic changes to engage in copious milk secretion. Lactation is an essential feature of mammalian life. For that reason, it is paramount to elucidate the molecular mechanisms necessary to initiate and to sustain lactation.

Most of humanity depends on lactation as a source of nourishment for children (1–3). The World Health Organization recommends exclusive breastfeeding as the optimal feeding strategy for at least the first six months of life (4). On a daily basis, women can secrete 800 milliliters of milk containing 32 grams of triglycerides, 7 g of protein and 57 g of lactose (5, 6). Furthermore, the production and consumption of bovine milk and dairy products is closely tied to the economic livelihoods of many societies around the world (7, 8). The first few weeks after parturition represent a period of increased milk yield and heightened metabolic activity of the mammary gland (9). Taken together, lactation is important for human society for both economic and nutritional reasons.

Mammalian neonates rely on milk for virtually all nutrients. For example, milk is the only source of nourishment for mouse pups for the first two weeks

of life. The mouse mammary gland has evolved to secrete copious amounts of not only milk proteins, but also milk lipids and lactose. Over a single lactation, the mouse mammary gland secretes over 30 grams of milk lipids. The fact that the mouse dam is capable of secreting her own body weight in lipids exemplifies the enormous biosynthetic capacity of the mammary gland (5, 10).

The mammary epithelial cells of the lobulo-alveolar system synthesize the organic components of milk. Within these cells, the ER organelle participates in the synthesis of virtually all organic milk components. ER homeostasis is sensitive to periodic cycles of metabolic stress (11). At the onset of lactation, sudden and intense periods of lipid and protein synthesis could perturb the ER environment. However, little is known about ER function in the context of lactation. Therefore the first part of the literature review will describe mammary gland development and milk synthesis. The second part will discuss the function of the ER and ER specific mechanisms that preserve homeostasis of this important cellular organelle.

Part I. Mammary Gland

Structure

The mammary gland is a heterogenous tissue composed of cell types that can be divided into two broad categories: parenchyma and stroma (12). Parenchyma is a term that refers to structures responsible for milk synthesis, ejection, and transport of milk to the nipple or teat. Milk synthesis occurs within

a structure known as the alveolus. Each alveolus is composed of a single layer of MEC encircling a lumen where milk is secreted. Evacuation of milk from the alveolar lumen, a process known as milk ejection, is facilitated by myoepithelial cell contraction. Myoepithelial cells surround each alveolus in the mammary gland. Suckling triggers a neuroendocrine reflex resulting in oxytocin release from the posterior pituitary gland. Oxytocin then binds to its cognate receptor present on myoepithelial cell and activates contraction (13). From the alveolar lumen, milk is delivered to the teat or nipple through a connected network of ducts. In the mouse, smaller ductal branches merge to a single primary duct directly connected to the nipple (10).

The parenchyma is surrounded by stroma, which is composed of a mixture of cell types such as connective tissue, fibroblasts, nerves, haematopoietic cells, blood vessels, and adipocytes (12–14). MEC and adipocytes are the predominant cells composing the parenchyma and stroma, respectively (12, 15). The MEC and adipocyte compartments dynamically change during mammary gland development.

Development

The principal stages of mammary gland development occur during fetal life, puberty, pregnancy, lactation and involution. During these developmental stages, the mammary gland undergoes morphological changes, which are driven primarily through hormonal signaling cascades (13, 16). The hallmark morphological changes that occur during pregnancy, lactation and involution

are the growth of the ductal system, formation of the lobular alveolar apparatus, and its subsequent destruction upon cessation of milk withdrawal, respectively (14). This section will highlight the morphological changes occurring to the MEC and adipocyte compartments, and the major hormones regulating these changes.

In utero, the mammary gland forms from the ectoderm (14). A primitive ductal structure is detectable as early as embryonic day 17 in mice but will remain relatively dormant until puberty (10, 14, 17). With the initiation of ovarian hormone production around 21 days of age and the onset of puberty in mice, the primitive ductal structure is elongated (17). The ovarian hormones estradiol and progesterone as well as the locally produced amphiregulin and insulin like growth factor I are responsible for ductal elongation during puberty (12, 16, 18). The terminal end buds (TEB) of the ductal tree are the sites of rapid proliferation and direct ductal elongation (14). By 10-12 weeks of age in mice, the TEB have infiltrated the stroma completely, thus resulting in TEB to regress. The adipocyte compartment occupies most of the gland relative to the MEC compartment in mature virgin animals.

The lobulo-alveolar apparatus is formed during the twenty-day gestation period in mice. The mammary gland prepares for lactation by initiating ductal side branching and inducing expression of genes associated with milk synthesis. Elevated levels of proliferation promote ductal side branching during the first half of pregnancy (10, 17). The ductal side branches are the origin of

alveolar structures (17). During pregnancy, prolactin and progesterone are responsible for promoting ductal side branching and alveolar formation (10). Prolactin promotes an increase in the expression of proteins and enzymes involved in milk synthesis during the second half of pregnancy (5, 14, 19, 20). During the last few days of pregnancy, the MEC compartment increases dramatically in size relative to mammary adipocytes. Also at this time, MEC can begin to synthesize milk components but circulating levels of progesterone prevents the onset of copious milk secretion (21, 22).

The loss of the placenta at parturition leads to the fall of progesterone levels (22). With loss of progesterone inhibition, copious amounts of milk are synthesized and secreted (5, 22, 23). To meet the sudden and intense demands of nursing pups, the alveolar structures expand and eventually fully occupy the mammary gland. A predominant MEC compartment, expanded alveolar lumen, and absent adipocyte compartment are hallmark morphological features of a fully lactating mammary gland (10). The hormones that promote alveolar expansion and subsequently, lactation, include prolactin, glucocorticoids and insulin (12, 16, 18, 24). Moreover, the pulsatile release of prolactin is essential to maintain lactation in rodents and humans (12, 25, 26).

Milk stasis at weaning induces the final stage of mammary gland development, involution. During involution the mammary gland undergoes remodeling (14). Mammary gland tissue remodeling is mediated through protease degradation of extracellular matrix, basement membrane

deterioration, and elevated MEC apoptosis. Collectively these distinctive features of involution lead to alveolar structure collapse (14, 27). Furthermore, alveolar structure collapse is concomitant with a decline in prolactin levels (28). Involution is reversible if suckling is reinitiated within 48 hours of weaning but by day 3 of involution, most of the alveoli have collapsed (14, 29). Consistent with alveolar collapse, apoptosis in MEC peaks on involution day 4 (29, 30). With increased MEC cell death, the adipocyte compartment reappears. Once involution is completed, the mammary gland resembles that of adult virgin mice, featuring a ductal system embedded in a prominent fatty stroma. Overall, involution is necessary to restore the mammary gland back to a pre-pregnant state. The remodeling process allows the mammary gland to proliferate and differentiate during subsequent pregnancies.

Milk Synthesis

Mammary epithelial cells are unique in synthesizing and secreting a complex fluid not only composed of proteins, but also copious amounts of carbohydrates and lipids. Milk provides complete nutrition for mouse pups during the first two weeks of life (5, 10).

Mouse milk is composed of 30% lipids, 12% proteins, and 5% lactose (10). The hallmark characteristic of a defective lactation in genetically manipulated mice is reduced pup growth, which is generally explained by defects in synthesis or secretion of one or more organic components of milk

(5, 23, 31–35). The remainder of Part I will focus specifically on the synthesis and secretion of the organic components of milk.

Milk Fat

Lipids are the most calorically dense component in milk and are vital to provide energy for neonatal growth (25). Ninety eight percent of milk fat is in the form of TAG (10, 36). Milk and adipose tissue TAG differ substantially in terms of the fatty acid composition. Accordingly, the next section is focused on fatty acid synthesis in the mammary gland.

Mouse milk fatty acids are divided into three categories: medium chain fatty acids, palmitate, and long chain fatty acids. The milk fatty acids categories are defined by their origin (37, 38). Medium chain fatty acids have lengths varying from 8 to 14 carbons and are synthesized in the cytosol of MEC. This process will be referred to as *de novo* lipogenesis. Long chain fatty acids have 18 or more carbons and can be saturated or unsaturated. Long chain milk fatty acids come to the MEC already assembled (or preformed). These fatty acids originate from the diet, hepatic lipogenesis, or from adipose tissue reserves. Finally, palmitic acid comes from both *de novo* lipogenesis and from the pool of preformed fatty acids (37).

When expressed on a molar basis, medium chain fatty acids, palmitate, and long chain fatty acids respectively account for 15-40%, 20-30%, and 30-70% of milk fatty acids (33, 39). Human milk is similar in that 15-35% of milk fatty acids are medium chain fatty acids. Several factors explain the variation

in the proportion of each category of fatty acid in milk (25). For example, mice fed a standard chow diet will have a higher level of medium chain fatty acids whereas those fed a high fat diet have a higher proportion of long chain milk fatty acids (10, 33).

During the transition from pregnancy to lactation, the mammary gland adjusts from fatty acid β-oxidation to *de novo* lipogenesis, in part by the robust induction of enzymes involved in *de novo* lipogenesis (40). In mice, the major carbon source for *de novo* lipogenesis is glucose. Glut1, a non-insulin dependent transporter, shuttles glucose into MEC (10, 25). Evidence suggests that prolactin regulates Glut1 expression (10). Once inside the MEC, glucose has two major fates, either used in the pentose phosphate shunt to generate NADPH in support of fatty acid synthesis or converted to pyruvate via glycolysis. Pyruvate then enters the mitochondria where it is converted to citrate (25). Citrate is transported from the mitochondria to the cytoplasm by the mitochondrial citrate transporter (SLC). Then two cytoplasmic enzymes, ATP citrate lyase (ACLY) and acety-CoA carboxylase (ACC), utilizes citrate to produce acetyl-CoA and convert acetyl-CoA into malonyl-CoA, respectively (33). ACC is the first rate-limiting step in fatty acid synthesis and is highly regulated by insulin (25, 33). Fatty acid synthase (FASN) utilizes malonyl-CoA and NADPH molecules to synthesize fatty acids. FASN catalyzes a series of condensation cycles, each requiring two NADPH molecules, to add two carbon units donated from malonyl-CoA to a growing fatty acyl chain. Another

cytoplasmic enzyme, thioesterase II, cleaves the growing fatty acyl chain through its acylthioester hydrolase activity at lengths between 8-14 carbons (25, 33), thus explaining the presence of short and medium chain fatty acids in milk fat. Once formed, medium chain fatty acids and palmitate can be desaturated by stearoyl-CoA desaturase 1 (SCD1), an ER membrane bound enzyme (33).

A portion of C16 fatty acids and all fatty acids with 18 carbons or more originate from outside of the mammary gland. Circulating chylomicrons transport TAG when the animal is in a fed state. During lactation, fatty acids are also mobilized from adipose tissue and transported to liver, where very low density lipoproteins (VLDL) are synthesized and secreted. TAG contained into chylomicrons and VLDL are targets by lipoprotein lipase (LPL) (10). LPL is attached to the endothelium layer of capillaries and is responsible for releasing preformed fatty acids from TAG (41). Preformed and *de novo* synthesized fatty acids must be activated in the form of acyl-CoA fatty acid by the enzyme, acyl-CoA-synthase (ACSL) (40)**.** Their incorporation into TAG can then proceed via a series of enzyme embedded into the smooth ER (25, 33).

TAG synthesis requires enzymes embedded into the ER to incorporate fatty acids to a glycerol-3-phosphate backbone (42). Fatty acids are acylated to the sn-1 and sn-2 position of the glycerol-3-phosphate backbone by glycerol-3-phosphate O-acyltransferase (GPAT) and 1-acylglycerol-3-phosphate O-acyltransferase (AGPAT) enzymes, respectively (11, 43). This is

followed by removal of the phosphate group from phosphatidic acid by the enzyme, phosphatidic acid phosphatase (PAP) or lipin, yielding diacylglycerol (DAG) (11, 43). A third fatty acid is then added to DAG by diacylglycerol O-acyltransferase enzyme (DGAT) (11). The mouse has 2 DGAT genes with the mammary expressing predominantly DGAT1. DGAT1 is not only necessary for milk lipid synthesis but it is also essential for mammary development (44, 45).

After newly synthesized milk TAGs have accumulated in the ER, they are released into the cytosol of MEC as cytoplasmic lipid droplets (CLD). Milk CLD travel to the apical plasma membrane of the MEC. Milk CLD fused with the MEC apical plasma membrane resulting in the secretion of milk lipids into the alveolar lumen (46). Milk lipid synthesis can occur during late gestation but milk secretion is inhibited until the onset of lactation. The fall of progesterone at parturition releases the inhibition of milk secretion and allows milk components to be secreted into the alveolar lumen (13, 15). Accordingly, histology sections of late pregnant mammary glands reveal multiple large CLDs inside the MEC whereas they are seen predominantly in the alveolar lumen upon lactation (14).

Milk lipids are secreted with a unique membrane structure, termed the milk fat globule membrane (MFGM) (46, 47). Evidence suggests that the MFGM is a tripartite membrane structure consisting of an outer membrane bilayer and an inner monolayer enveloping the milk TAG core (44, 48, 49). The outer membrane bilayer is thought to originate from the MEC apical plasma

membrane whereas the inner membrane is thought to be contributed by the ER membrane. Collectively, the proposed tripartite membrane structure of MFGM accounts for roughly 50-70% of the phospholipid fraction in milk (36).

Butyrophilin, adipophilin (ADPH), and xanthine oxidoreductase (XO) are three proteins present in MFGM and shown to be involved with MFGM secretion (44). Butyrophilin is a type 1 transmembrane protein and has been detected on the MEC apical plasma membrane (36, 50). Electron micrographs of mammary glands collected from butyrophilin null female mice displayed abnormally large lipid droplets in the MEC, suggesting that butyrophilin is involved in milk lipid secretion (51). Evidence suggests that ADPH regulates milk CLD size. Histology sections from late gestation ADPH null mice revealed small CLDs in the MEC (52). Furthermore, the appearance of large CLDs in MEC correlated with increased ADPH expression (50). XO mRNA is highly expressed in MEC with mRNA levels increasing dramatically during late gestation, remaining high throughout lactation, and decreasing at involution. XO protein has been detected at the MEC apical plasma membrane in the middle of lactation (19). XO protein accounts for 1-2% of total mammary soluble protein in both cow and mouse, reflecting its conserved abundance in MEC (19, 50).

Recent evidence suggests that XO expression is regulated by a transcription coactivator, Cidea. Cidea null lactating mice had diminished XO mRNA and protein levels in addition to reduced total milk lipids and milk fatty

acids (31). The protein content and volume of milk collected from Cidea null mice were not altered, suggesting a lipid secretion defect. MECs collected from wildtype mice exhibited an increase of Cidea mRNA and protein levels during pregnancy and further elevation of both during lactation. Cidea protein was also detected in milk, thus suggesting that Cidea co-regulates XO mediated milk lipid secretion in MEC (31).

Milk Protein

Milk protein is essential to support postnatal growth. Mouse milk contains approximately 6-12% proteins, represented predominantly by casein and whey proteins. The major casein proteins found in mouse milk are β-casein followed by αs-1 and αs-2 casein, γ-casein, κ-casein and ε-casein. The major whey proteins in mouse milk are whey acidic protein (WAP), lactoferrin, and α-lactalbumin (53). Milk protein expression is tightly linked to lactation, and therefore is also regarded as an indicator of mammary gland differentiation.

Milk protein synthesis in MEC cell culture is induced by the combination of insulin, prolactin, and glucocorticoids (54). One mechanism by which insulin regulates milk protein expression is through the serine/threonine kinase Akt1. Akt1 has been shown to be significantly upregulated during pregnancy and lactation in the mammary gland (55). Overexpression of constitutively active Akt1 resulted in elevated β and ε-casein, WAP, and α-lactalbumin expression (56). Furthermore, the lactogenic hormone prolactin stimulates the activation

of STAT5a, which subsequently upregulates milk protein gene expression (28). In addition, recent evidence suggests that sustained Akt activation induces prolactin production by MEC (57). Together, these findings elucidate a direct mechanism whereby Akt induces local prolactin production followed by the activation of Jak2-Stat5 and ultimately resulting in the production of milk protein.

The caseins are a family of proteins found only in milk. The caseins have very little secondary structure but some are glycosylated in the ER (58, 59). Once synthesized, caseins form a macromolecular complex with minerals, termed micelles (38). The primary mineral in casein micelles is calcium. Casein micelles are then packaged into secretory vesicles and transported to the MEC apical plasma, followed by exocytosis and ultimately secretion of casein in the alveolar lumen (13).

Lactose

The major carbohydrate in milk for most mammals is lactose (22). Lactose is crucial for milk secretion because it acts as an osmotic regulator and drives water into the MEC golgi lumen (10, 38, 60). As a result, the rate of lactose synthesis regulates water flux into milk and ultimately determines milk volume (13, 60).

Lactose is a disaccharide composed of glucose and galactose. Glucose is the precursor for galactose. Interestingly, the UDP-galactose-4-epimerase (GALE) enzyme, which catalyzes the conversion of UDP-glucose to UDP-

galactose, is induced during lactation and decline with weaning (61). The final enzymatic step involved in lactose synthesis occurs in the Golgi and is performed by the lactose synthase complex. This enzyme complex is composed of the ubiquitious protein β1-4 galactosyltransferase and the mammary specific protein α-lactalbumin (10, 27). Mice lacking α-lactalbumin have no lactose synthase activity and no milk lactose. As a result, they synthesize milk with a high solid content and suffer from a secretion defect (60). Once synthesized in the golgi, lactose is packaged into secretory vesicles. The secretory vesicles are transported to the apical MEC plasma membrane resulting in the exocytosis of lactose in the MEC alveolar lumen (13).

Part II. ER

Role in synthesis of milk proteins and triglycerides

The ER is the site of synthesis of secreted proteins and where the assembly of TAG and phospholipid occurs (43, 62). The ER is a continuous network of flattened sac like structures radiating from the nucleus into the cytosol of the cell. The ER consists of phospholipid rich membrane bilayers enclosing an internal luminal space. Secreted and transmembrane proteins are made in regions of the ER studded with ribosomes, termed the rough ER. TAG and amphiphatic phospholipids are made in regions of the ER devoid of ribosomes, called the smooth ER (43).

Rough ER

It is estimated that the rough ER handles roughly 75% of all proteins made by professional secretory cells, such as hepatocytes (11, 63). Nascent proteins destined for the rough ER are recognized by a N-terminal short signal sequence, directed by a signal recognition particle, and translocated into the rough ER lumen by the Sec61 protein channel. Once inside the ER lumen, the polypeptides undergo a variety of post-translational modifications until the protein reaches its mature state (64). One of the main post-translational modifications for secretory and membrane-bound proteins is glycosylation, with asparagine linked (N-linked) glycosylation present in most modified glycoproteins (58). Some of the casein and whey milk proteins are modified by N-linked glycosylation (58, 65, 66).

The final three branch-carbohydrate structure present for N-linked glycosylation is composed of nine mannoses, two N-acetylglucosamines and three terminal glucose residues (64, 67). This structure is synthesized one sugar at a time and arranged in different combinations. This complex carbohydrate branched structure is formed at first in the cytosol and then in the ER lumen by ER membrane bound glycosyltransferases (58). Once the final carbohydrate structure is made, the unit is transferred to the nascent polypeptide on a specific asparagine residue inside the lumen of the rough ER (68).

Removal of the terminal mannose residue of the oligosaccharide complex results in irreversible extraction of the glycoprotein from the calnexin and calreticulin chaperone complex. The major lectin involved in mannose trimming is the ER-degradation enhancing α-mannosidase like protein 1 (EDEM1). EDEM1 contains a mannosidase domain and can also act as a chaperone by binding to non-native proteins (64). The glycoprotein is then available for binding to lectins. Lectin proteins are known to bind and modify N-linked glycans in order to assist in protein folding (64). In mammals, the major glycan binding lectin proteins are OS-9 and XTP3-B (68). OS-9 and XTP3-B contain mannose-6-phosphate receptor homology MRH domains, which allow these lectin proteins to bind to the exposed mannose residue (67).

Smooth ER

An important function of the smooth ER in MEC is synthesis of TAG and amphiphatic phospholipids (43). Virtually all milk lipids appear in the form of TAG whereas phospholipids are major components of ER membranes and must be synthesized abundantly to sustain the extensive ER network of MEC engaged in milk synthesis.

Cells secreting large amounts of protein display highly elaborate ER (69–71). The size of the ER could influence its capacity to properly fold proteins or synthesize lipids, and one mechanism to restore ER homeostasis is to increase ER luminal capacity (72). Increasing the ER phospholipid membrane bilayer, termed ER biogenesis, is coordinated in part by

upregulating phospholipid synthesis (69, 70). Furthermore, inhibiting phospholipid synthesis has been shown to disrupt ER morphology, indicating that phospholipid synthesis is integral to the maintenance and promotion of ER membranes (73).

Amphiphatic phospholipids are composed of two hydrophobic fatty acyl groups and a hydrophilic phosphorylated alcohol group attached to a glycerol backbone (74). Enzymes in the Kennedy pathway assemble phospholipids (11, 69). The predominant phospholipid is phosphatidylcholine (PC) and is estimated to constitute 40-80% of the total membrane mass (62, 74). The synthesis of the second most abundant phospholipid, phosphatidylethanolamine (PE) mirrors PC synthesis due to similar enzymatic reactions (43, 74). However, PC levels within a cell change more dynamically than PE levels (74). Therefore, I will focus on PC to describe enzymatic steps involved in phospholipid synthesis.

The synthesis of PC is similar to that of TAG, except that DAG is condensed with a cytidylylphosphointermediate rather than a third fatty acid. Synthesis of the cytidylylphosphointermediate begins with the indispensable nutrient choline (74). Choline kinase (CHK), the first step in the Kennedy pathway, phosphorylates choline (69, 74). Choline cytidyltransferase (PCYT1) generates the cytidylylphosphointermediate by transferring a cytidine moiety to the phosphorylated choline and is the rate-limiting step in the Kennedy pathway (43, 74). Finally, the cytidylylphosphointermediate is transferred to

DAG by cholinephosphotransferase (CHPT1), resulting in the synthesis of PC (74). Alternatively, PC can be synthesized by phosphatidylethanolamine N-methyltransferase (PEMT), which is a bifunctional enzyme that can methylate PE to PC (43, 46, 62, 69, 74). Similar to TAG synthesizing enzymes, PCYT1, CHPT1, and PEMT have been detected on the ER membrane (43, 74).

CLD formation is tightly coupled to the smooth endoplasmic reticulum, as previously mentioned (Mammary Section Part I). In CLD, phospholipids surround the TAG core, with both TAG and phospholipids synthesis occurring in the smooth ER (44, 75).

ER Homeostatic Systems

In order to sustain the fidelity of lipid, phospholipid, and protein synthesis, ER homeostasis must be preserved. A variety of cellular conditions can perturb the ER luminal environment such as calcium depletion, oxidative stress, hypoxia, and misfolded protein accumulation (76). Chronic or acute disruptions in ER homeostasis elicit a cellular condition known as ER stress. In the broadest sense, ER stress occurs when the demands placed on the ER surpass its ability to handle them. Prolonged ER stress has detrimental consequences, including apoptosis. Therefore, the cell has adapted by developing two regulatory homeostatic systems aimed at resolving ER stress, the UPR and ERAD (77). The UPR and ERAD systems will be discussed in further detail.

UPR Functions and Elements

If the ER luminal environment is disturbed, the UPR is initiated in an attempt to restore ER homeostasis. UPR refers to a highly conserved signaling cascade that detects stress inside the ER lumen and initiate adaptations promoting cell survival (11, 76, 78). The UPR broadly consists of three branches, with each branch controlled by an ER stress sensor. The three ER transmembrane stress sensors are PERK (double stranded RNA-activated protein kinase PKR-like ER kinase), ATF6 (activating transcription factor 6), and IRE1 (inositol requiring enzyme 1) (Figure 2.1). UPR signaling in metazoans results from the activation of one or more ER stress sensors, thus enabling an array of cellular outcomes (79). The particular combination of ER stress sensors that is activated varies by cell type, nature of the insults, and the required cellular response. Ultimately, the activation of each ER stress sensor leads to the production of a basic leucine zipper domain (bZIP) transcription factor, which subsequently induces transcriptional networks alleviating ER stress (79). In the next section, the UPR sensors, PERK and ATF6, are covered briefly. The IRE1 sensor is discussed more extensively because it gives rise to the transcription factor, XBP1, which is one of the proteins studied in this work.

ER Sensors

PERK

PERK is a type 1 ER transmembrane protein with serine/threonine kinase activity on its cytosolic domain (76). Normally, PERK is retained in an

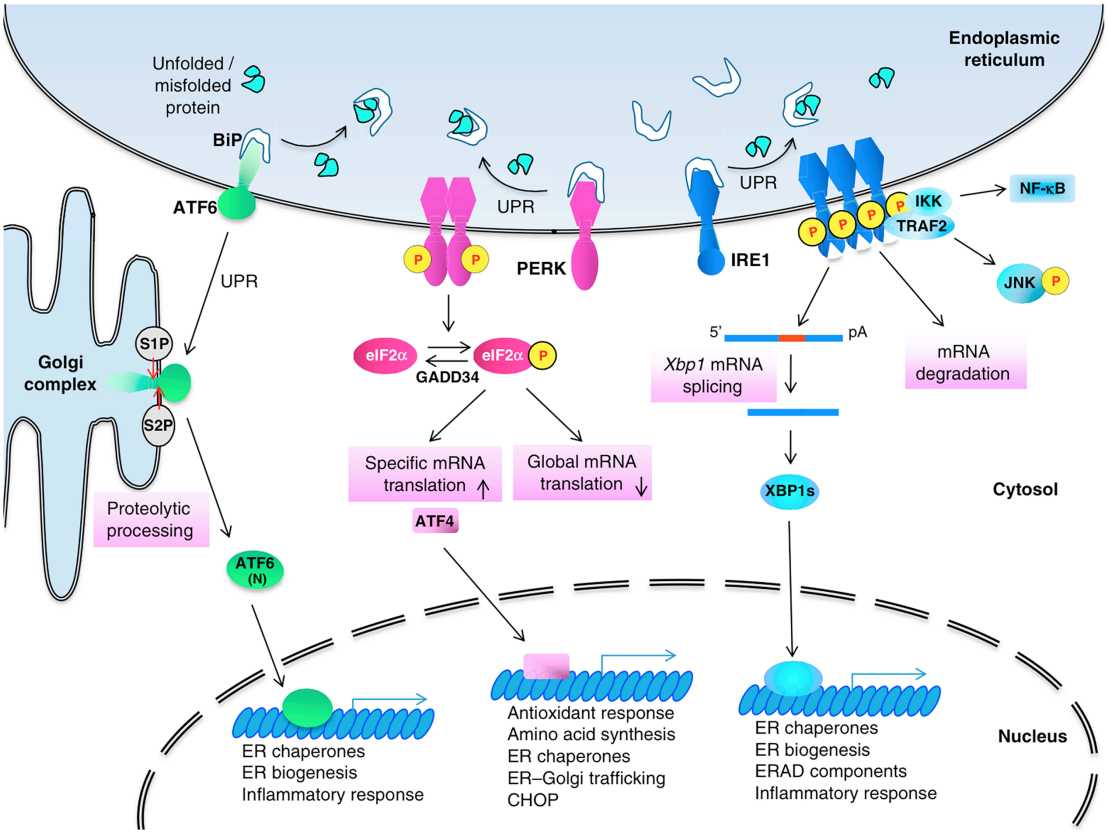

Figure 2.1 UPR signaling in metazoans.

A general illustration depicting the activation of the three metazoan ER transmembrane stress sensors of the UPR signaling cascade. Illustration is adapted from Kaufman et al 2012 (76).

inactive monomeric state by Bip, a mammalian ER resident HSP70 chaperone protein. Upon ER stress conditions, Bip dissociates, leading to the oligomerization and activation of PERK (79). Once activated, PERK specifically phosphorylates eIF2α, which in turn inhibits the translation initiation complex and ribosomal translation (80).

Despite suppressed protein translation during PERK activation, a subset of mRNAs is preferentially translated. One of these is ATF4 mRNA, which encodes a bZIP transcription factor (76). ATF4 mRNA contains positive and inhibitory short open reading frames in the 5'-untranslated region (respectively known as uORF1 and uORF2). In the absence of ER stress, the translation initiation complex is abundant and ribosomes reach the inhibitory uORF2, which results in ribosome release and reduced translation of ATF4 mRNA. PERK mediated phosphorylation of eIF2α under ER stress conditions reduces the availability of the translation initiation complex. Therefore, after scanning through uORF1, the translation initiation complex is not acquired again until the ribosomes have reached the coding region, thus bypassing the inhibitory uORF2 and facilitating ATF4 mRNA translation (81).

Two downstream target genes of ATF4 are C/EBP homologous protein (CHOP) and growth arrest and DNA damage-inducible 34 (GADD34) (76, 80). CHOP is a transcription factor that promotes apoptosis whereas GADD34 encodes a phosphatase that counteracts PERK mediated phosphorylation of eIF2α (79). GADD34 activation results in the removal of the protein translation

brake and, combined with CHOP activation, promotes apoptosis (82). Globally, PERK activation promotes ER homeostasis by diminishing protein folding demands, followed by cell death if ER homeostasis can not be restored.

ATF6

The second ER stress sensor, ATF6, is a type II transmembrane protein with a larger luminal domain than PERK (76, 79). Once Bip dissociates from the ATF6 luminal domain during ER stress, ATF6 is trafficked to the Golgi for proteolytic cleavage (79). The full length ATF6 is cleaved by site 1 and 2 Golgi proteases to release the N-terminal cytosolic fragment (76, 79, 80). The N-terminal ATF6 fragment enters the nucleus where it acts as a dimer to activate its own subset of genes or as a heterodimer with XBP1 to regulate overlapping genes. Activated genes function in protein folding, ERAD, and other ER homeostasis systems (83, 84). Furthermore, overexpression of ATF6 in cell culture promoted ER membrane expansion by increasing phospholipid synthesis, indicating that ATF6 has a potential overlapping role in ER membrane biogenesis with XBP1 (85).

IRE1

IRE1 is the only ER stress sensor found in yeast. Metazoans have two IRE1 homologues with IRE1α expressed ubiquitously and IRE1β expression restricted to the intestinal epithelium. IRE1 is a type 1 ER transmembrane protein composed of cytosolic, transmembrane, and luminal domains. IRE1

shares structural similarities with PERK and is endowed with serine/threonine kinase activity. In addition, IRE1 also has endoribonuclease (RNase) located in its cytosolic domain (76). The ER luminal domain of IRE1 is responsible for sensing stress inside the ER lumen (86). Once ER stress is sensed, the ER luminal domain undergoes oligomerization.

Oligomerization of the IRE1 luminal domain positions the cytosolic kinase domains for trans-autophosphorylation, leading to the activation of its enzymatic activities (79, 86). Oligomerization was suggested by fluorescence live cell imaging. Under basal conditions, human IRE1 displayed a diffuse distribution within the ER membrane. However after ER stress induction, discrete IRE1 foci were observed in the ER membrane, suggesting oligomerization (87). Structural analysis and X-ray crystallography of yeast IRE1 predicted oligomerization of the yeast IRE1 luminal domain (86). Mutating a tightly packed lysine residue at the predicted human IRE1 dimerization interface prevented discrete foci formation during ER stress (87). Taken together, these data suggest that oligomerization is essential for IRE1 activation in yeast and metazoans.

Two different activation models have been proposed to explain IRE1 oligomerization (88). In metazoans, Bip restrain IRE1 activity under normal condition by binding to its luminal domain; IRE1 activity is unleashed when Bip moves to unfolded protein aggregates accumulating under ER stress (89). Coimmunoprecipitation experiments support this model because under

unstressed conditions Bip was bound to the luminal IRE1 domain and ER stress inducer treatment diminished Bip binding (90). However, this model does not seem to apply in yeast because deleting Bip binding regions did not cause a constitutively active IRE1, and IRE1 can form discrete foci under ER stress conditions in yeast mutants lacking the Bip homologue, Kar2 (88, 90). Rather oligomerization in yeast appears to be driven by direct binding of unfolded proteins to IRE1. Structural analysis of yeast IRE1 luminal domain predicted a groove for unfolded protein binding. Furthermore, overexpression of purified IRE1 luminal domain in yeast resulted in attenuated protein aggregation due to direct binding of this domain to unfolded proteins (91, 92).

The activation of the two enzymatic activities of IRE1 follows oligomerization. The endoribonuclease activity of IRE1 has two mRNA cleavage functions. The first cleavage activity is specific for XBP1 (X-Box Binding Protein 1). It specifically removes a 26 base pair internal segment from XBP1 mRNA (93, 94). This results in a shift in the reading frame allowing for the synthesis of a 54 kDa protein (sXBP1). In absence of this frameshift, translation leads to a shorter and unstable 33 kDa protein (uXBP1) (76, 95). This unconventional IRE1 mediated mRNA splicing was first observed in the yeast XBP1 homologue HAC1 (96–98). In 2002, XBP1 mRNA species missing the 26 nucleotide fragment were identified in C. elegans undergoing ER stress, but not in unstressed cells (95). The stable 54 kDa protein is a transcription

factor recognizing ER stress response elements in the promoter region of target genes (76, 99–102).

The endoribonuclease activity of IRE1 also participates in a second less specific process known as regulated IRE1 dependent decay of mRNAs (RIDD). RIDD refers to nonspecific cleavage of a broad range of mRNAs destined for protein translation on the ER. In this process, the IRE1 endonuclease does not have identifiable consensus sequences but rather attacks mRNA free ends. Consequently, RIDD alleviates ER stress by minimizing the flux of incoming nascent proteins in the ER (79, 103). Interestingly, insulin, TAG, and cholesterol related transcripts were identified as targets of RIDD in experimental models where IRE1 was hyperactivated (104, 105).

The kinase activity of IRE1 can also be uncoupled from its endoribonuclease activity (79). IRE1 kinase activity has been shown to activate JUN N-terminal kinases (JNK) and in this way elicit a cellular inflammatory response (106). Under chronic ER stress, IRE1 hyperactivation has been implicated in eliciting a cellular inflammatory response through JNK activation (11). For example, increased JNK phosphorylation has been associated with intestinal epithelial cells lacking XBP1 and mice with a null mutation in one XBP1 allele fed a high fat diet (107, 108).

XBP1 Function

Evidence for an essential role for XBP1 first came from non-vertebrate systems and cultured mammalian cells. In 1996, three independent research groups identified the yeast XBP1 homologue, HAC1 (96–98). HAC1 was identified as a gene encoding a bZIP transcription factor that, when reintroduced in IRE1 yeast mutants, restored survival during treatment with an ER stress inducer. Notably, Cox and colleagues reported that HAC1 mRNA was spliced in wild type yeast cells in the presence of an ER stress inducer (98). This unconventional splicing event was abolished in IRE1 yeast mutants, indicating that HAC1 mRNA splicing required IRE1. Collectively, these studies show that HAC1 is acting downstream of IRE1 and is an essential transcription factor of UPR signaling. The mammalian homologue, XBP1, was identified in higher eukaryotic systems by utilizing *C. elegans* (18, 109). These studies demonstrated, that similar to yeast, IRE1 mediated site-specific mRNA cleavage of XBP1.

Mammalian cell culture systems were the first to associate XBP1 signaling with highly elaborate ER structures in secretory cells. Overexpressing XBP1 in fibroblasts resulted in an increase in cell size with a parallel increase in ER size and volume (69, 70). Furthermore, fibroblasts overexpressing XBP1 had elevated levels of PC due to an increase in PCYT1 activity, the rate-limiting step of PC synthesis. The higher levels of PCYT1 activity was not associated with any changes in mRNA levels, suggesting that XBP1 upregulates PC synthesis in a post-transcriptional manner (69).

However the molecular mechanism of whereby XBP1 regulates ER membrane biogenesis still requires investigation.

Total XBP1 Knockout

In an effort to characterize the *in vivo* function of XBP1, a global XBP1 knock out mouse model was generated. However global depletion of XBP1 resulted in embryonic lethality beginning at embryonic day 12. Reduced proliferative and elevated apoptotic signals were reported in the liver of null XBP1 mice, indicating that XBP1 signaling is indispensable during fetal development (110). More recently, the Glimcher research group developed floxed XBP1 mice that allow for tissue specific ablation of XBP1 and circumvent the embryonic lethality of global XBP1 ablation. Findings from relevant tissue specific XBP1 experimental models are reviewed below.

XBP1 ablation in B cells

Plasma B cells, once differentiated, are capable of secreting large quantities of immunoglobulins (111). An essential role for XBP1 in plasma B cells was first suggested in 2001 when chimeric mice with XBP1 null lymphoids exhibited reduced circulating levels of immunoglobulins (112). Later studies utilizing cultured plasma B cells implicated XBP1 signaling in the differentiation and secretory function of plasma B cells. In response to differentiation stimuli, spliced XBP1 expression was induced in cultured purified B cells (111). XBP1 overexpression *in vitro* resulted in a dramatic increase of immunoglobulin secretion whereas XBP1 depletion reduced

expression of genes involved in secretion (111, 113). Furthermore, spliced XBP1 synthesis was initiated in response to differentiation stimuli even in the absence of immunoglobulin synthesis, suggesting that XBP1 signaling precedes increased immunoglobulin synthesis (114).

In 2009, a floxed XBP1 mouse model was used to ablate XBP1 specifically in B cells (115). This study substantiated earlier findings in that depletion of XBP1 in B cells inhibited terminal differentiation and impaired immunoglobulin production in response to immunization. In contrast, XBP1 deletion had no effect on the function and differentiation of memory cells, which are a distinct class of B cells that differentiate independently of plasma B cells. Interestingly, XBP1 depleted plasma B cells exhibited a lack of ER and Golgi expansion but the total number of B cells was unchanged. This suggests that the decrease in immunoglobulin production seen *in vivo* is due to a secretory machinery deficit in plasma B cells. Overall, this study demonstrated that XBP1 signaling is indispensable for differentiation and secretory function of plasma B cells (115).

In addition, XBP1 signaling has been implicated in the hematopoietic stem cells that give rise to B cells. Knock down of XBP1 signaling decreased the number of viable cultured hematopoietic cells and significantly upregulated gene expression related to apoptosis pathways (116). This was an interesting finding since the phenotypes described for B cells are independent of apoptosis.

XBP1 ablation in pancreas

The pancreas has both exocrine and endocrine functions accounting respectively for the synthesis and secretion of digestive enzymes and hormones (i.e. insulin, glucagon, etc.). A role for XBP1 signaling in the pancreas was first described in a XBP1 germ line global knock out mouse model whereby embryonic lethality was circumvented by directing XBP1 transgenic expression to the liver (117). Mutant pups exhibited severe growth retardation and died shortly after birth due to a lack of XBP1 mediated acinar production of digestive enzymes. Furthermore, pancreatic acinar cells exhibited abnormal ER morphology, suggesting that their secretory capacity was impaired in the absence of XBP1. Unmitigated ER stress induced by increased postnatal zymogen demands resulted in significant increase in *CHOP* mRNA and subsequent apoptosis in pancreatic acinar cells of mutant pups. Interestingly, the global deletion of XBP1 also resulted in disrupted ER morphology and diminished enzyme production in the salivary glands (117).

Due to the multiple defects observed in the XBP1 germline global knock out model, the Glimcher group later utilized floxed XBP1 mice to conditionally delete XBP1 specifically in the pancreatic acinar cells (118). Similar to the transgenic XBP1 model, pancreatic acinar cells exhibited diminished ER abundance and reduced digestive enzyme transcripts. Interestingly, about 10% of pancreatic acinar cells with intact XBP1 expression were able to compensate for the conditional ablation of XBP1 expression in the pancreas,

suggesting robust ability of pancreatic acinar cells with XBP1 expression to adapt (118).

Specifically ablating XBP1 in pancreatic β-cells resulted in elevated blood glucose levels, lower serum insulin levels, reduced β-pancreatic islet area, and higher ratios of proinsulin to insulin (104). Glucose stimulated insulin secretion was severely reduced in the absence of XBP1. Furthermore, the pancreatic β-cells displayed abnormal ER morphology and fewer dense insulin granules. These findings suggest that impaired insulin processing and secretion accounts for the hyperglycemia. The reduced β-pancreatic islet area was due to decreased proliferative signals with no change in apoptosis (104, 117). Taken together, these findings suggest a role for XBP1 in mediating proliferative and apoptotic signals and maintaining the secretory capacity in the pancreas.

XBP1 ablation in liver

A functional role of XBP1 in hepatic metabolism was first described in 2008 (119). Liver specific ablation of XBP1 with the Mx1 inducible Cre resulted in a decrease of circulating plasma TAG, cholesterol, and free fatty acids and a marked reduction in the hepatic expression of lipogenic genes, *DGAT2, SCD1,* and *ACC* (119). These results were confirmed using a second liver specific Cre (105). Consistent with this notion, silencing XBP1 expression in cultured hepatocytes resulted in decreased FASN and SREBP1c promoter

activity (120). Together, these results suggest XBP1 directly regulates the transcription of genes involved in hepatic lipid metabolism.

Liver specific ablation of IRE1 resulted in a mild hepatic steatotic phenotype unaccompanied by any changes in lipogenic gene expression (121). Lipid accumulation in the liver was explained predominantly by impaired hepatic VLDL secretion and by attenuated expression of genes involved in VLDL formation [protein disulfide isomerase (PDI) and microsomal TAG transfer protein (MTP)]. Overexpressing PDI in IRE1 null hepatocytes partially rescued TAG secretion whereas overexpressing XBP1 resulted in full restoration of TAG secretion as well as PDI transcripts and MTP activity (121). Although the direct role of XBP1 in regulating lipogenic gene expression was not supported, these findings indicate that XBP1 directs hepatic TAG secretion by regulating PDI expression and MTP activity.

XBP1 ablation in intestinal cells

Intestinal epithelial cells secrete antimicrobials in order to preserve their protective barrier. Deleting XBP1 in intestinal epithelial cells resulted in spontaneous inflammation and an almost complete absence of antimicrobial secreting Paneth cells (107). Ablating XBP1 elicited an ER stress response as evidenced by increased *CHOP* mRNA abundance and JNK phosphorylation. Elevated apoptotic signals in Paneth cells accounted for their decreased number. Paneth cells lacking XBP1 exhibited abnormally dense ER structures and fewer secretory granules. Consistent with the role of XBP1 in maintaining

secretory function in other cell types, Paneth cells challenged with an endotoxin were incapable of secreting antimicrobials (107). Overall, the absence of XBP1 impaired the secretory function of the intestinal epithelial Paneth cells and incapacitated their ability to handle environmental pathogens.

XBP1 ablation in neurons

Accumulation of misfolded proteins has been shown to contribute to the pathology of neurodegenerative disorders. One pathology in Parkinson disease is accumulation of misfolded proteins. Moreover, signs of elevated ER stress have been detected in postmortem brain sections from humans affected by Parkinson disease (122). Specifically ablating XBP1 in the central and peripheral nervous system resulted in a dramatic decrease in dopaminergic neuron viability (122, 123). Elevated ER stress was detected but no differences were observed in the overall number of neurons or *CHOP* transcript levels, indicating that deficiency of XBP1 in dopaminergic neurons did not promote apoptosis. In contrast to previously described tissue specific models, neuronal deletion of XBP1 did not result in disrupted ER morphology. Rather, dopaminergic neurons lacking XBP1 exhibited large dense aggregates, increased accumulation of polyubiquitinated proteins, and elevated markers of autophagy, suggesting that XBP1 deficiency impaired the ability to eliminate misfolded proteins.

Overall XBP1 Function

Collectively, the findings from tissue specific ablation experiments illustrate the requirement for XBP1 in fulfilling the secretory demands of cells. XBP1 is obviously important for secretory capacity through ER biogenesis in many cell types. Unresolved ER stress response elicited by XBP1 deficiency ultimately promotes apoptotic pathways and results in cell death.

ERAD Functions and Elements

Secretory and transmembrane proteins account for roughly 75% of the total proteins synthesized within professional secretory cells (11). The ER acts as a quality control center for these proteins because they only leave once they reach their mature state (68). Defects in protein folding and post-translational modifications are inevitable in professional secretory cells and can result in the formation of protein aggregates. The cell responds not only via the UPR, but also via a process designed to eliminate misfolded proteins, termed ERAD. To date, over 60 human diseases have been linked to malfunctions of the ERAD pathway, including familial hypercholesterolemia, neonatal diabetes, Walcott-Rallison syndrome, Huntington's disease, and cystic fibrosis (64, 124).

ERAD is a general term that refers to the process of translocating misfolded proteins from the ER lumen to the cytosol for ubiquitin mediated proteasomal degradation (68, 125). Currently, three different mammalian ERAD pathways have been identified: ERAD-L, ERAD-M, and ERAD-C (68, 126, 127). ERAD-L, ERAD-M, ERAD-C target proteins with misfolded luminal,

transmembrane or cytosolic domains, respectively (68, 126, 128). In addition, ERAD-L can be further classified into ERAD-Ls (misfolded soluble luminal proteins) and ERAD-Lm (transmembrane proteins with the misfolded domain facing the ER lumen) (127–129). All ERAD pathways involve ER embedded transmembrane complexes and require the coordination of multiple proteins to facilitate substrate recognition, delivery, and transfer to cytosolic proteasomes (Figure 2.2) (68).

All ERAD pathways involve an ER embedded E3 ubiquitin ligase marking misfolded proteins for degradation. The most well characterized metazoan E3 ligase is hydroxymethyglutaryl reductase degradation 1 (HRD1) (68, 126). HRD1 containing ERAD complex contains the metazoan protein, suppressor/enhancer of lin-12-like 1 (Sel1L) (126). Sel1L is a type 1 transmembrane protein with a large luminal domain and serves as an adaptor protein for HRD1 (68, 130, 131). Despite conflicting results in yeast and mammalian cell culture, the dependence of HRD1 on Sel1L was confirmed by the discovery that *in vivo* HRD1 levels are reduced in the absence of Sel1L (126, 132, 133). Sel1L can recruit other proteins to the ERAD transmembrane protein complex, such as EDEM1, osteosarcoma 9 (OS9), and endoplasmic reticulum lectin 1 (XTP3B) (126). Furthermore, these proteins are post-translationally modified by glycosylation (67). Sel1L and these recruited proteins provide substrate specificity for both the ERAD-L and ERAD-M pathways. A current research focus is the identification of HRD1/ Sel1L

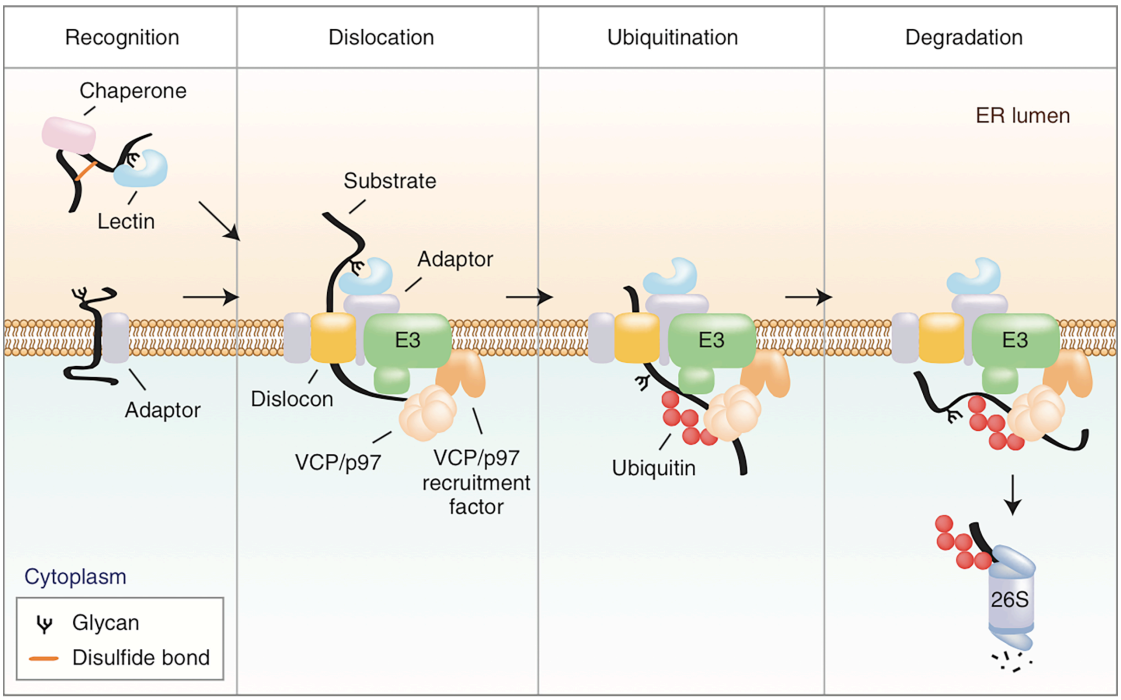

Figure 2.2 ERAD-L pathway in metazoans.

A general illustration depicting the ERAD-L pathway. ERAD-L involves an ER embedded transmembrane complex and requires the coordination of multiple proteins to facilitate substrate recognition, delivery, and transfer to cytosolic proteasomes. Illustration is adapted from Christianson et al 2013 (125).

substrates. For example, a recent study uncovered that Sel1L regulates the degradation of a glycosylated ATF6 precursor (128).

Total Sel1L Knockout

One approach to assess the functional importance of HRD1 driven ERAD complexes is to knockout Sel1L. A global deletion of Sel1L was embryonic lethal due to elevated apoptotic signals, induction of ER stress, and abnormal ER morphology in hepatocytes (134). In cell culture, null Sel1L embryonic fibroblasts exhibited diminished degradation of a constitutively misfolded protein as well as attenuated protein secretion. Furthermore, embryonic development of the pancreas was inhibited in the absence of Sel1L (135). Taken together, these findings establish an absolute requirement for Sel1L during embryonic development.

Heterozygous Sel1L Knockout

To circumvent embryonic lethality, mice heterozygous for the null Sel1L allele were studied (130). These animals were phenotypically normal on chow diet, however when challenged with high fat diet, heterozygous mice were hyperglycemic and exhibited reductions in glucose stimulated insulin secretion. The pancreatic β-cell mass was dramatically reduced, suggesting that it accounts for the reduction in insulin secretion. The reduced β-cell mass was associated with decreased proliferation with no changes in apoptosis. Furthermore, Sel1L heterozygous pancreatic β-cells exhibited an ER stress response when challenged with high concentrations of glucose in cell culture

(130). Overall these findings illustrate that Sel1L plays a role in maintaining the secretory function of pancreatic β-cells during conditions that induce chronic ER stress.

Inducible and tissue specific Sel1L ablation

Postnatal global depletion of Sel1L was performed using a tamoxifen inducible Cre. Following global Sel1L induced deletion, mice died within two to three weeks. Death was attributed in large part to a severe defect in the exocrine pancreas (126). Pancreatic amylase and lipase mRNA and enzymatic activities were significantly reduced, resulting in impaired food digestion and absorption. Increase in apoptotic signals in parallel with reduced proliferative signals were observed in the exocrine pancreas. ER morphology was abnormal and markers of ER stress, including spliced XBP1, were elevated (126).

In addition, Sel1L was ablated specifically in adipose tissue. These mice were protected from body weight gain during high fat diet feeding (136). This protection was associated with elevated serum TAG levels and increased liver fat accumulation, suggesting a defect in plasma lipid clearance. Inadequate LPL enzyme secretion was demonstrated as a primary mechanism explaining this phenotype. Sel1L deletion inhibited the formation of an ER membrane embedded complex that is critical for secretion of mature LPL (136). Interestingly, this complex operates independently of HRD1 and ERAD, suggesting the possibility that Sel1L has other unidentified functions.

Summary

In conclusion, the mammary gland is an extraordinarily efficient organ in terms of synthesis and secretion of both proteins and lipids. Yet little is known about systems maintaining ER biogenesis and homeostasis in the mammary gland. Accordingly, the overall objective of this research was to investigate the roles of XBP1 and Sel1L in the mammary gland during the metabolically demanding period of lactation. We specifically ablated XBP1 and Sel1L signaling in the mammary gland by utilizing the floxed XBP1 and floxed Sel1L mice, respectively. We hypothesized that XBP1 deletion in the MEC would affect lipid and protein synthesis and result in impaired lactation due to severely reduced milk protein and fat content. Furthermore, we hypothesized that Sel1L deletion in the MEC would affect protein synthesis and sensitize MEC to apoptosis, thus resulting in severely reduced milk protein content and accelerated involution.

References

1. Kornides, M., and Kitsantas, P. (2013) Evaluation of breastfeeding promotion, support, and knowledge of benefits on breastfeeding outcomes. *J. Child Health Care* **17**, 264–73

2. Bhutta, Z. A., Chopra, M., Axelson, H., Berman, P., Boerma, T., Bryce, J., Bustreo, F., Cavagnero, E., Cometto, G., Daelmans, B., de Francisco, A., Fogstad, H., Gupta, N., Laski, L., Lawn, J., Maliqi, B., Mason, E., Pitt, C., Requejo, J., Starrs, A., Victora, C. G., and Wardlaw, T. (2010) Countdown to 2015 decade report (2000-10): taking stock of maternal, newborn, and child survival. *Lancet* **375**, 2032–44

3. Pérez-Escamilla, R., Curry, L., Minhas, D., Taylor, L., and Bradley, E. (2012) Scaling up of breastfeeding promotion programs in low- and middle-income countries: the “breastfeeding gear” model. *Adv. Nutr.* **3**, 790–800

4. Imdad, A., Yakoob, M. Y., and Bhutta, Z. A. (2011) Effect of breastfeeding promotion interventions on breastfeeding rates, with special focus on developing countries. *BMC Public Health* **11**, S24

5. Schwertfeger, K. L., McManaman, J. L., Palmer, C. A., Neville, M. C., and Anderson, S. M. (2003) Expression of constitutively activated Akt in the mammary gland leads to excess lipid synthesis during pregnancy and lactation. *J. Lipid Res.* **44**, 1100–12

6. Jenness, R. (1979) The Composition of Human Milk. *Semin. Perinatol.* **3**, 225–239

7. Capuco, A. V, and Akers, R. M. (2009) The origin and evolution of lactation. *J. Biol.* **8**, 37

8. Haug, A., Høstmark, A. T., and Harstad, O. M. (2007) Bovine milk in human nutrition--a review. *Lipids Health Dis.* **6**, 1–16

9. Bell, A. W. (1995) Regulation of organic nutrient metabolism during transition from late pregnancy to early lactation. *J. Anim. Sci.* **73**, 2804–2819

10. Anderson, S. M., Rudolph, M. C., McManaman, J. L., and Neville, M. C. (2007) Secretory activation in the mammary gland: it's not just about milk protein synthesis! *Breast Cancer Res.* **9**, 204

11. Fu, S., Watkins, S. M., and Hotamisligil, G. S. (2012) The role of endoplasmic reticulum in hepatic lipid homeostasis and stress signaling. *Cell Metab.* **15**, 623–34

12. Hennighausen, L., and Robinson, G. W. (2005) Information networks in the mammary gland. *Nat. Rev. Mol. Cell Biol.* **6**, 715–25

13. McManaman, J. L., Reyland, M. E., and Thrower, E. C. (2006) Secretion and Fluid Transport Mechanisms in the Mammary Gland: Comparisons with the Exocrine Pancreas and the Salivary Gland. *J. Mammary Gland Biol. Neoplasia* **11**, 249–268

14. Richert, M. M., Schwertfeger, K. L., Ryder, J. W., and Anderson, S. M. (2000) An atlas of mouse mammary gland development. *J. Mammary Gland Biol. Neoplasia* **5**, 227–41

15. Russell, T. D., Palmer, C. A., Orlicky, D. J., Fischer, A., Rudolph, M. C., Neville, M. C., and McManaman, J. L. (2007) Cytoplasmic lipid droplet accumulation in developing mammary epithelial cells: roles of adipophilin and lipid metabolism. *J. Lipid Res.* **48**, 1463–75

16. Brisken, C., and O'Malley, B. (2010) Hormone action in the mammary gland. *Cold Spring Harb. Perspect. Biol.* **2**, a003178

17. Watson, C. J., and Khaled, W. T. (2008) Mammary development in the embryo and adult: a journey of morphogenesis and commitment. *Development* **135**, 995–1003

18. Horseman, N. D., and Gregerson, K. a (2014) Prolactin actions. *J. Mol. Endocrinol.* **52**, R95–106

19. McManaman, J. L., Palmer, C. A., Wright, R. M., and Neville, M. C. (2002) Functional regulation of xanthine oxidoreductase expression and localization in the mouse mammary gland: evidence of a role in lipid secretion. *J. Physiol.* **545**, 567–579

20. Pauloin, A., and Chanat, E. (2012) Prolactin and epidermal growth factor stimulate adipophilin synthesis in HC11 mouse mammary epithelial cells via the PI3-kinase/Akt/mTOR pathway. *Biochim. Biophys. Acta* **1823**, 987–96

21. Nguyen, D. A., Parlow, A. F., and Neville, M. C. (2001) Hormonal regulation of tight junction closure in the mouse mammary epithelium during the transition from pregnancy to lactation. *J. Endocrinol.* **170**, 347–56

22. Neville, M. C., and Morton, J. (2001) Lactogenesis: The Transition from Pregnancy to Lactation. *Pediatr. Clin. North Am.* **48**, 35–52

23. Rudolph, M. C., Russell, T. D., Webb, P., Neville, M. C., and Anderson, S. M. (2011) Prolactin-mediated regulation of lipid biosynthesis genes in vivo in the lactating mammary epithelial cell. *AM J Physiol Endocrinol Metab.* **300**, 1059–1068

24. Svennersten-Sjaunja, K., and Olsson, K. (2005) Endocrinology of milk production. *Domest. Anim. Endocrinol.* **29**, 241–58

25. Neville, M. C., and Picciano, M. F. (1997) Regulation of Milk Lipid Secretion and Composition. *Annu. Rev. Nutr.* **17**, 159–184

26. McNeilly, A. S. (1980) Prolactin and the control of gonadotrophin secretion in the female. *J. Reprod. Fertil.* **58**, 537–49

27. De la Cruz, L., Steffgen, K., Martin, A., McGee, C., and Hathaway, H. (2004) Apoptosis and involution in the mammary gland are altered in mice lacking a novel receptor, beta1,4-Galactosyltransferase I. *Dev. Biol.* **272**, 286–309

28. Wagner, K.-U., and Schmidt, J. W. (2011) The two faces of Janus kinases and their respective STATs in mammary gland development and cancer. *J. Carcinog.* **10**, 50–59

29. Ning, Y., Hoang, B., Schuller, A. G. P., Cominski, T. P., Hsu, M.-S., Wood, T. L., and Pintar, J. E. (2007) Delayed mammary gland involution in mice with mutation of the insulin-like growth factor binding protein 5 gene. *Endocrinology* **148**, 2138–47

30. Chapman, R. S., Lourenco, P. C., Tonner, E., Flint, D. J., Selbert, S., Takeda, K., Akira, S., Clarke, A. R., and Watson, C. J. (1999) Suppression of epithelial apoptosis and delayed mammary gland involution in mice with a conditional knockout of Stat3. **6**, 2604–2616

31. Wang, W., Lv, N., Zhang, S., Shui, G., Qian, H., Zhang, J., Chen, Y., Ye, J., Xie, Y., Shen, Y., Wenk, M. R., and Li, P. (2012) Cidea is an essential

transcriptional coactivator regulating mammary gland secretion of milk lipids. *Nat. Med.* **18**, 235–244

32. Bobrovnikova-Marjon, E., Hatzivassiliou, G., Grigoriadou, C., Romero, M., Cavener, D. R., Thompson, C. B., and Diehl, J. A. (2008) PERK-dependent regulation of lipogenesis during mouse mammary gland development and adipocyte differentiation. *Proc. Natl. Acad. Sci. U. S. A.* **105**, 16314–9

33. Rudolph, M. C., Monks, J., Burns, V., Phistry, M., Marians, R., Foote, M. R., Bauman, D. E., Anderson, S. M., and Neville, M. C. (2010) Sterol regulatory element binding protein and dietary lipid regulation of fatty acid synthesis in the mammary epithelium. *Am. J. Physiol. Endocrinol. Metab.* **299**, E918–27

34. Wan, Y., Saghatelian, A., Chong, L.-W., Zhang, C.-L., Cravatt, B. F., and Evans, R. M. (2007) Maternal PPAR gamma protects nursing neonates by suppressing the production of inflammatory milk. *Genes Dev.* **21**, 1895–908

35. Neville, M. C., Webb, P., Ramanathan, P., Mannino, M. P., Pecorini, C., Monks, J., Anderson, S. M., and MacLean, P. (2013) The insulin receptor plays an important role in secretory differentiation in the mammary gland. *Am. J. Physiol. Endocrinol. Metab.* **305**, E1103–14

36. Mather, I. H., and Keenan, T. W. (1998) Origin and secretion of milk lipids. *J. Mammary Gland Biol. Neoplasia* **3**, 259–73

37. Griffiths, B., Lewis, C. a, Bensaad, K., Ros, S., Zhang, Q., Ferber, E. C., Konisti, S., Peck, B., Miess, H., East, P., Wakelam, M., Harris, A. L., and Schulze, A. (2013) Sterol regulatory element binding protein-dependent regulation of lipid synthesis supports cell survival and tumor growth. *Cancer Metab.* **1**, 3

38. Neville, M. C. (1990) The physiological basis of milk secretion. *Ann. N. Y. Acad. Sci.* **586**, 1–11

39. Smith, B. S., Gagn, H. T., Pitelka, D. R., and Abraham, S. (1969) The Effect of Dietary Fat on Lipogenesis in Mammary Gland and Liver from Lactating and Virgin Mice. *Biochem* **115**, 807–815

40. Rudolph, M. C., Neville, M. C., and Anderson, S. M. (2007) Lipid synthesis in lactation: diet and the fatty acid switch. *J. Mammary Gland Biol. Neoplasia* **12**, 269–81

41. Wang, Y., Tong, J., Li, S., Zhang, R., Chen, L., Wang, Y., Zheng, M., Wang, M., Liu, G., Dai, Y., Zhao, Y., and Li, N. (2011) Over-expression of human lipoprotein lipase in mouse mammary glands leads to reduction of milk triglyceride and delayed growth of suckling pups. *PLoS One* **6**, e20895

42. Reue, K., and Brindley, D. N. (2008) Thematic Review Series: Glycerolipids. Multiple roles for lipins/phosphatidate phosphatase enzymes in lipid metabolism. *J. Lipid Res.* **49**, 2493–503

43. Fagone, P., and Jackowski, S. (2009) Membrane phospholipid synthesis and endoplasmic reticulum function. *J. Lipid Res.* **50 Suppl**, S311–6

44. Olofsson, S.-O., Boström, P., Andersson, L., Rutberg, M., Perman, J., and Borén, J. (2009) Lipid droplets as dynamic organelles connecting storage and efflux of lipids. *Biochim. Biophys. Acta* **1791**, 448–58

45. Cases, S., Zhou, P., Shillingford, J. M., Wiseman, B. S., Dee, J., Angle, C. S., Hennighausen, L., Werb, Z., and Farese, R. V (2004) Development of the mammary gland requires DGAT1 expression in stromal and epithelial tissues. *Development* **131**, 3047–3055

46. McManaman, J. L. (2014) Lipid transport in the lactating mammary gland. *J. Mammary Gland Biol. Neoplasia* **19**, 35–42

47. Wu, C. C., Howell, K. E., Neville, M. C., Yates, J. R., and McManaman, J. L. (2000) Proteomics reveal a link between the endoplasmic reticulum and lipid secretory mechanisms in mammary epithelial cells. *Electrophoresis* **21**, 3470–82

48. Spertino, S., Cipriani, V., De Angelis, C., Giuffrida, M. G., Marsano, F., and Cavaletto, M. (2011) Proteome profile and biological activity of caprine, bovine and human milk fat globules. *Mol. Biosyst.*

49. Robenek, H., Hofnagel, O., Buers, I., Lorkowski, S., Schnoor, M., Robenek, M. J., Heid, H., Troyer, D., and Severs, N. J. (2006) Butyrophilin controls milk fat globule secretion. *Proc. Natl. Acad. Sci. U. S. A.* **103**, 10385–90

50. Chong, B. M., Reigan, P., Mayle-Combs, K. D., Orlicky, D. J., and McManaman, J. L. (2011) Determinants of adipophilin function in milk lipid formation and secretion. *Trends Endocrinol. Metab.* **22**, 211–7

51. Ogg, S. L., Weldon, A. K., Dobbie, L., Smith, A. J. H., and Mather, I. H. (2004) Expression of butyrophilin (Btn1a1) in lactating mammary gland is essential for the regulated secretion of milk-lipid droplets. *Proc. Natl. Acad. Sci. U. S. A.* **101**, 10084–9

52. Russell, T. T., Schaack, J., Orlicky, D. J., Palmer, C., Chang, B. H.-J., Chan, L., and McManaman, J. L. (2011) Adipophilin regulates maturation of cytoplasmic lipid droplets and alveolae in differentiating mammary glands. *J. Cell Sci.* **124**, 3247–3253

53. Boumahrou, N., Andrei, S., Miranda, G., Henry, C., Panthier, J. J., Martin, P., and Bellier, S. (2009) The major protein fraction of mouse milk revisited using proven proteomic tools. *J. Physiol. Pharmacol.* **60**, 113–1118

54. Rhoads, R. E., and Grudzien-Nogalska, E. (2007) Translational regulation of milk protein synthesis at secretory activation. *J. Mammary Gland Biol. Neoplasia* **12**, 283–92

55. Chodosh, L. A., Gardner, H. P., Rajan, J. V, Stairs, D. B., Marquis, S. T., and Leder, P. A. (2000) Protein kinase expression during murine mammary development. *Dev. Biol.* **219**, 259–76

56. Boxer, R. B., Stairs, D. B., Dugan, K. D., Notarfrancesco, K. L., Portocarrero, C. P., Keister, B. a, Belka, G. K., Cho, H., Rathmell, J. C., Thompson, C. B., Birnbaum, M. J., and Chodosh, L. a (2006) Isoform-specific requirement for Akt1 in the developmental regulation of cellular metabolism during lactation. *Cell Metab.* **4**, 475–90

57. Chen, C.-C., Stairs, D. B., Boxer, R. B., Belka, G. K., Horseman, N. D., Alvarez, J. V, and Chodosh, L. a (2012) Autocrine prolactin induced by the Pten-Akt pathway is required for lactation initiation and provides a direct link between the Akt and Stat5 pathways. *Genes Dev.* **26**, 2154–68

58. Vijay, I. K. (1998) Developmental and hormonal regulation of protein N-glycosylation in the mammary gland. *J. Mammary Gland Biol. Neoplasia* **3**, 325–36

59. Ginger, M. R., and Grigor, M. R. (1999) Comparative aspects of milk caseins. *Comp. Biochem. Physiol. B. Biochem. Mol. Biol.* **124**, 133–45

60. Stacey, A., Schnieke, A., Kerr, M., Scott, A., McKee, C., Cottingham, I., Binas, B., Wilde, C., and Colman, A. (1995) Lactation is disrupted by

alpha-lactalbumin deficiency and can be restored by human alpha-lactalbumin gene replacement in mice. *Proc. Natl. Acad. Sci. U. S. A.* **92**, 2835–9

61. Prestoz, L. L., Daude, N., Cournu, I., Shin, Y. S., and Petry, K. G. (1998) Differential UDP-galactose-4'-epimerase (GALE) enzymatic activity and mRNA expression in the rat mammary gland during lactation. *FEBS Lett.* **431**, 391–4

62. Lagace, T. A., and Ridgway, N. D. (2013) The role of phospholipids in the biological activity and structure of the endoplasmic reticulum. *Biochim. Biophys. Acta* **1833**, 2499–510

63. Andrews, T., and Tata, J. R. (1971) Protein Synthesis by Membrane-Bound and Free Ribosomes of Secretory and Non-Secretory Tissues. *Biochem. J.* **121**, 683–694

64. Brodsky, J. L. (2012) Cleaning Up: ER-Associated Degradation to the Rescue. *Cell* **151**, 1163–1167

65. O'Riordan, N., Kane, M., Joshi, L., and Hickey, R. M. (2014) Structural and functional characteristics of bovine milk protein glycosylation. *Glycobiology* **24**, 220–36

66. Liu, B., and Newburg, D. S. (2013) Human milk glycoproteins protect infants against human pathogens. *Breastfeed. Med.* **8**, 354–62

67. Hebert, D. N., and Molinari, M. (2012) Flagging and docking: dual roles for N-glycans in protein quality control and cellular proteostasis. *Trends Biochem. Sci.* **37**, 404–10

68. Smith, M. H., Ploegh, H. L., and Weissman, J. S. (2011) Road to ruin: targeting proteins for degradation in the endoplasmic reticulum. *Science* **334**, 1086–90

69. Sriburi, R., Bommiasamy, H., Buldak, G. L., Robbins, G. R., Frank, M., Jackowski, S., and Brewer, J. W. (2007) Coordinate regulation of phospholipid biosynthesis and secretory pathway gene expression in XBP-1(S)-induced endoplasmic reticulum biogenesis. *J. Biol. Chem.* **282**, 7024–34

70. Sriburi, R., Jackowski, S., Mori, K., and Brewer, J. W. (2004) XBP1: a link between the unfolded protein response, lipid biosynthesis, and biogenesis of the endoplasmic reticulum. *J. Cell Biol.* **167**, 35–41

71. Moore, K., and Hollien, J. (2012) The unfolded protein response in secretory cell function. *Annu. Rev. Genet.* **46**, 165–83

72. Chan, Y.-H. M., and Marshall, W. F. (2012) How cells know the size of their organelles. *Science* **337**, 1186–9

73. Testerink, N., van der Sanden, M. H. M., Houweling, M., Helms, J. B., and Vaandrager, A. B. (2009) Depletion of phosphatidylcholine affects endoplasmic reticulum morphology and protein traffic at the Golgi complex. *J. Lipid Res.* **50**, 2182–92

74. Lykidis, A., and Jackowski, S. (2001) Regulation of Mammalian Cell Membrane Biosynthesis. *Prog. Nucleic Acid Res. Mol. Biol.* **65**, 361–393

75. Olofsson, S.-O., Boström, P., Andersson, L., Rutberg, M., Levin, M., Perman, J., and Borén, J. (2008) Triglyceride containing lipid droplets and lipid droplet-associated proteins. *Curr. Opin. Lipidol.* **19**, 441–7

76. Cao, S. S., and Kaufman, R. J. (2012) Unfolded protein response. *Curr. Biol.* **22**, R622–R626

77. Travers, K. J., Patil, C. K., Wodicka, L., Lockhart, D. J., Weissman, J. S., and Walter, P. (2000) Functional and genomic analyses reveal an essential coordination between the unfolded protein response and ER-associated degradation. *Cell* **101**, 249–58

78. Ron, D., and Walter, P. (2007) Signal integration in the endoplasmic reticulum unfolded protein response. *Nat. Rev. Mol. Cell Biol.* **8**, 519–29

79. Walter, P., and Ron, D. (2011) The unfolded protein response: from stress pathway to homeostatic regulation. *Science* **334**, 1081–6

80. Ryno, L. M., Wiseman, R. L., and Kelly, J. W. (2013) Targeting unfolded protein response signaling pathways to ameliorate protein misfolding diseases. *Curr. Opin. Chem. Biol.* **17**, 1–7

81. Vattem, K. M., and Wek, R. C. (2004) Reinitiation involving upstream ORFs regulates ATF4 mRNA translation in mammalian cells. *Proc. Natl. Acad. Sci. U. S. A.* **101**, 11269–74

82. Lee, A.-H., and Glimcher, L. H. (2009) Intersection of the unfolded protein response and hepatic lipid metabolism. *Cell. Mol. Life Sci.* **66**, 2835–50

83. Wu, J., Rutkowski, D. T., Dubois, M., Swathirajan, J., Saunders, T., Wang, J., Song, B., Yau, G. D.-Y., and Kaufman, R. J. (2007) ATF6alpha optimizes long-term endoplasmic reticulum function to protect cells from chronic stress. *Dev. Cell* **13**, 351–64

84. Yamamoto, K., Sato, T., Matsui, T., Sato, M., Okada, T., Yoshida, H., Harada, A., and Mori, K. (2007) Transcriptional induction of mammalian ER quality control proteins is mediated by single or combined action of ATF6alpha and XBP1. *Dev. Cell* **13**, 365–76

85. Bommiasamy, H., Back, S. H., Fagone, P., Lee, K., Meshinchi, S., Vink, E., Sriburi, R., Frank, M., Jackowski, S., Kaufman, R. J., and Brewer, J. W. (2009) ATF6alpha induces XBP1-independent expansion of the endoplasmic reticulum. *J. Cell Sci.* **122**, 1626–36

86. Korennykh, A. V, Egea, P. F., Korostelev, A. A., Finer-Moore, J., Zhang, C., Shokat, K. M., Stroud, R. M., and Walter, P. (2009) The unfolded protein response signals through high-order assembly of Ire1. *Nature* **457**, 687–93

87. Li, H., Korennykh, A. V, Behrman, S. L., and Walter, P. (2010) Mammalian endoplasmic reticulum stress sensor IRE1 signals by dynamic clustering. *Proc. Natl. Acad. Sci. U. S. A.* **107**, 16113–8

88. Pincus, D., Chevalier, M. W., Aragón, T., van Anken, E., Vidal, S. E., El-Samad, H., and Walter, P. (2010) BiP binding to the ER-stress sensor Ire1 tunes the homeostatic behavior of the unfolded protein response. *PLoS Biol.* **8**, 1–14

89. Liu, C. Y., Schröder, M., and Kaufman, R. J. (2000) Ligand-independent dimerization activates the stress response kinases IRE1 and PERK in the lumen of the endoplasmic reticulum. *J. Biol. Chem.* **275**, 24881–5

90. Kimata, Y., Oikawa, D., Shimizu, Y., Ishiwata-Kimata, Y., and Kohno, K. (2004) A role for BiP as an adjustor for the endoplasmic reticulum stress-sensing protein Ire1. *J. Cell Biol.* **167**, 445–56

91. Gardner, B. M., and Walter, P. (2011) Unfolded proteins are Ire1-activating ligands that directly induce the unfolded protein response. *Science* **333**, 1891–4

92. Kimata, Y., Ishiwata-Kimata, Y., Ito, T., Hirata, A., Suzuki, T., Oikawa, D., Takeuchi, M., and Kohno, K. (2007) Two regulatory steps of ER-

stress sensor Ire1 involving its cluster formation and interaction with unfolded proteins. *J. Cell Biol.* **179**, 75–86

93. Lee, K., Tirasophon, W., Shen, X., Michalak, M., Prywes, R., Okada, T., Yoshida, H., Mori, K., and Kaufman, R. J. (2002) IRE1-mediated unconventional mRNA splicing and S2P-mediated ATF6 cleavage merge to regulate XBP1 in signaling the unfolded protein response. *Genes Dev.* **16**, 452–66

94. Nekrutenko, A., and He, J. (2006) Functionality of unspliced XBP1 is required to explain evolution of overlapping reading frames. *Trends Genet.* **22**, 645–8

95. Calfon, M., Zeng, H., Urano, F., Till, J. H., Hubbard, S. R., Harding, H. P., Clark, S. G., and Ron, D. (2002) IRE1 couples endoplasmic reticulum load to secretory capacity by processing the XBP-1 mRNA. *Nature* **415**, 92–6

96. Nikawa, J., Akiyoshi, M., Hirata, S., and Fukuda, T. (1996) Saccharomyces cerevisiae IRE2 / HAC1 is involved in IRE1-mediated KAR2 expression. *Nucleic Acids Res.* **24**, 4222–4226

97. Mori, K., Kawahara, T., Yoshida, H., Yanagi, H., and Yura, T. (1996) Signalling from endoplasmic reticulum to nucleus: transcription factor with a basic-leucine zipper motif is required for the unfolded protein-response pathway. *Genes to Cells* **1**, 803–817

98. Cox, J. S., and Walter, P. (1996) A Novel Mechanism for Regulating Activity of a Transcription Factor That Controls the Unfolded Protein Response. *Cell* **87**, 391–404

99. Lee, A.-H., Iwakoshi, N. N., and Glimcher, L. H. (2003) XBP-1 Regulates a Subset of Endoplasmic Reticulum Resident Chaperone Genes in the Unfolded Protein Response. *Mol. Cell. Biol.* **23**, 7448–7459

100. Clauss, I. M., Chu, M., Zhao, J., and Glimcher, L. H. (1996) The basic domain / leucine zipper protein hXBP-1 preferentially binds to and transactivates CRE-like sequences containing an ACGT core. *Nucleic Acids Res.* **24**, 1855–1864

101. Yamamoto, K., Yoshida, H., Kokame, K., Kaufman, R. J., and Mori, K. (2004) Differential contributions of ATF6 and XBP1 to the activation of endoplasmic reticulum stress-responsive cis-acting elements ERSE, UPRE and ERSE-II. *J. Biochem.* **136**, 343–50

102. Acosta-Alvear, D., Zhou, Y., Blais, A., Tsikitis, M., Lents, N. H., Arias, C., Lennon, C. J., Kluger, Y., and Dynlacht, B. D. (2007) XBP1 controls diverse cell type- and condition-specific transcriptional regulatory networks. *Mol. Cell* **27**, 53–66

103. Han, D., Lerner, A. G., Vande Walle, L., Upton, J.-P., Xu, W., Hagen, A., Backes, B. J., Oakes, S. A., and Papa, F. R. (2009) IRE1alpha kinase activation modes control alternate endoribonuclease outputs to determine divergent cell fates. *Cell* **138**, 562–75

104. Lee, A.-H., Heidtman, K., Hotamisligil, G. S., and Glimcher, L. H. (2011) Dual and opposing roles of the unfolded protein response regulated by IRE1alpha and XBP1 in proinsulin processing and insulin secretion. *Proc. Natl. Acad. Sci. U. S. A.* **108**, 8885–90

105. So, J.-S., Hur, K. Y., Tarrio, M., Ruda, V., Frank-Kamenetsky, M., Fitzgerald, K., Koteliansky, V., Lichtman, A. H., Iwawaki, T., Glimcher, L. H., and Lee, A.-H. (2012) Silencing of Lipid Metabolism Genes through IRE1α-Mediated mRNA Decay Lowers Plasma Lipids in Mice. *Cell Metab.* **16**, 487–499

106. Urano, F., Wang, X., Bertolotti, A., Zhang, Y., Chung, P., Harding, H. P., and Ron, D. (2000) Coupling of Stress in the ER to Activation of JNK Protein Kinases by Transmembrane Protein Kinase IRE1. *Science (80-.).* **287**, 664–666

107. Kaser, A., Lee, A.-H., Franke, A., Glickman, J. N., Zeissig, S., Tilg, H., Nieuwenhuis, E. E. S., Higgins, D. E., Schreiber, S., Glimcher, L. H., and Blumberg, R. S. (2008) XBP1 links ER stress to intestinal inflammation and confers genetic risk for human inflammatory bowel disease. *Cell* **134**, 743–56

108. Özcan, U., Cao, Q., Yilmaz, E., Lee, A.-H., Iwakoshi, N. N., Ozdelen, E., Tuncman, G., Gorgun, C., Glimcher, L. H., and Hotamisligil, G. S. (2004) Endoplasmic Reticulum Stress Links Obesity , Insulin Action , and Type 2 Diabetes. *Science (80-.).* **306**, 457–461

109. Shen, X., Ellis, R. E., Lee, K., Liu, C., Yang, K., Solomon, A., Yoshida, H., Morimoto, R., Kurnit, D. M., Mori, K., Kaufman, R. J., and Arbor, A. (2001) Complementary Signaling Pathways Regulate the Unfolded Protein Response and Are Required for C . elegans Development. *Cell* **107**, 893–903

110. Reimold, A. M., Etkin, A., Clauss, I., Perkins, A., Friend, D. S., Zhang, J., Horton, H. F., Scott, A., Orkin, S. H., Byrne, M. C., Grusby, M. J., and Glimcher, L. H. (2000) An essential role in liver development for transcription factor XBP-1. *Genes Dev.* **14**, 152–157

111. Iwakoshi, N. N., Lee, A.-H., Vallabhajosyula, P., Otipoby, K. L., Rajewsky, K., and Glimcher, L. H. (2003) Plasma cell differentiation and the unfolded protein response intersect at the transcription factor XBP-1. *Nat. Immunol.* **4**, 321–9

112. Reimold, A. M., Iwakoshi, N. N., Manis, J., Vallabhajosyula, P., Szomolanyi-tsuda, E., Gravallese, E. M., Friend, D., Grusby, M. J., Alt, F., and Glimcher, L. H. (2001) Plasma cell differentiation requires the transcription factor XBP-1. *Nature* **412**, 300–307

113. Shaffer, A. L., Shapiro-Shelef, M., Iwakoshi, N. N., Lee, A.-H., Qian, S.-B., Zhao, H., Yu, X., Yang, L., Tan, B. K., Rosenwald, A., Hurt, E. M., Petroulakis, E., Sonenberg, N., Yewdell, J. W., Calame, K., Glimcher, L. H., and Staudt, L. M. (2004) XBP1, downstream of Blimp-1, expands the secretory apparatus and other organelles, and increases protein synthesis in plasma cell differentiation. *Immunity* **21**, 81–93

114. Hu, C.-C. A., Dougan, S. K., McGehee, A. M., Love, J. C., and Ploegh, H. L. (2009) XBP-1 regulates signal transduction, transcription factors and bone marrow colonization in B cells. *EMBO J.* **28**, 1624–36

115. Todd, D. J., McHeyzer-Williams, L. J., Kowal, C., Lee, A.-H., Volpe, B. T., Diamond, B., McHeyzer-Williams, M. G., and Glimcher, L. H. (2009) XBP1 governs late events in plasma cell differentiation and is not required for antigen-specific memory B cell development. *J. Exp. Med.* **206**, 2151–9

116. Kurata, M., Yamazaki, Y., Kanno, Y., Ishibashi, S., Takahara, T., Kitagawa, M., and Nakamura, T. (2011) Anti-apoptotic function of Xbp1 as an IL-3 signaling molecule in hematopoietic cells. *Cell Death Dis.* **2**, e118

117. Lee, A.-H., Chu, G. C., Iwakoshi, N. N., and Glimcher, L. H. (2005) XBP-1 is required for biogenesis of cellular secretory machinery of exocrine glands. *EMBO J.* **24**, 4368–80

118. Hess, D. A., Humphrey, S. E., Ishibashi, J., Damsz, B., Lee, A.-H., Glimcher, L. H., and Konieczny, S. F. (2011) Extensive pancreas

regeneration following acinar-specific disruption of Xbp1 in mice. *Gastroenterology* **141**, 1463–72

119. Lee, A.-H., Scapa, E. F., Cohen, D. E., and Glimcher, L. H. (2008) Regulation of hepatic lipogenesis by the transcription factor XBP1. *Science* **320**, 1492–6

120. Ning, J., Hong, T., Ward, A., Pi, J., Liu, Z., Liu, H.-Y., and Cao, W. (2011) Constitutive role for IRE1α-XBP1 signaling pathway in the insulin-mediated hepatic lipogenic program. *Endocrinology* **152**, 2247–55

121. Wang, S., Chen, Z., Lam, V., Han, J., Hassler, J., Finck, B. N., Davidson, N. O., and Kaufman, R. J. (2012) IRE1α-XBP1s Induces PDI Expression to Increase MTP Activity for Hepatic VLDL Assembly and Lipid Homeostasis. *Cell Metab.* **16**, 473–86

122. Valdés, P., Mercado, G., Vidal, R. L., Molina, C., Parsons, G., Court, F. A., Martinez, A., Galleguillos, D., Armentano, D., Schneider, B. L., and Hetz, C. (2014) Control of dopaminergic neuron survival by the unfolded protein response transcription factor XBP1. *Proc. Natl. Acad. Sci. U. S. A.*, 1–6

123. Hetz, C., Lee, A.-H., Gonzalez-Romero, D., Thielen, P., Castilla, J., Soto, C., and Glimcher, L. H. (2008) Unfolded protein response transcription factor XBP-1 does not influence prion replication or pathogenesis. *Proc. Natl. Acad. Sci. U. S. A.* **105**, 757–62

124. Guerriero, C. J., and Brodsky, J. L. (2012) The delicate balance between secreted protein folding and endoplasmic reticulum-associated degradation in human physiology. *Physiol. Rev.* **92**, 537–76

125. Olzmann, J. A., Kopito, R. R., and Christianson, J. C. (2013) The Mammalian Endoplasmic Reticulum-Associated Degradation System. *Cold Spring Harb. Perspect. Biol.* **5**, 1–17

126. Sun, S., Shi, G., Han, X., Francisco, A. B., Ji, Y., Mendonça, N., Liu, X., Locasale, J. W., Simpson, K. W., Duhamel, G. E., Kersten, S., Iii, J. R. Y., Long, Q., and Qi, L. (2014) Sel1L is indispensable for mammalian endoplasmic reticulum-associated degradation, endoplasmic reticulum homeostasis, and survival. *Proc. Natl. Acad. Sci. U. S. A.* **111**, 6115

127. Carvalho, P., Goder, V., and Rapoport, T. A. (2006) Distinct ubiquitin-ligase complexes define convergent pathways for the degradation of ER proteins. *Cell* **126**, 361–73

128. Horimoto, S., Ninagawa, S., Okada, T., Koba, H., Sugimoto, T., Kamiya, Y., Kato, K., Takeda, S., and Mori, K. (2013) The unfolded protein response transducer ATF6 represents a novel transmembrane-type endoplasmic reticulum-associated degradation substrate requiring both mannose trimming and SEL1L. *J. Biol. Chem.*, 0–20

129. Bernasconi, R., Galli, C., Calanca, V., Nakajima, T., and Molinari, M. (2010) Stringent requirement for HRD1, SEL1L, and OS-9/XTP3-B for disposal of ERAD-LS substrates. *J. Cell Biol.* **188**, 223–35

130. Francisco, A. B., Singh, R., Sha, H., Yan, X., Qi, L., Lei, X., and Long, Q. (2011) Haploid insufficiency of suppressor enhancer Lin12 1-like (SEL1L) protein predisposes mice to high fat diet-induced hyperglycemia. *J. Biol. Chem.* **286**, 22275–82

131. Mueller, B., Lilley, B. N., and Ploegh, H. L. (2006) SEL1L, the homologue of yeast Hrd3p, is involved in protein dislocation from the mammalian ER. *J. Cell Biol.* **175**, 261–70

132. Gardner, R. G., Swarbrick, G. M., Bays, N. W., Cronin, S. R., Wilhovsky, S., Seelig, L., Kim, C., and Hampton, R. Y. (2000) Endoplasmic reticulum degradation requires lumen to cytosol signaling: Transmembrane control of Hrd1p by Hrd3p. *J. Cell Biol.* **151**, 69–82

133. Iida, Y., Fujimori, T., Okawa, K., Nagata, K., Wada, I., and Hosokawa, N. (2011) SEL1L protein critically determines the stability of the HRD1-SEL1L endoplasmic reticulum-associated degradation (ERAD) complex to optimize the degradation kinetics of ERAD substrates. *J. Biol. Chem.* **286**, 16929–39

134. Francisco, A. B., Singh, R., Li, S., Vani, A. K., Yang, L., Munroe, R. J., Diaferia, G., Cardano, M., Biunno, I., Qi, L., Schimenti, J. C., and Long, Q. (2010) Deficiency of suppressor enhancer Lin12 1 like (SEL1L) in mice leads to systemic endoplasmic reticulum stress and embryonic lethality. *J. Biol. Chem.* **285**, 13694–703

135. Li, S., Francisco, A. B., Munroe, R. J., Schimenti, J. C., and Long, Q. (2010) SEL1L deficiency impairs growth and differentiation of pancreatic epithelial cells. *BMC Dev. Biol.* **10**, 1–13

136. Sha, H., Sun, S., Francisco, A. B., Ehrhardt, N., Xue, Z., Liu, L., Lawrence, P., Mattijssen, F., Guber, R. D., Panhwar, M. S., Brenna, J. T., Shi, H., Xue, B., Kersten, S., Bensadoun, A., Péterfy, M., Long, Q., and Qi, L. (2014) The ER-associated degradation adaptor protein Sel1L regulates LPL secretion and lipid metabolism. *Cell Metab.* **20**, 458–70

CHAPTER 3

EFFECT OF XBP1 MAMMARY EPITHELIAL CELL ABLATION ON MILK COMPOSITION, MAMMARY GLAND DEVELOPMENT, AND ENDOPLASMIC RETICULUM MORPHOLOGY[1]

Lactation represents a metabolically demanding phase of mammalian life. In the mouse, milk is the only source of nourishment for the first two weeks of life. Milk synthesis occurs in alveolar structures composed of a single layer of MEC. In order to become fully functional, MEC acquire a number of cellular characteristics during late pregnancy, including the development of an elaborate ER system. Recent work suggests that the transcription factor, XBP1, could be important for differentiation and function of MEC. XBP1 has been shown to promote ER biogenesis as well as positively regulate lipogenesis. Despite emerging evidence implicating XBP1 signaling to the function of other secretory cells, the role of XBP1 in the secretory function of MEC has not been addressed directly. To this end, we specifically ablated XBP1 in MEC during late pregnancy and lactation. The absence of XBP1 in the MEC caused an 80% pup growth deficit. Surprisingly, the modest 20-30% milk composition change was insufficient to account for the severe lactation

[1] Davis, K. R., Giesy, S. L., Krumm, C., Long, Q., Harvatine, K. J., and Boisclair, Y. R. (2015) XBP1 is required for expansion of the mammary epithelial compartment in early lactation. *In preparation.*

impairment. Whole mount and histology analysis of mammary glands demonstrated that inadequate expansion of the MEC compartment is the primary reason for the inadequate lactation performance. Consistent with previous findings, lack of XBP1 in MEC resulted in lower ER abundance during late pregnancy and absence of ER compartment expansion between late pregnancy and early lactation. The failure of MEC compartment to completely occupy the gland was associated with reciprocal changes in proliferative and apoptotic signals. Overall, our findings establish that XBP1 signaling is absolutely necessary for ER biogenesis and expansion in the MEC during lactation. These defects lead to a reduced MEC compartment and a severely impaired lactation.

Introduction

Lactation represents a dynamic and metabolically demanding stage in life for most mammals. Milk is a complex fluid that is synthesized and secreted by the mammary gland to provide complete nutrition for neonates. In the mouse, milk is the only source of nourishment for the first two weeks of life (1). Over the course of a single lactation, the mouse mammary gland can synthesize and secrete over 30 grams of triglycerides, 12 grams of proteins, and 5 grams of lactose (2). Milk synthesis occurs in a mammary specific structure known as the alveolus. Alveolar structures are composed of a single layer of MEC encircling a lumen where milk is secreted (3). In order to become fully functional, MEC acquire a number of cellular characteristics during late pregnancy, including the development of an elaborate ER system (4). The ER is not only required for the synthesis of secreted proteins but is also the site where fatty acids are assembled into TAG and phospholipids (5, 6).

Three lines of evidence suggest that the transcription factor, XBP1, could be important for differentiation and function of MEC (7–9). First, XBP1 promotes ER biogenesis as shown by an increased size of the ER compartment after forced overexpression of XBP1 in fibroblasts (10, 11). Furthermore, studies examining other secretory cells reported diminished ER abundance and suppressed protein secretion in the absence of XBP1 (12, 13). Second, XBP1 is vital component of a highly conserved signaling cascade

responsible for restoring ER homeostasis when the ER is confronted with various stresses, including increased protein synthesis demands. Specifically, a disruption of ER homeostasis elicits a cellular ER stress response and results in the activation of the ER transmembrane stress sensor IRE1 (7, 14). Activated IRE1 specifically cleaves a 26 base pair internal segment from XBP1 transcripts. This results in a shift in the reading frame allowing for the production of the active transcription factor, spliced XBP1 (15–17). Finally, XBP1 signaling has been implicated as a positive regulator of lipogenesis in hepatocytes, which could be relevant to the mammary gland because it differentiates to a metabolically active lipogenic gland during lactation (4, 18, 19).

Interestingly, Gregor et al recently reported that XBP1 ablation in adipose tissue caused a modest reduction in lactation performance (20). Despite emerging evidence implicating XBP1 signaling to the function of other secretory cells, the role of XBP1 in the secretory function of MEC has not been addressed directly. To this end, we specifically ablated XBP1 in MEC during late pregnancy and lactation. XBP1 ablation did not impact mammary gland development during pregnancy but severely impaired lactation. This defect was accounted by failure to maintain the ER compartment and an adequate MEC population.

Materials and Methods

Animals

All procedures were approved by Cornell Institutional Animal Care and Use Committee. $XBP1^{f/f}$ mice with loxP sites on either side of exon 2 in the XBP1 gene were obtained from Dr. Laurie Glimcher (21). $XBP1^{f/f}$ mice were maintained on a C57BL/6 background. BLG-Cre mice expressing a copy of the Cre recombinase under the control of the ovine β-lactoglobulin promoter were previously described (22, 23). BLG-Cre mice were maintained on a mixed background. Experimental animals were generated by intercrossing $XBP1^{f/f}$ females with $XBP1^{f/f}$ males carrying one copy of the BLG-Cre transgene. Offspring retained for studies were either $XBP1^{f/f}$ (designated WT) or $XBP1^{f/f}$ carrying BLG-Cre transgene (designated $\Delta XBP1^{MEC}$). Litters were weaned and genotyped at 3 weeks of age.

All animals were housed in an environment with a constant ambient temperature (22°C) and photoperiod (lights on between 0600 and 1800 hours). Throughout the experiments, mice were fed *ab libitum* of a standard rodent chow diet containing 5% fat and 19% protein (Harlan Tekland 7912, Madison, WI). All terminal procedures involved euthanasia by CO_2 asphyxiation.

Measurement of pup growth and analysis of milk components

Reciprocal mating crosses were performed at 10 weeks of age (WT females x $\Delta XBP1^{MEC}$ males; $\Delta XBP1^{MEC}$ females x WT males) (n=6-11 dams

per genotype). Parturition was considered lactation day 0 (L0) and litter sizes were standardized to 9 pups on lactation day 1 (L1). Each litter was weighed from L1 to L14. On L14, pups were removed from the dam for two hours to allow for mammary gland filling. Dams were anesthetized by IP injection with Avertin (Sigma-Aldrich, St. Louis, MO) followed immediately by administration of oxytocin (4 IU IP). Each mammary gland was milked for 10-15 minutes. The milking procedure involved massage of the gland combined with collection of milk droplet appearing at the tip of the nipple with a pipetteman. The milk yield ranged from 45 to 260 µl**.** Milk was diluted 1:1 with phosphate buffered saline (PBS) to reduce viscosity, sonicated to ensure homogeneity, and frozen until analyzed. Lactose concentration in milk was determined by the Galactose and Lactose Colormetric Assay kit (Sigma-Aldrich). Milk protein content was measured by the Bradford assay using reconstituted milk powder as a standard. To visualize individual milk proteins, diluted milk (10 µl) was separated on 13% SDS-polyacrylamide gels and stained with Coomassie Blue (24). Milk samples were analyzed for fat content and fatty acid profile as described in (25). Briefly, approximately 60 mg of diluted whole milk were weighed into glass extraction tubes followed by the addition of dual internal standards (17:0 triglycerides and 19:0 methyl esters). Milk lipids were extracted by hexane:isopropanol extraction and methylated overnight (40°C) in 1% methanolic sulfuric acid. Gas chromatography was used to quantify methyl

esters as previously described (26). Milk fat concentration was assessed based on the dilution of the internal standards.

Isolation of mammary epithelial cells

WT and ΔXBP1^{MEC} female mice were mated and evaluated daily for the presence of a copulatory plug (designated pregnancy day 0). Subsets of females were euthanized at P14, P18, L0, and L5 (n=5-8 dams each genotype and mammary gland stage). Mammary epithelial cells (MEC) were isolated according to a recently validated procedure (27). In brief, the two abdominal mammary glands were dissected and the individual lymph nodes were removed. A small portion of each gland was dissected and snap frozen in liquid nitrogen. The remaining abdominal mammary glands were transferred to a glass plate on ice and minced to a paste consistency for approximately 4 minutes. Glands were incubated in a 50 mL conical tube with 5 mL of digestion buffer (DMEM containing 1 mg/mL trypsin, 2 mg/mL collagenase A, 50 mM sodium fluoride, and 1 mM sodium orthovanadate) for 30 minutes in a shaking water bath (37°C, 200 rpm). After incubation, the digestion reaction was quenched with 1 mL of fetal bovine serum. The digested mammary gland was transferred to a 15 mL conical tube containing 14 mL of wash buffer (1xPBS, 50 mM sodium fluoride, 1 mM sodium orthovanadate, 2 mM phenylmethanesulfonyl fluoride). MEC were pelleted by centrifugation (9300g for 10 min at 4°C) and the supernatant was discarded. The pellet was

resuspended in wash buffer and the washing procedure was repeated two more times. After discarding the last supernatant, the MEC pellet was frozen at -80°C until isolation of total RNA.

Analysis of mammary development

WT and ΔXBP1^{MEC} female mice were mated and evaluated daily for the presence of a copulatory plug (pregnancy day 0). Subsets of mice were euthanized at P14, P18, L1, L5, and L14 (n=2-3 dams for each genotype and development stage). The right abdominal mammary gland was spread onto a glass plate for whole mount analysis (28). In brief, spread glands were fixed overnight in Carnoy's solution (60% ethanol, 30% chloroform, 10% acetic acid). After overnight fixation, glands were postfixed in 70% ethanol, rehydrated in decreasing concentrations of ethanol, and stained in carmine-alum. When uniformly stained, glands were dehydrated in increasing ethanol concentrations, cleared in xylene overnight, and secured with using Permount. Whole mounts were photographed using an Axiovert 40 microscope (Zeiss) and a dissecting microscope. For H&E analysis, the right thoracic mammary gland was fixed overnight in 10% buffered formalin and postfixed in 70% ethanol. Glands were embedded in paraffin and stained in hematoxylin and eosin. H&E histological sections were photographed using an Axiovert 40 microscope (Zeiss) bright light microscopy at 10X and 40X magnifications as previously described (28).

Total RNA isolation and analysis of gene expression

Isolated MEC and snap frozen tissues (mammary gland, liver, gastrocnemius muscle) collected from various subsets of animals were lyzed with Qiazol (Qiagen, Valencia, CA). Total RNA was isolated and purified using RNeasy Mini columns and on-column RNase-free DNase treatment (Qiagen). Quantity and integrity of total RNA were determined using the RNA Nano Lab Chip Kit and Bioanalyzer (Agilent, Palto Alto, CA). Reverse transcription reactions were performed with 1 µg of RNA and 1 µl of 10X random primers in a total 10 µl volume with the high-capacity cDNA reverse transcription kit and RNase Inhibitor (Applied Biosystems, Foster City, CA). Gene expression was analyzed with quantitative real-time PCR assays using Power SYBR Green Mix (Applied Biosystems). Real-time PCR assays were performed in duplicate with a total 25 µl reaction volume containing 500 nM concentration of each primer and reverse transcribed RNA [25 ng except 2.5 ng for the internal standard gene *β-2 microglobulin* (*B2M)*]. The sequence of all primers used is given in Appendix I. mRNA data were analyzed using a relative standard curve of pooled cDNA from either mammary gland (MG), MEC, liver, or muscle, as indicated in figure legends. mRNA data was normalized to *B2M* expression by analyzing *B2M* expression as a covariate. The standard curve for each assay was a seven serial 2-fold dilution. Unknown samples expression levels were calculated from the standard curve, except when quantifying changes in the

expression of total and spliced XBP1 across pregnancy and lactation. In this case, data were analyzed by the efficiency-corrected ΔCT method, with all assays performed at the same detection threshold level (29). For each assay, the slope of the standard curve was used to calculate PCR efficiencies (E) by using $E = 10^{(-1/slope)}$. The quantity of each XBP1 isoform was calculated using = E^{-CT}. Arbitrary expression values were standardized to input of total RNA.

Ki67 immunohistochemistry and TUNEL assay

Mammary gland sections were prepared from the right thoracic mammary gland collected at P18 and L5 (n=5 for each genotype and mammary gland stage). Sections were immunostained with a rabbit monoclonal anti-Ki67 (Abcam, 1:50) and counterstained with DAPI (Vector Laboratories, Burlingame, CA). Sections were photographed using an Axiovert 40 microscope (Zeiss) equipped with AxioCam camera. Images were used to quantify Ki67-positive cells and DAPI-stained nuclei. The percentage of Ki67-positive cells was calculated by dividing the number of Ki67-positive cells with the total number of DAPI-stained nuclei. TUNEL assay was performed by using the DeadEnd™ Colorimetric TUNEL System (Promega, Madison, WI) and sections were counterstained with DAPI (Vector Laboratories). Images were obtained as previously described. The percentage of TUNEL-positive cells was calculated by dividing the number of TUNEL-positive cells with the total number of DAPI-stained nuclei.

Transmission Electron Microscopy

The right thoracic mammary gland was dissected from subsets of WT and ΔXBP1^{MEC} mice at P18 and L5 (n=2 for each genotype and development stage). Tissue cubes (1 mm^3) were prepared from each gland and immersed into Karnovsky's Fixative (16% paraformaldehyde, 50% glutaraldehyde, 0.2M sodium phosphate buffer, pH 7.2; Electron Microscopy Sciences, Hatfield, PA). Fixation was for 1 hour on ice followed by overnight at 4°C. Samples were then washed with 0.1M sodium phosphate buffer three times for ten minutes. Samples were embedded EMbed 812 (Electron Microscopy Sciences) and then processed into 65 nm sections with the Leica Ultracut Ultramicrotome system. Images were captured using the JEM-1400 TEM. Embedding, processing and imaging were on a fee-for-service basis at the Electron Microscopy and Histology Core Facility at Weill Cornell Medical College.

Western Blotting

Inguinal mammary glands were obtained from subsets of WT and ΔXBP1^{MEC} mice at day 5 of lactation and used for preparation of total protein extracts. Briefly, 50 mg of mammary gland tissue was homogenized in 50 µl RIPA buffer (10 mM tris-HCl (pH 7.4), 150 mM sodium chloride, 1% nonidet P-40, 1 mM phenylmethylsulfonyl fluoride, 1 mM ethylenediaminetetraacetic acid (EDTA), 1 mM sodium flouride, 0.25% sodium deoxycholate, and 10%

glycerol), supplemented with protease and phosphatase inhibitors (Halt TM phosphatase inhibitor mixture EDTA-free, Thermo Scientific, Waltham, MA). Protein concentrations were determined using the BCA protein assay (Thermo Scientific). Fixed protein amounts (60 ug) were separated on 7-10% SDS-PAGE gels. Separated proteins were then transferred onto nitrocellulose membranes (Protran, Schleicher & Schuell Bioscience, Keene, NH) and blocked for 1 hour at room temperature in tris-buffered saline with tween-20 (TBS-T) (0.05M tris-HCl (pH 7.4), 0.2M sodium chloride and 0.1% Tween-20) supplemented with 5% wt/vol nonfat dried skim milk. Membranes were then incubated overnight at 4^0C with specific primary antibodies: IRE1-α (Cell Signaling, Danvers, MA), Stat 3 (Santa Cruz Biotechnology, Dallas, TX), phospho-Stat 3 Tyr 705 (Cell Signaling), and β-Actin (Cell Signaling). Primary antibodies were diluted 1:1000 in blocking solution. For direct quantitative analysis, membranes were incubated with 1:20,000 dilution of IRDye 800 anti-rabbit secondary antibody (LI-COR Biotechnology, Lincoln, NE) and then visualized using the LI-COR Odyssey infrared imaging system.

Statistical Analysis

Analyses were performed using the fit model procedure of JMP Pro 11.0 statistical software (SAS Institute, Cary, NC). Mammary expression of XBP1 transcript isoforms during pregnancy and lactation were analyzed by a model accounting for the fixed effect of development. Variation accounted by

development was partitioned into three preplanned orthogonal contrasts: development (Dev, pregnancy vs lactation), stage of pregnancy (Preg, P14 vs P18), and stage of lactation (Lact, L0 vs L5). Pup growth data were analyzed by fit model procedure including fixed effect of genotype, day of lactation, and their interaction. All other variables were analyzed within development stages (P14, P18, or L5) by a model accounting for either genotype (WT or $\Delta XBP1^{MEC}$) or tissue type (MG or MEC). Statistical significance was set at $P<0.05$.

Results

XBP1 expression is elevated in the mammary epithelial compartment in late pregnancy

Final differentiation of the mammary epithelium occurs in late pregnancy and includes the acquisition of an extensive ER compartment. To determine whether XBP1 expression varies in the epithelial compartment, we isolated MEC from wild type mice on pregnancy day 14 (P14), P18, lactation day 0 (L0), and L5. Isolation of MEC from contaminating adipocytes was assessed by comparing perilipin expression in the intact mammary gland (MG) and the resulting MEC preparation. Perilipin was used to assess purity of the MEC preparation because it is a gene expressed in adipocytes but silent in epithelial cells (27).

As shown in Figure 3.1A, perilipin expression in MEC was less than 5% of MG expression at all stages of the pregnancy and lactation, confirming successful isolation. Next, we assayed the mRNA abundance of both spliced XBP1 and total XBP1 in MEC in order to determine the proportion of XBP1 transcripts that have undergone IRE1 mediated splicing. Spliced XBP1 abundance was higher during pregnancy than lactation (Figure 3.1B, Dev, $P < 0.04$) and higher at P18 than at P14 (Preg, $P < 0.04$). The same overall effects were seen for total XBP1, although expression only tended to be higher at P18 than P14 (Preg, $P < 0.1$). Finally, the ratio of spliced to total XBP1 was significantly higher at P18 than at P14 (Preg, $P < 0.01$). These results indicate

Figure 3.1 Mammary XBP1 expression in late pregnancy and lactation.

Mammary epithelial cells (MEC) were isolated from mammary glands of wild type (WT) mice on either pregnancy day 14 (P14), pregnancy day 18 (P18), lactation day 0 (L0), or lactation day 5 (L5). **(A)** Total RNA was isolated and analyzed by quantitative RT-PCR for perilipin mRNA abundance in both MG and MEC. At each stage of development, expression is relative to MG mRNA and each bar represents the mean ± SE of perilipin mRNA abundance (n=5-11 for each tissue and development stage). *P<0.001. **(B)** Spliced and total XBP1 mRNA were measured by quantitative RT-PCR in isolated MEC. At each stage of development, expression is relative to P14, except for the ratio of spliced to total XBP1. Each bar represents the mean ± SE of indicated mRNA abundance (n=5-8 for each development stage). Each variable was analyzed by contrasts accounting for the effect of mammary development (Dev, pregnancy vs lactation), stage of pregnancy (Preg, P14 vs P18) or stage of lactation (Lact, L0 vs L5). The P-values of these contrasts are given when $P < 0.10$.

A

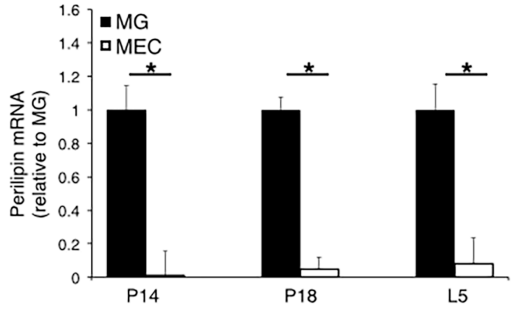
MG
MEC
Perilipin mRNA (relative to MG)
1.6
1.4
1.2
1
0.8
0.6
0.4
0.2
0
*
*
*
P14
P18
L5

B

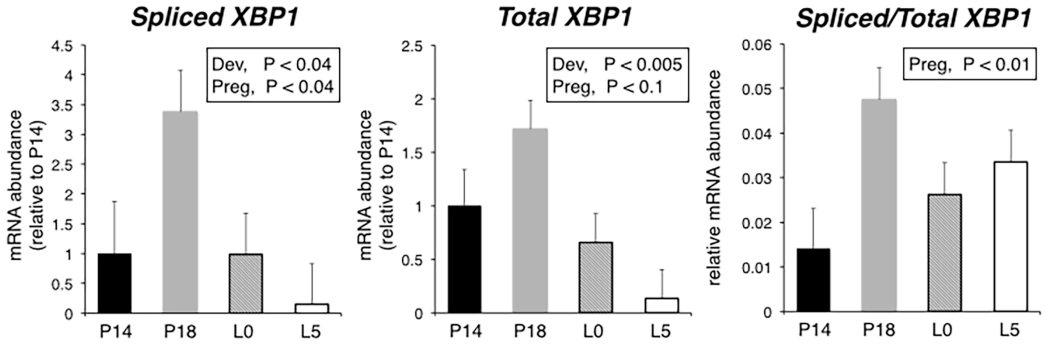
Spliced XBP1
Dev, P < 0.04
Preg, P < 0.04
mRNA abundance (relative to P14)
4.5
4
3.5
3
2.5
2
1.5
1
0.5
0
P14
P18
L0
L5
Total XBP1
Dev, P < 0.005
Preg, P < 0.1
mRNA abundance (relative to P14)
2.5
2
1.5
1
0.5
0
P14
P18
L0
L5
Spliced/Total XBP1
Preg, P < 0.01
relative mRNA abundance
0.06
0.05
0.04
0.03
0.02
0.01
0
P14
P18
L0
L5

that expression of the transcriptionally active XBP1 isoform is elevated in late pregnancy, consistent with a role for XBP1 in the final differentiation of the mammary epithelial cell compartment.

BLG-Cre mediated recombination of XBP1 transcripts in the mammary epithelial cells

To examine the role of XBP1 signaling in the mammary epithelial compartment during pregnancy and lactation, we generated experimental female mice carrying floxed XBP1 alleles in absence or presence of one copy of the BLG-Cre transgene (respectively referred to in the following text as WT and $\Delta XBP1^{MEC}$). Mice of both genotypes were mated and MEC were isolated at P14, P18, and L5. The isolation procedure was as efficient in $\Delta XBP1^{MEC}$ in terms of epithelial enrichment as in WT (see Appendix II).

To measure BLG-Cre mediated recombination of XBP1, we designed a quantitative RT-PCR assay where the forward and reverse primers are respectively located in exon 1 and exon 2 regions. XBP1 loxP sites are positioned in the introns flanking exon 2 thus resulting in the removal of exon 2 upon Cre-mediated recombination (21). In MEC collected from $\Delta XBP1^{MEC}$ mice, exon 2 containing XBP1 transcripts were reduced to 7, 4, and 16% of abundance detected in WT MEC at P14, P18, and L5, respectively (Figure 3.2A, $P < 0.001$). In contrast, abundance of exon 2 containing transcripts did not differ at L5 across genotypes in liver and skeletal muscle (Figure 3.2B).

Figure 3.2 Effect of BLG-Cre mediated recombination on XBP1 transcript abundance.

Mice harboring floxed XBP1 alleles in absence (WT) or presence of the β-lactoglobulin transgene ($\Delta XBP1^{MEC}$) were studied on either pregnancy day 14 (P14), pregnancy day 18 (P18), or lactation day 5 (L5). **(A)** Mammary epithelial cells (MEC) were isolated from the mammary gland (MG) of WT and $\Delta XBP1^{MEC}$ mice at P14, P18, and L5. Exon 2-containing XBP1 mRNA was measured by quantitative RT-PCR in isolated MEC. At each stage of development, expression is relative to WT mRNA and each bar represents the mean ± SE of exon 2-containing XBP1 mRNA abundance (n=5-11 dams for each genotype and development stage). ^{a,b} $P<0.001$. **(B)** Exon 2-containing XBP1 mRNA was measured by quantitative RT-PCR in liver and muscle collected from WT and $\Delta XBP1^{MEC}$ mice at L5. For each tissue, expression is relative to WT mRNA and each bar represents the mean ± SE of exon 2-containing XBP1 mRNA abundance (n=5 mice for each genotype and tissue).

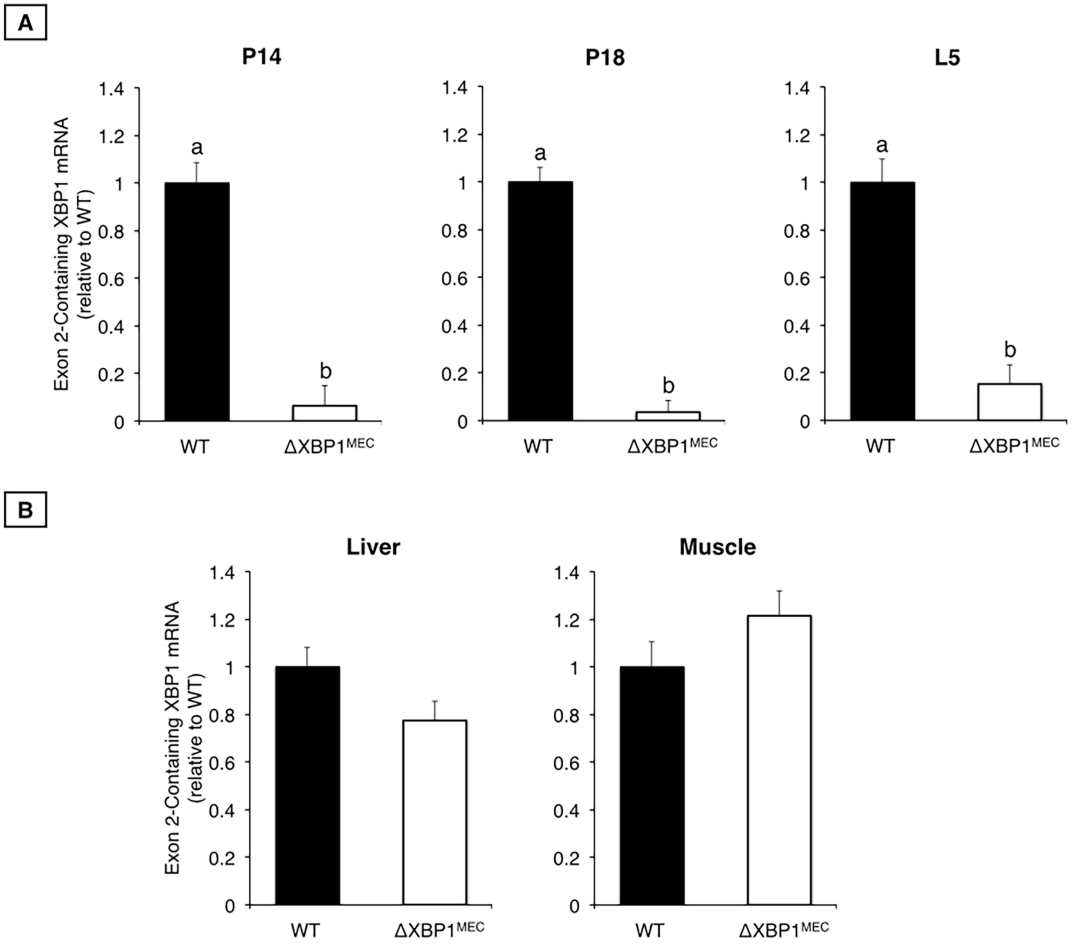
A
P14
P18
L5
Exon 2-Containing XBP1 mRNA (relative to WT)
1.4
1.2
1
0.8
0.6
0.4
0.2
0
a
b
WT
ΔXBP1MEC
B
Liver
Muscle

These results demonstrate that Cre-mediated recombination of XBP1 occurs in MEC as early as P14 and does not occur in liver and skeletal muscle.

XBP1 expression is required for normal lactation

Next we assessed effects of XBP1 ablation in MEC by measuring pup growth over the first 14 days of lactation. In this study, any effect of pup genotype was eliminated by performing reciprocal mating (i.e. WT dam x floxed male carrying BLG-Cre; $\Delta XBP1^{MEC}$ dam x WT male) and litter sizes were normalized to 8-9 pups/dam. Pup weight did not differ at L1 but a growth deficit became obvious by L3 for pups nursed by $\Delta XBP1^{MEC}$ dams (Figure 3.3). Between day 1 and 14 of lactation, pups nursed by WT dams gained 4.8 grams whereas pups nursing by $\Delta XBP1^{MEC}$ dams gained only 1.23 grams (Genotype x Day, $P < 0.0001$). By day 14 of lactation, individual pup weight averaged 6.4 grams for WT litters but only 2.6 grams for $\Delta XBP1^{MEC}$ litters (Genotype, $P < 0.0001$). To rule out the possibility that the lactation defect in $\Delta XBP1^{MEC}$ dams related to non-recombination effects of the BLG-Cre transgene, we generated female mice carrying one WT and one floxed XBP1 allele in presence of the BLG-Cre transgene ($\Delta XBP1^{+/-}$). Pups nursing from these dams grew at a similar rate as pups nursing from WT dams (see Appendix III). These results indicate that XBP1 ablation in the mammary epithelial compartment impairs lactation.

To determine whether XBP1 absence altered milk composition, milk

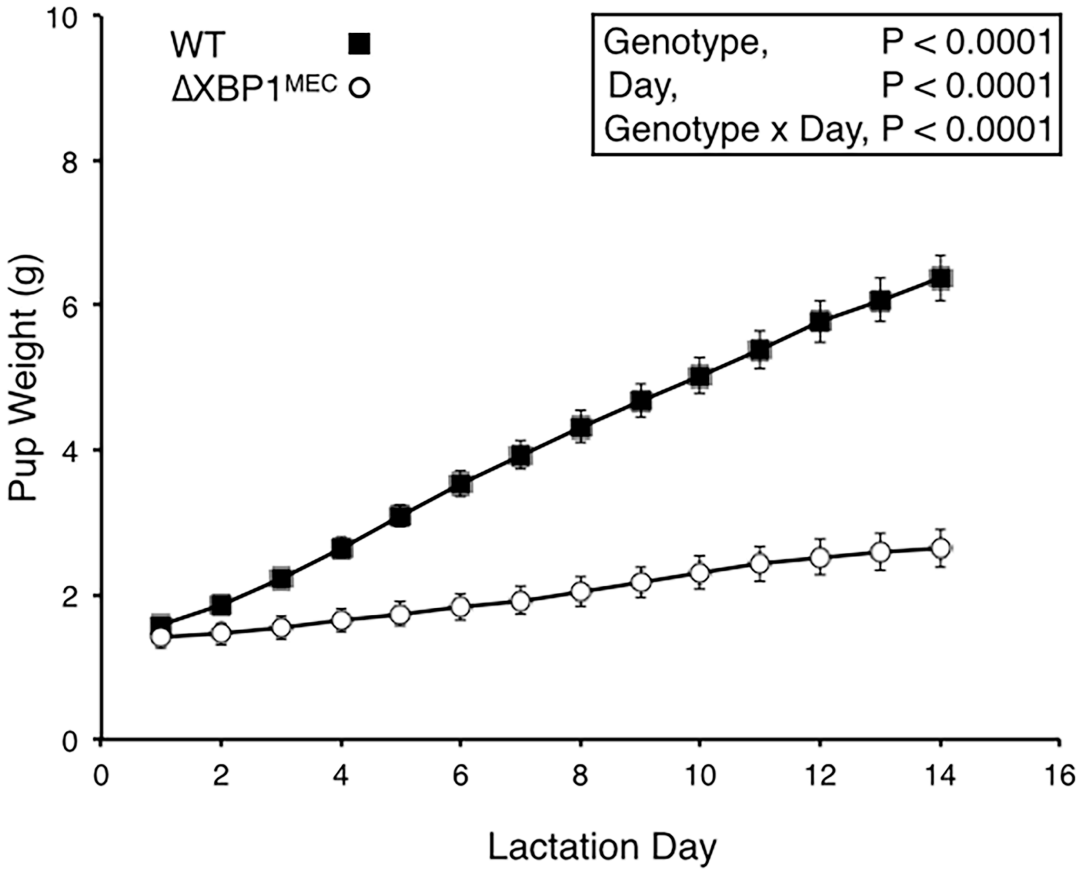

Figure 3.3 Effect of mammary specific ablation of XBP1 on pup growth.

Mice harboring wild type XBP1 (WT) or null XBP1 in mammary epithelial cells ($\Delta XBP1^{MEC}$) were studied between day 1 and 14 of lactation (n=6-11 dams for each genotype). Litters were standardized to 8-9 pups and weighed each day. Each curve represents the average weight of individual pups nursing from either WT dams or $\Delta XBP1^{MEC}$ dams. The significant effects of genotype, day, and genotype x day interaction are reported.

was collected from dams of both genotype at L14, and analyzed for major organic components. The milk concentrations of lactose and protein were respectively 37% and 21% lower in ΔXBP1^{MEC} than WT dams (Figure 3.4A, $P < 0.001$ and $P < 0.01$ respectively). SDS-Page analysis of milk showed that the lower protein content was accounted by a reduction of major milk specific proteins, including the caseins, lactoferrin, and the whey acidic protein (Figure 3.4B). In contrast, total milk fat content was increased by 24% in ΔXBP1^{MEC} milk (Figure 3.4A, $P < 0.01$). Gas chromatography analysis of milk fat did not reveal a genotype effect on the content of individual fatty acids (results not shown) or on the content of fatty acids grouped according to their origin (mammary origin, C<16; mammary and non-mammary origin, C=16; non-mammary origin, C>16) (Figure 3.4C).

We next asked whether changes in MEC gene expression contributed to XBP1 effects on milk composition. In agreement with reduced protein content in ΔXBP1^{MEC} milk, expression of the mammary specific proteins whey acidic protein (*WAP*) and β casein (β-*Csn)* were lower in ΔXBP1^{MEC} than in WT MEC (Figure 3.5A, $P < 0.03$ and $P < 0.09$). XBP1 ablation had no effect on the expression of genes engaged in milk lipid synthesis, (*Fasn, Scd1, Dgat1*) (Figure 3.5B) but upregulated expression of 3 genes involved in the formation of lipid droplets and their secretion into milk (*Btn, XO,* and *Cidea*; Figure 3.5C, $P < 0.05$). Finally, XBP1 ablation did not alter expression of the rate limiting

Figure 3.4 Effect of mammary specific ablation of XBP1 on milk composition.

Mice harboring wild type (WT) or null XBP1 in mammary epithelial cells ($\Delta XBP1^{MEC}$) were studied on day 14 of lactation. **(A)** Milk was collected from WT or $\Delta XBP1^{MEC}$ dams and analyzed for lactose, protein, and fat content. Bars represent the mean ± SE of the indicated milk component (n=5-8 dams per genotype). ^{a,b} $P<0.001$. ^{c,d} $P<0.01$. **(B)** Milk was analyzed by SDS-PAGE and Coomassie blue staining (n=5 per genotype). Two representative samples are shown for each genotype. Position of the molecular weight markers are shown on the left whereas identity of milk proteins is given on the right (Lf: lactoferrin, SA: serum albumin, α-CSN: α-casein, β-CSN: β-casein, γ-CSN: γ-casein, ε-CSN: ε-casein, WAP: whey acidic protein). **(C)** The fatty acid profile of milk was analyzed by gas chromatography (n=7-8 dams for each genotype). Fatty acids were grouped by categories reflecting their chain length [less than 16 carbons (C<16), exactly 16 carbons (C=16), or more than 16 carbons (C>16)] and each category was expressed as a % of total fatty acids.

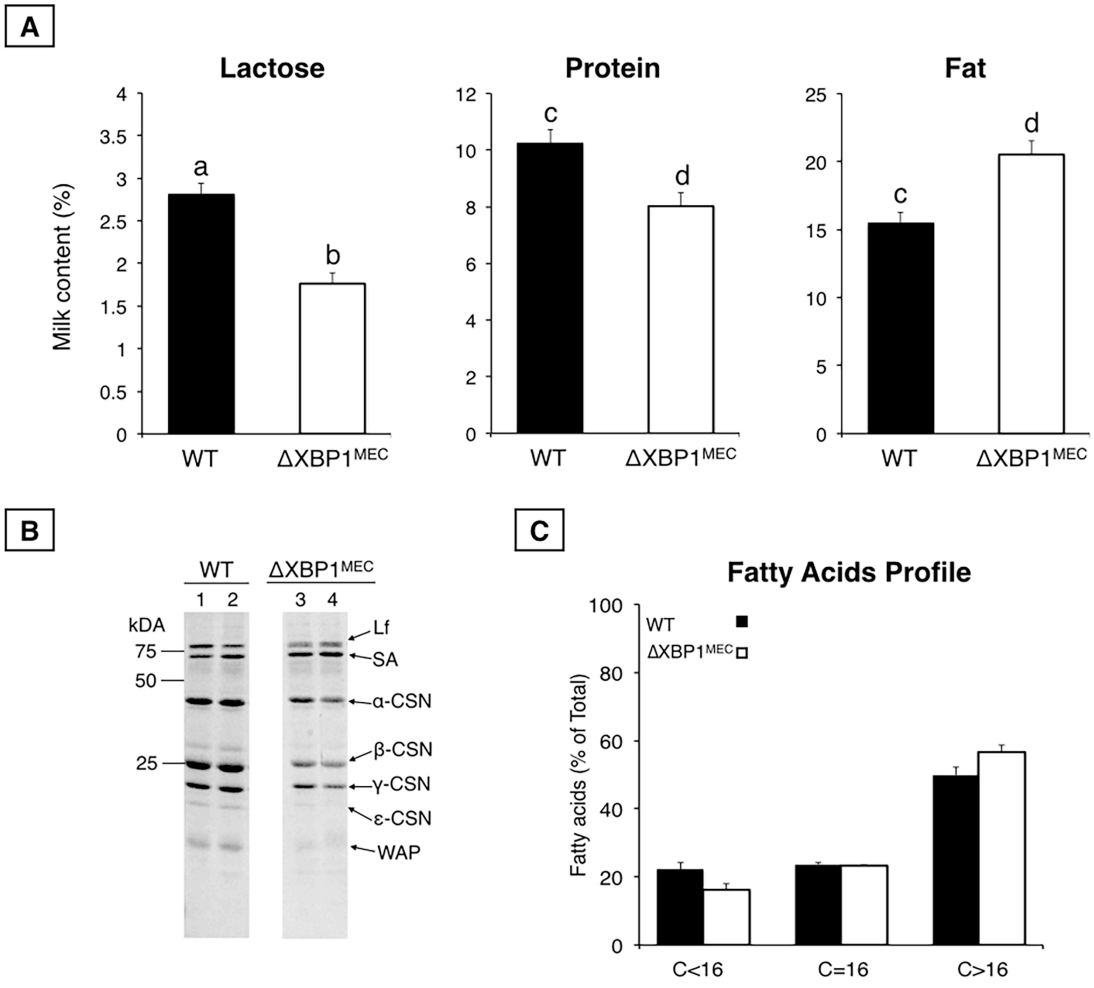
A
Lactose
Protein
Fat
Milk content (%)
a
b
c
d
c
d
WT
ΔXBP1MEC
B
WT
ΔXBP1MEC
1 2
3 4
kDA
75
50
25
Lf
SA
α-CSN
β-CSN
γ-CSN
ε-CSN
WAP
C
Fatty Acids Profile
WT
ΔXBP1MEC
Fatty acids (% of Total)
C<16
C=16
C>16

Figure 3.5 Effect of mammary specific ablation of XBP1 on expression of genes engaged in the synthesis of organic milk components.

Mammary epithelial cells (MEC) were isolated on day 5 of lactation from the mammary gland of mice harboring wild type XBP1 (WT) or null XBP1 in mammary epithelial cells ($\Delta XBP1^{MEC}$). Total RNA was isolated and analyzed by quantitative RT-PCR for expression of genes involved in **A:** synthesis of milk proteins [whey acidic protein (*WAP*) and β-casein (*β-Csn*)], **B:** synthesis of milk lipids [fatty acid synthase (*Fasn*), stearoyl-Coenzyme A desaturase 1 (*SCD1*), diacylglycerol O-acyltransferase 1 (*Dgat1*)], **C:** lipid droplet formation [butyrophilin (*Btn*), xanthine dehydrogenase (*XO*), and cell death inducing DNA fragmentation factor (*Cidea*)], **D:** lactose synthesis [UDP galactose-4-epimerase (*Gale*), α-lactalbumin (*α-lalba*), and UPD-Gal: βGlcNAc β1,4-galactosyltransferase (*β4Galt1*)]. For each gene, expression is relative to WT mRNA with bars representing the mean ± SE of indicated mRNA abundance (n=5-8 dams for each genotype). ^{a,b} $P<0.03$. ^{c,d} $P<0.09$.

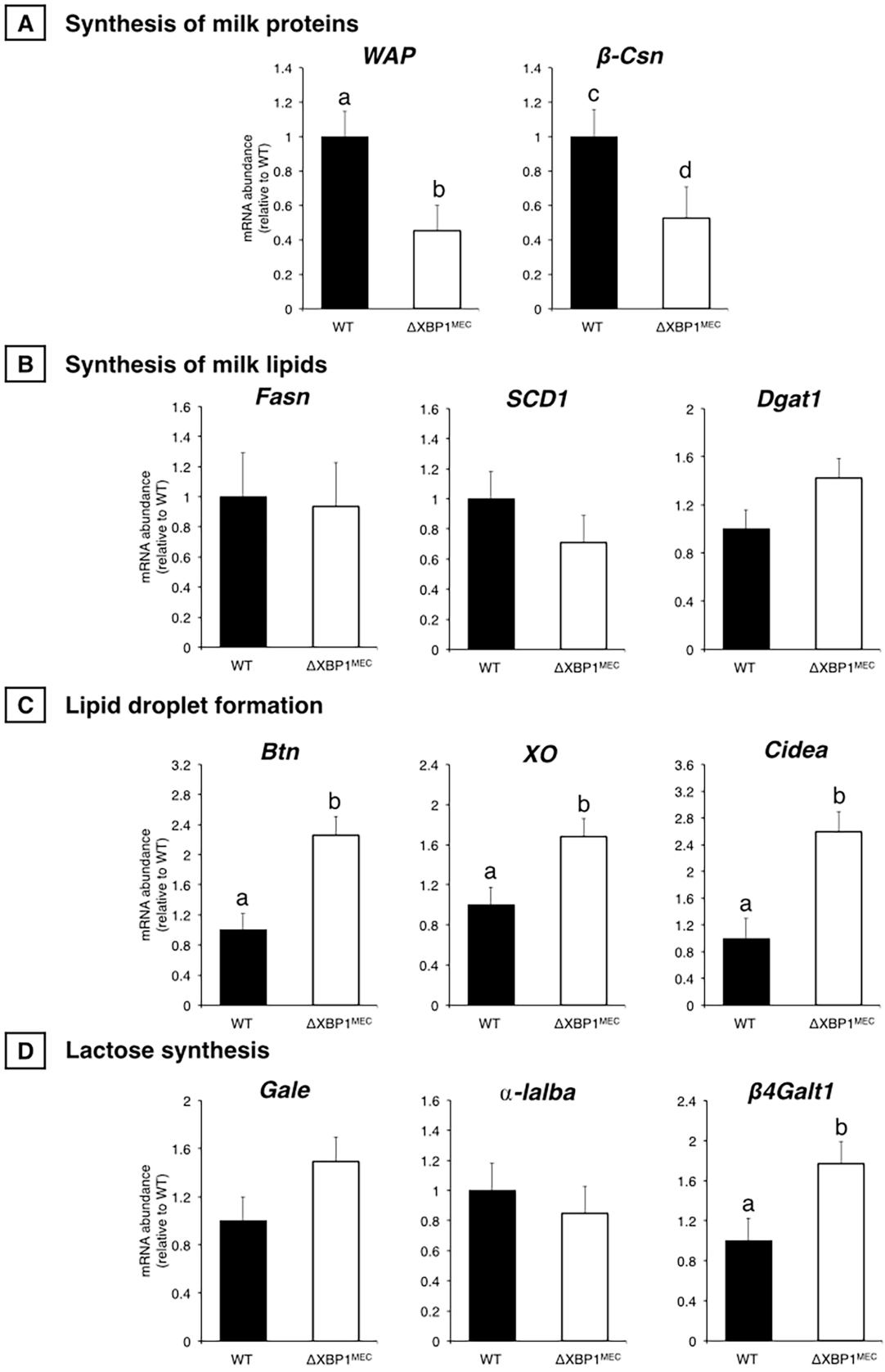
A
Synthesis of milk proteins
WAP
β-Csn
mRNA abundance (relative to WT)
a
b
c
d
WT
ΔXBP1MEC
B
Synthesis of milk lipids
Fasn
SCD1
Dgat1
C
Lipid droplet formation
Btn
XO
Cidea
D
Lactose synthesis
Gale
α-lalba
β4Galt1

enzyme responsible for galactose synthesis (*GALE*) and had no consistent effect on the expression of the two genes encoding the lactose synthase enzyme (*α-lalba* and *B4GALT1*) (Figure 3.5D). Overall, these changes in gene expression are consistent with the reciprocal changes seen in protein and fat content of ΔXBP1^{MEC} milk but do not explain the lower lactose content.

XBP1 ablation impairs alveolar expansion

The 80% growth deficit seen in litters nursed by ΔXBP1^{MEC} dams cannot be explained solely by the 20-30% change in milk composition. Accordingly, we asked whether mammary development was altered by XBP1 absence in MEC. Mammary glands were collected from WT and ΔXBP1^{MEC} female mice at P14, P18, L1, L5, and L14 and analyzed by whole mount and H&E staining (Figure 3.6). At P14, P18, and L1, WT and ΔXBP1^{MEC} mice had similar degree of ductal branching and alveolar density (Figure 3.6A) as well as similar epithelial and adipose tissue compartments (Figure 3.6B). Mammary glands collected from the two genotypes did not differ at P18 in terms of morphological indices of epithelial differentiation (accumulation of lipid droplets, expansion of alveolar lumen) but obvious differences appeared by L5 (Figure 3.6B). In WT glands, alveolar structures were fully expanded and completely displaced the adipocyte compartment. In contrast, ΔXBP1^{MEC} glands had fewer and poorly expanded alveoli and retained a prominent adipocyte compartment. These morphological differences remained obvious in

Figure 3.6 Effect of mammary specific ablation of XBP1 on mammary gland development.

Mice harboring wild type XBP1 (WT) or null XBP1 in mammary epithelial cells ($\Delta XBP1^{MEC}$) were sacrificed on pregnancy day 14 or 18 (P14, P18) or on lactation days 1, 5, or 14 (L1, L5 or L14) (n=2-3 dams for each genotype and development stage). The fourth mammary gland was collected for analysis. **(A)** Glands were analyzed by the whole mount procedure and photographed at low magnification (all images) and higher magnification (bottom right hand corner for L5 and L14). A single representative photograph is shown at each stage of development for each genotype. **(B)** Hematoxylin and eosin (H&E) stained mammary gland sections were photographed at 10X magnification (all images) and 40X magnification (bottom right hand corner). At P18 and L5, alveolar structures are shown by red arrowheads and adipocytes are shown by black arrowheads. A single representative photograph is shown at each stage of development for each genotype.

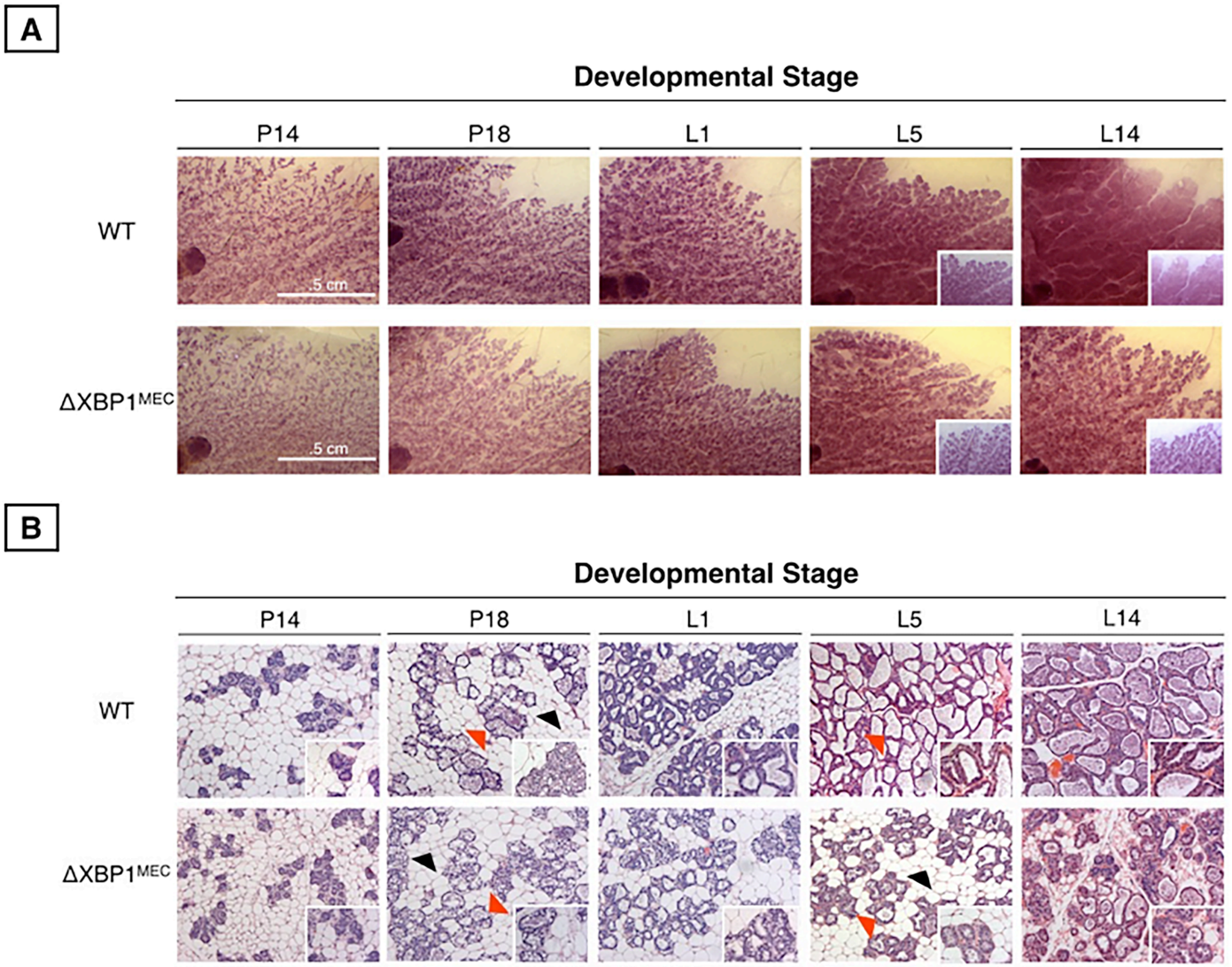
A
Developmental Stage
P14
P18
L1
L5
L14
WT
ΔXBP1MEC
.5 cm
.5 cm
B
Developmental Stage
P14
P18
L1
L5
L14
WT
ΔXBP1MEC

ΔXBP1^{MEC} at L14 with the addition that many mammary alveoli were totally collapsed. Overall, these results suggest that inadequate expansion of the MEC compartment is the primary reason for the inadequate lactation performance of ΔXBP1^{MEC} dams.

XBP1 ablation has reciprocal effects on proliferation and apoptosis

To understand why the epithelial compartment fails to expand during lactation in ΔXBP1^{MEC}, indices of proliferation and apoptosis were measured at P18 when no morphological differences were observed and at L5 when an epithelial deficit was first observed. No differences were seen in the Ki67 index of proliferation at P18. By L5, however, ΔXBP1^{MEC} experienced a 71% reduction in epithelial cell proliferation compared to WT mice (Figure 3.7B, $P < 0.01$). On the other hand, apoptosis measured by TUNEL tended to be higher in ΔXBP1^{MEC} than in WT MEC at P18 (Figure 3.8B, $P < 0.15$) and followed by a 20 fold increase in ΔXBP1^{MEC} compared to WT MEC at L5 (Figure 3.8, $P < 0.001$). Collectively, these data show that the epithelial deficit of ΔXBP1^{MEC} is accounted by reciprocal changes in both proliferation and apoptosis, with the latter apparently having a greater impact during lactation.

XBP1 ablation reduces ER abundance and increases expression of genes involved in phospholipid synthesis

Absence of XBP1 caused a reduction in the size and activity of the ER

Figure 3.7 Effect of mammary specific ablation of XBP1 on the proliferation of mammary epithelial cells.

Mice harboring wild type XBP1 (WT) or null XBP1 in mammary epithelial cells ($\Delta XBP1^{MEC}$) were sacrificed at pregnancy day 18 (P18) or lactation day 5 (L5). The third mammary gland was collected and subjected to Ki67 immunohistochemistry. **(A)** Representative photomicrograph used for quantification of Ki67 immunoreactivity (red) and DAPI stained nuclei (blue). **(B)** The percentage of DAPI stained epithelial cells positive for Ki67 signal was calculated. Proliferation is expressed relative to WT for each development stage and each bar represents the mean ± SE (n=5 dams for each genotype and development stage). ^{a,b} $P<0.01$.

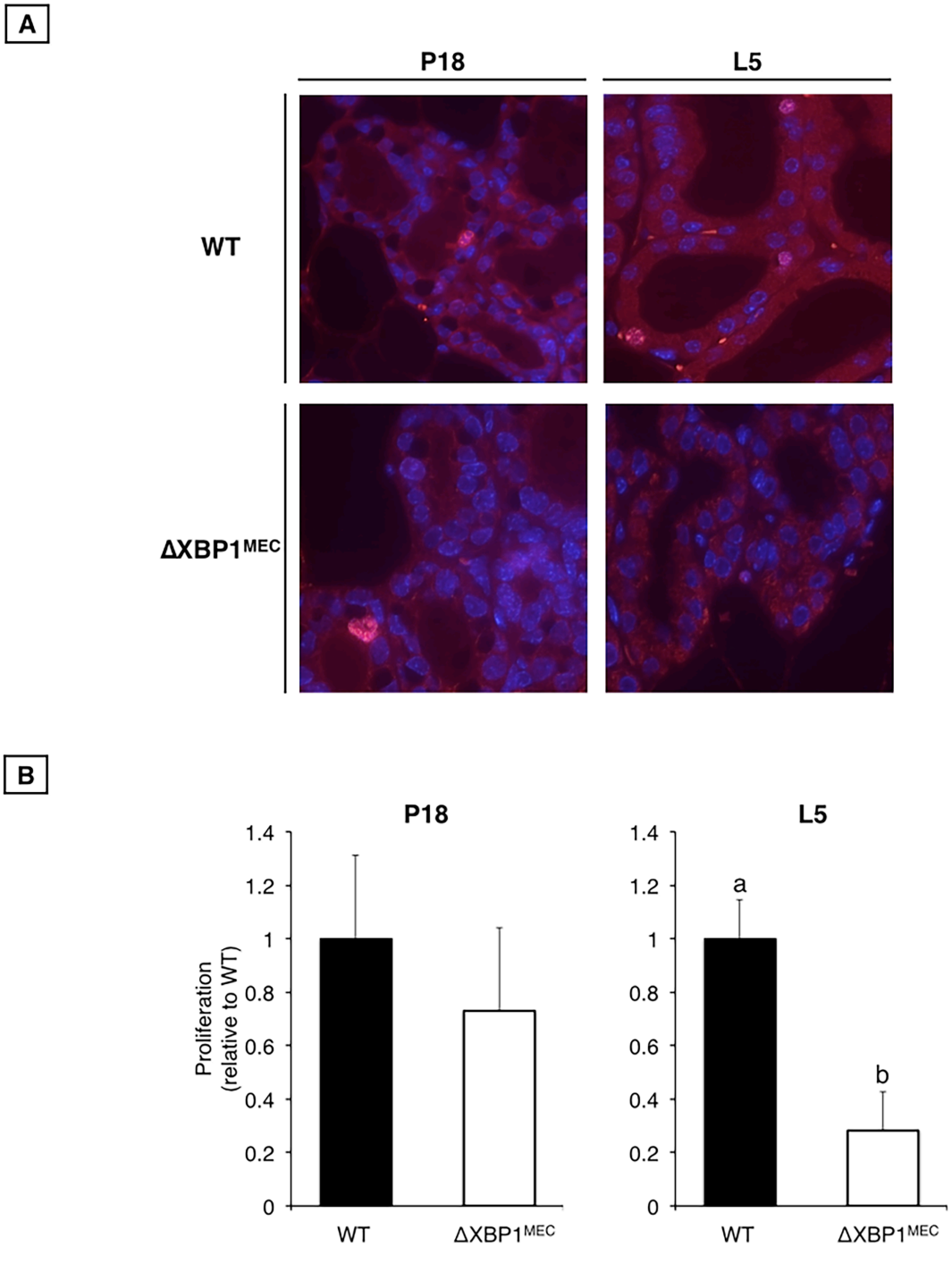
A
P18
L5
WT
ΔXBP1MEC
B
P18
L5
Proliferation (relative to WT)
1.4
1.2
1
0.8
0.6
0.4
0.2
0
a
b
WT
ΔXBP1MEC

Figure 3.8 Effect of mammary specific ablation of XBP1 on apoptosis of mammary epithelial cells.

Mice harboring wild type XBP1 (WT) or null XBP1 in mammary epithelial cells ($\Delta XBP1^{MEC}$) were sacrificed at pregnancy day 18 (P18) or lactation day 5 (L5). The third mammary gland was collected and subjected to TUNEL assay. **(A)** Representative photomicrograph used for quantification of the TUNEL signal (green) and DAPI stained nuclei (blue). **(B)** The percentage of DAPI stained epithelial cells positive for TUNEL signal was calculated. Apoptosis is expressed relative to WT for each development stage and each bar represents the mean ± SE (n=5 dams for each genotype and development stage). ^{a,b} $P<0.15$. ^{c,d} $P<0.001$.

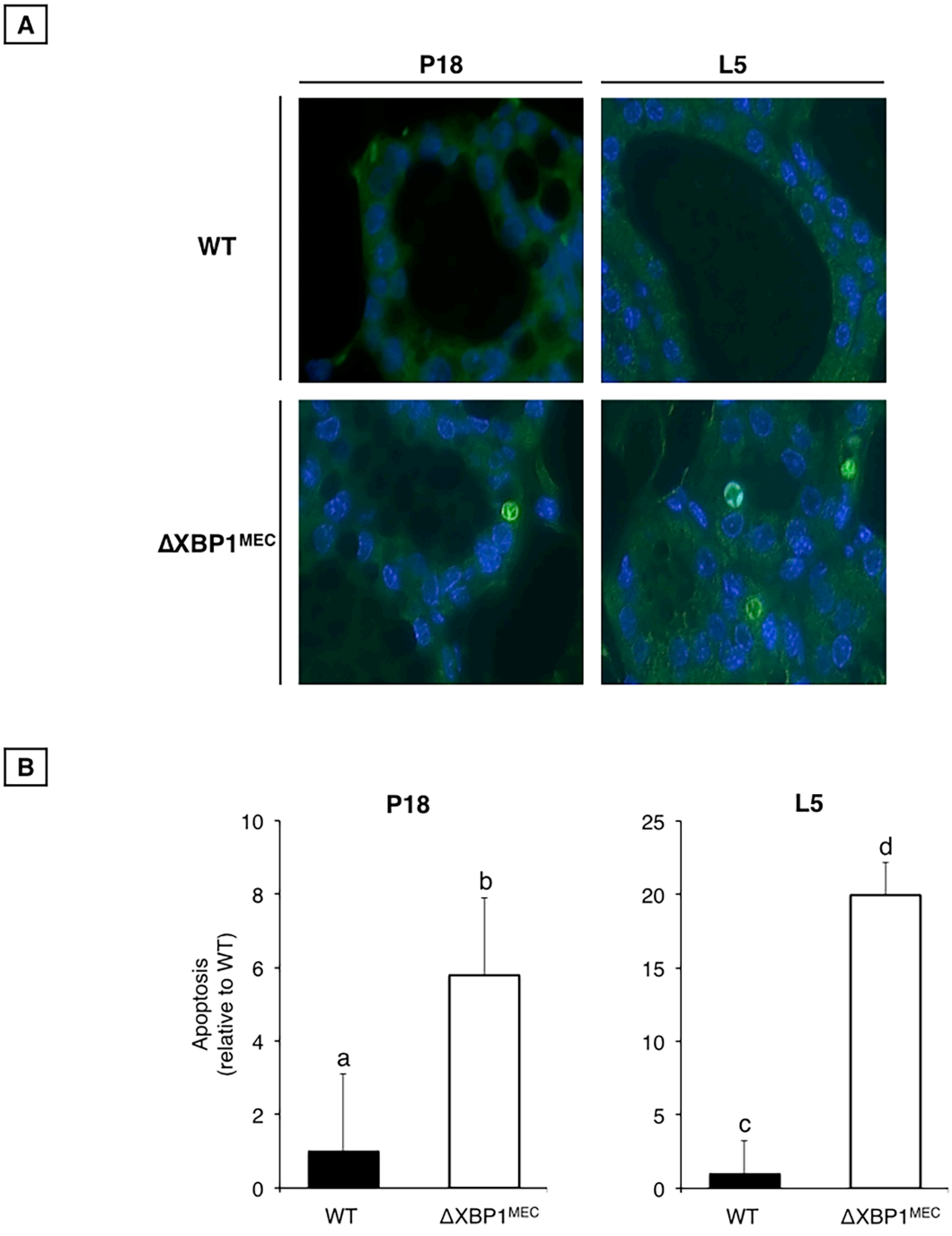
A
P18
L5
WT
ΔXBP1MEC
B
P18
L5
Apoptosis (relative to WT)
10
8
6
4
2
0
25
20
15
10
5
0
a
b
c
d
WT
ΔXBP1MEC
WT
ΔXBP1MEC

compartment and apoptosis in other secretory cells (13, 30–32). Accordingly, we investigated the cellular morphology of MEC utilizing transmission electron microscopy (TEM) (Figure 3.9A). The ER compartment was easily seen in WT MEC at P18 and increased substantially in abundance at L5, consistent with the key role played by the ER compartment in secretory activation (1). In contrast, ribbons of elaborate ER networks were less abundant in ΔXBP1^{MEC} at P18 and completely failed to increase in abundance and complexity at L5. Notably, the only ER structures visible at L5 were broken and very short. XBP1 has been shown to support ER biogenesis by stimulating the synthesis of phospholipids (10, 11). Transcript abundance of genes involved in the synthesis of phosphatidylethanolamine (PE) and phosphatidylcholine (PC) were assessed at L5 in MEC (Figure 3.9B) (33). Levels of two enzymes involved in de novo PC synthesis, either from PE (*PEMT*) or from CDP choline (*Pcyt1*) were upregulated in ΔXBP1^{MEC} MEC cells (Figure 3.9B, $P < 0.01$). In contrast, transcript levels of the enzyme regulating the conversion of CDP ethanolamine to PE (*Pcyt2*) were identical in both genotypes. Collectively, these data show that development of an adequate ER compartment in lactation is dependent on the presence of XBP1.

XBP1 ablation induces markers of ER stress

Finally, we assessed whether the absence of XBP1 signaling elicited an ER stress response in the epithelial compartment at L5. Absence of XBP1

Figure 3.9 Effect of mammary specific ablation of XBP1 on ER morphology and expression of phospholipid synthesis genes.

Mice harboring wild type XBP1 (WT) or null XBP1 in mammary epithelial cells ($\Delta XBP1^{MEC}$) were sacrificed on pregnancy day 18 (P18) or on lactation day 5 (L5). **(A)** The third mammary gland was collected and analyzed by transmission electron microscopy (n=2 dams per genotype and development stage). Representative images are shown. Nucleus (N), lipid droplet (LD), and mitochondria (M) are labeled. ER structures are shown by red arrows. **(B)** Mammary epithelial cells were isolated from WT or $\Delta XBP1^{MEC}$ dams on day 5 of lactation. Total RNA was analyzed by quantitative RT-PCR for expression of genes involved in phospholipid synthesis [phosphate cytidylyltransferase 2 ethanolamine (*Pcyt2*), phosphate cytidylyltransferase 1 (*Pcyt1*), and phosphatidylethanolamine N-methyltransferase (*Pemt*)]. For each gene, expression is relative to WT mRNA with bars representing mean ± SE of indicated mRNA abundance (n=5 dams per genotype). ^{a,b} $P<0.01$.

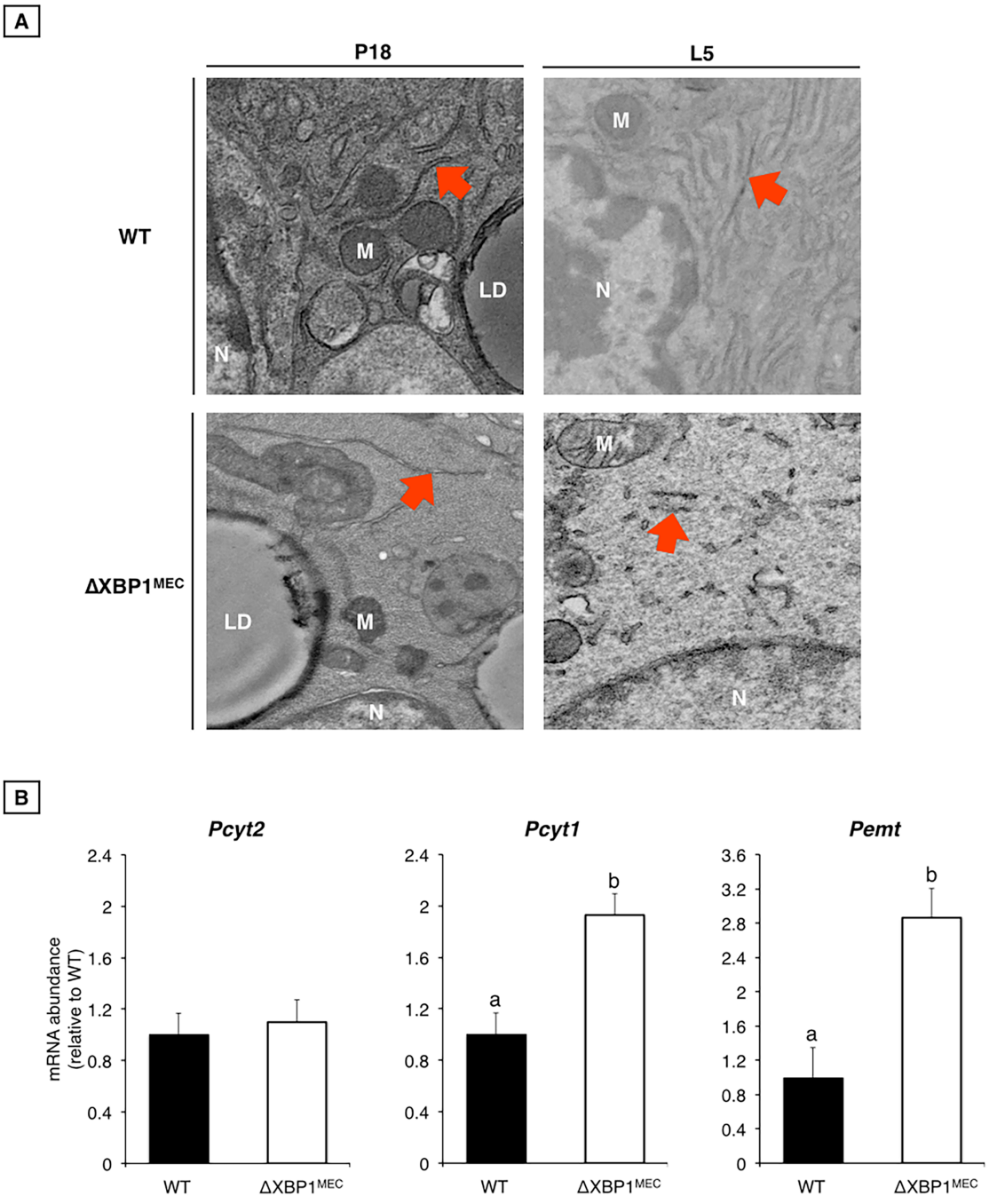
A
P18
L5
WT
ΔXBP1MEC
M
LD
N
B
Pcyt2
Pcyt1
Pemt
mRNA abundance (relative to WT)
2.4
2
1.6
1.2
0.8
0.4
0
3.6
3.2
2.8
a
b
WT
ΔXBP1MEC

results in a marked upregulation of IREα protein in the mammary gland (Figure 3.10A, $P < 0.03$). We also evaluated transcript abundance of three previously reported downstream targets of XBP1: *Wfs*, *Erdj3*, *EDEM1*. Only *EDEM1* transcript abundance was significantly downregulated in MEC collected from $\Delta XBP1^{MEC}$ compared to WT MEC (Figure 3.10B, $P < 0.005$). Next, we assessed expression of endpoints associated with apoptosis developing upon ER stress (*CHOP* mRNA) and upon involution of the mammary gland (phospho STAT3). *CHOP* mRNA abundance was increased more than 6 fold in $\Delta XBP1^{MEC}$ MEC (Figure 3.10D, $P < 0.001$). Absence of XBP1 did not alter STAT3 abundance but led to a 47% increase in its activation via tyrosine phosphorylation (Figure 3.10C, $P < 0.001$). These findings suggest that both *CHOP* and STAT3 dependent mechanisms play a role in increasing MEC apoptosis in $\Delta XBP1^{MEC}$ lactating mice.

Figure 3.10 Effect of mammary specific ablation of XBP1 on markers of ER stress response.

Mice harboring wild type XBP1 (WT) or null XBP1 in mammary epithelial cells ($\Delta XBP1^{MEC}$) were studied on day 5 of lactation. **(A)** Total cellular extracts were prepared from the fifth mammary gland and analyzed by western immunoblotting using antibodies specific for IRE1α. IRE1α signal was normalized to the actin signal. All samples were run on the same blot. Two representative samples are shown for each genotype. Expression is relative to WT and each bar represents mean ± SE (n=5 dams per genotype). [a,b] $P<0.03$. **(B)** Mammary epithelial cells were isolated from the fourth mammary gland and total RNA was analyzed by quantitative RT-PCR for expression of XBP1 response genes [wolfram syndrome 1 homolog (*Wfs*), DnaJ Hsp40 homolog (*Erdj3*), ER degradation enhancer mannosidase α-like 1 (*Edem1*)]. For each gene, expression is relative to WT mRNA, with bars representing mean ± SE of indicated mRNA abundance (n=5-8 dams per genotype). [a,b] $P<0.005$. **(C)** Mammary gland protein extracts were analyzed by western immunoblotting using antibodies specific for tyrosine 705 phosphorylated STAT3 (pSTAT), total STAT3. Total STAT3 was normalized to the actin signal whereas pSTAT3 was normalized to total STAT3. All samples were run on the same blot. Two representative samples are shown for each genotype. Expression is relative to WT and each bar represents mean ± SE of indicated protein abundance (n=5 dams per genotype). [a,b] $P<0.001$. **(D)** Expression of DNA-damage inducible transcript 3 (*CHOP*) was analyzed by quantitative RT-PCR. Expression is relative to WT mRNA, with bars representing mean ± SE (n=5-8 dams per genotype). [a,b] $P<0.001$.

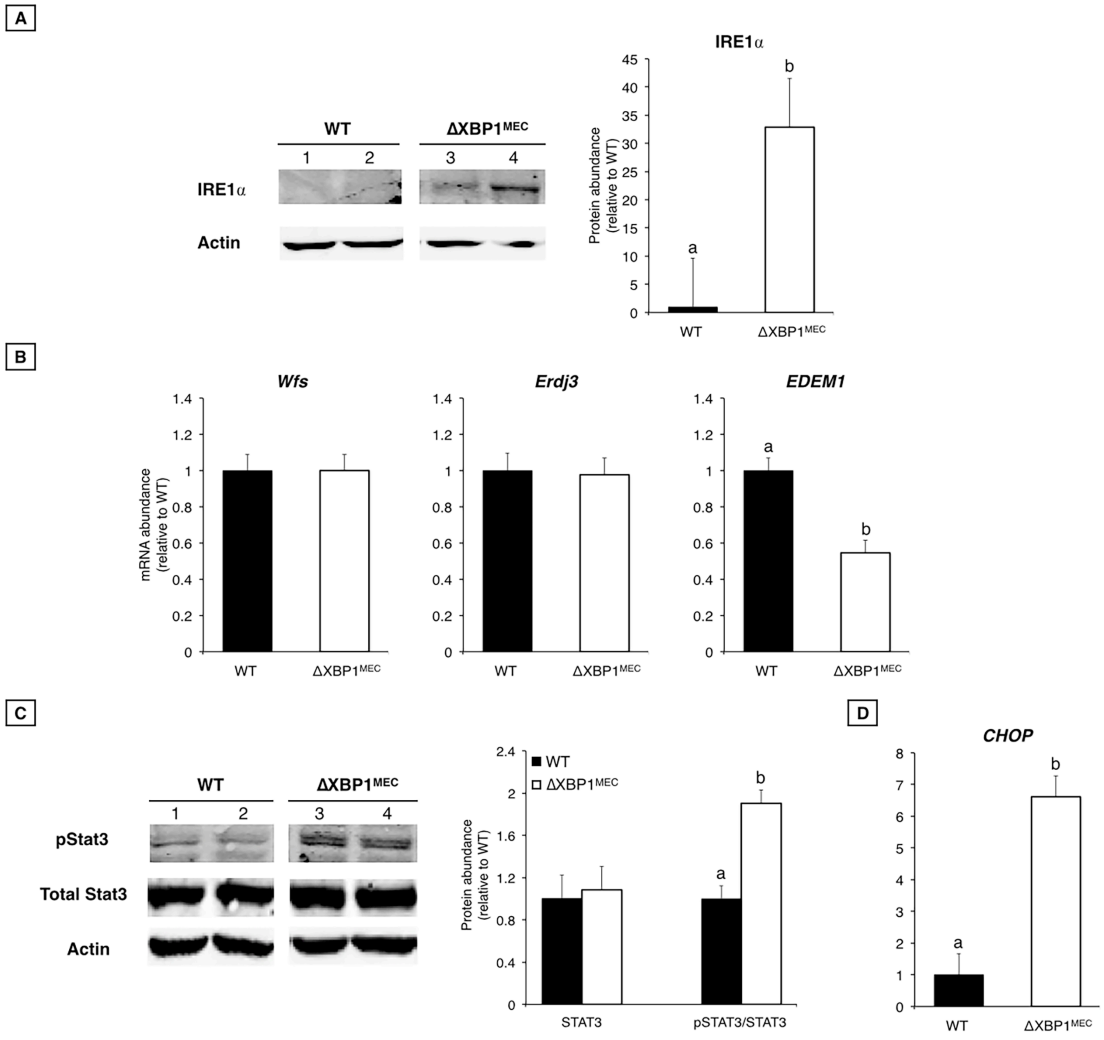
A
WT
ΔXBP1MEC
1
2
3
4
IRE1α
Actin
IRE1α
Protein abundance (relative to WT)
a
b
WT
ΔXBP1MEC
B
Wfs
Erdj3
EDEM1
mRNA abundance (relative to WT)
C
pStat3
Total Stat3
Actin
WT
ΔXBP1MEC
STAT3
pSTAT3/STAT3
D
CHOP

Discussion

MEC are unique among professional secretory cells for their ability to secrete not only proteins but also large quantities of TAG and lactose (1). The ER is involved in the synthesis of each of these organic milk components. Milk proteins are synthesized in the rough ER, whereas the assembly of milk triglycerides and the formation of milk fat droplets occur in the smooth ER (5). The major carbohydrate in milk, lactose, is synthesized in the Golgi and co-secreted in milk with mammary specific proteins (caseins and α-lactalbumin) (34). Accordingly, the MEC is a unique system to assess the role of XBP1 in maintaining ER biogenesis and homeostasis.

The adipose tissue compartment is predominant in the mammary gland during pregnancy and early lactation (1). Therefore, it was necessary to isolate MEC to assess developmental changes in XBP1 expression and the consequences of XBP1 ablation specifically in the epithelial compartment. Analysis of mRNA changes in MEC suggested that XBP1 expression is regulated during late pregnancy and lactation. Spliced XBP1 transcripts were transiently elevated at P18, corresponding to the time MEC undergo secretory activation (1). The only other study where XBP1 regulation was studied in the context of mouse lactation was performed in gonadal adipose tissue (20). In contrast to our findings, spliced and total XBP1 expression was increased on day 5 of lactation relative to day 18 of pregnancy (20). The authors attributed XBP1 induction to the lactogenic hormone, prolactin. Prolactin signaling also

plays a major role in MEC secretory activation (4, 35). Prolactin mediated activation of down stream targets have been shown to increase milk protein production in MEC (36, 37). Furthermore, a correlation of XBP1 expression with protein secretion has been demonstrated in studies of plasma B cells (12, 38). Upon differentiation, plasma B cells initiate sudden and intense production of immunoglobulin. Similar to our findings in MEC, spliced XBP1 expression was increased when cultured plasma B cells were experimentally forced to differentiate (39). Collectively, these data suggest that XBP1 upregulation is a necessary event for copious protein secretion by professional secretory cells, including MEC.

Ablating XBP1 in the adipocytes decreased pup growth with no significant changes in milk composition (20). This finding, taken together with the induction of XBP1 expression in the MEC, led us to ask whether ablating XBP1 in the predominant compartment of the mammary gland also impairs lactation. The absence of XBP1 in the MEC caused an 80% pup growth deficit by day 14 of lactation. We first asked whether changes in milk composition contributed to this XBP1 effect. Milk from $\Delta XBP1^{MEC}$ dams was lower in protein and lactose content. These XBP1 effects were consistent with changes in the expression of relevant genes for milk proteins (i.e. reduced *WAP* and *β-csn* expression) but not for lactose. Specifically, expression of genes encoding the lactose synthase complex (*α-lalba* and *β4Galt1*) and the rate limiting enzyme for lactose synthesis (*Gale*) were not reduced, the latter was

surprising because XBP1 was recently shown to regulate GALE transcription in liver (40). Moreover, GALE mRNA and activity levels increase at the onset of lactation (41).

Previous studies implicated XBP1 as a positive regulator of lipogenesis. Specifically, ablating XBP1 in the liver impaired lipid synthesis and resulted in reduced circulating levels of plasma TAG, cholesterol and fatty acids (18). This phenotype was attributed to decreased expression of key genes involved in lipogenesis, including *Dgat2*, *SCD1*, and *ACC* (18, 42). Our work shows, however, that XBP1 does not stimulate lipogenesis in MEC as milk lipids were actually increased. This conclusion remained true even when considering only medium and short chain fatty acids (C<16), which are synthesized exclusively by MEC. Absence of effects on mammary de novo lipogenesis was also supported by a lack of XBP1 effect on the expression of *Fasn* and *SCD1*.

Furthermore, XBP1 has also been implicated in the assembly and secretion of liver lipids. Specifically, VLDL secretion is dependent on microsomal triglyceride-transfer protein (MTP), a heterodimer protein complex that includes a protein disulfide isomerase (PDI) component (43). Conditionally deleting IRE1 in liver resulted in mild lipid accumulation and reduced TAG secretion with no changes in de novo lipogenesis. Reduced PDI expression and MTP activity accounted for the impaired assembly of lipid rich VLDL particles and the defect in liver TAG secretion. Reintroducing XBP1 expression in cultured null IRE1 hepatocytes completely restored TAG secretion, PDI

mRNA expression and MTP activity, indicating that XBP1 regulates hepatic VLDL secretion (19). Assembly and secretion of lipids in MEC is via lipid droplets that are formed at the smooth ER. Lipid droplet formation depends on the mammary specific proteins butyrophilin (BTN) and xanthine oxidoreductase (XO) (44, 45). Another protein, Cidea, was recently shown to stimulate milk lipid secretion by upregulating XO expression (46). Upregulation of *BTN, XO,* and *Cidea* in absence of XBP1 may explain increased fat content of $\Delta XBP1^{MEC}$ milk.

The modest composition change seen in milk of $\Delta XBP1^{MEC}$ dams was insufficient to account for the 80% growth deficit of these litters. Therefore, we investigated whether $\Delta XBP1^{MEC}$ dams suffered a mammary development defect. Despite efficient XBP1 deletion in the MEC at P14, our results indicate that mammary glands from $\Delta XBP1^{MEC}$ dams were indistinguishable from WT glands during pregnancy. There were no observable differences in terms of branching morphogenesis and alveolar structure formation at P14, P18, or L1. Moreover, milk fat droplets were equally visible in MEC from WT and $\Delta XBP1^{MEC}$ dams at P18. By the time a pup growth deficit become obvious at L5, notable defects became apparent in the mammary gland of $\Delta XBP1^{MEC}$ dams. First, many alveolar structures were flat and remained unfilled. Second, the epithelial compartment failed to completely invade the mammary gland leading to the continued presence of a substantial adipose tissue compartment. Both defects were still obvious on day 14 of lactation. Presence

of many unfilled alveoli in ΔXBP1^{MEC} glands suggest impaired biosynthetic activity in MEC. The ER is involved in the biosynthesis of milk lactose, proteins, and TAG, and its expansion is a key feature of lactogenesis in MEC. (47). XBP1 signaling has been implicated in inducing ER biogenesis; overexpressing XBP1 in cultured fibroblast cells increases ER membrane size as well as the protein level of the rate limiting enzyme of PC synthesis, PCYT1 (10, 11). Conversely, depletion of XBP1 results in diminished ER expansion in pancreatic acinar cells, salivary glands, and plasma B cells (13, 30, 31). Consistent with these data, lack of XBP1 in MEC resulted in lower ER abundance at P18, and absence of ER compartment expansion between P18 and L5. Moreover, the ER ribbons were completely missing at L5. Unexpectedly, these changes were associated with an increase rather than a decrease in the genes involved in PC synthesis, suggesting the possibility of a compensatory response.

The failure of MEC to completely occupy the mammary gland at L5 in ΔXBP1^{MEC} dams was associated with a reduction in MEC proliferation. Interestingly, XBP1 promoted the malignant phenotype via a stimulation of proliferative pathways in cultured luminal breast cancer cells (48–50). Moreover, a reduced pancreatic β-cell mass after XBP1 ablation was accounted for by reduced proliferation with no changes in apoptosis (51). In the case of MEC, however, the lack of XBP1 had an even greater effect on apoptosis, causing a 20 fold stimulation at L5. Interestingly, the ER stress

occurring upon XBP1 deletion in pancreatic acinar cells and in paneth cells is associated with *CHOP* mRNA induction and apoptosis (13, 32). CHOP is a pro-apoptotic transcription factor and is induced by ER stress activation of the PERK pathway (7, 8). These observations suggest that increased *CHOP* expression contributed to increased apoptosis in MEC lacking XBP1. We also note that XBP1 ablation also increased STAT3 activation, which is known to drive apoptosis in MEC (4, 35, 52). These data suggest that CHOP and STAT3 are both involved in stimulating apoptosis and in inducing an involution like phenotype in $\Delta XBP1^{MEC}$ mammary gland (i.e. smaller epithelial compartment combined with a significant adipocyte population).

In conclusion, our findings establish that XBP1 signaling is absolutely necessary for ER biogenesis and ER expansion in the mammary epithelial cell during late pregnancy and lactation. In the absence of XBP1, MEC have depressed biosynthetic activity and are more susceptible to apoptosis. These defects lead to a reduced mammary epithelial compartment and a severely impaired lactation.

References

1. Anderson, S. M., Rudolph, M. C., McManaman, J. L., and Neville, M. C. (2007) Secretory activation in the mammary gland: it's not just about milk protein synthesis! *Breast Cancer Res.* **9**, 204

2. Schwertfeger, K. L., McManaman, J. L., Palmer, C. A., Neville, M. C., and Anderson, S. M. (2003) Expression of constitutively activated Akt in the mammary gland leads to excess lipid synthesis during pregnancy and lactation. *J. Lipid Res.* **44**, 1100–12

3. McManaman, J. L., Reyland, M. E., and Thrower, E. C. (2006) Secretion and Fluid Transport Mechanisms in the Mammary Gland: Comparisons with the Exocrine Pancreas and the Salivary Gland. *J. Mammary Gland Biol. Neoplasia* **11**, 249–268

4. Richert, M. M., Schwertfeger, K. L., Ryder, J. W., and Anderson, S. M. (2000) An atlas of mouse mammary gland development. *J. Mammary Gland Biol. Neoplasia* **5**, 227–41

5. Fagone, P., and Jackowski, S. (2009) Membrane phospholipid synthesis and endoplasmic reticulum function. *J. Lipid Res.* **50 Suppl**, S311–6

6. Fu, S., Watkins, S. M., and Hotamisligil, G. S. (2012) The role of endoplasmic reticulum in hepatic lipid homeostasis and stress signaling. *Cell Metab.* **15**, 623–34

7. Ron, D., and Walter, P. (2007) Signal integration in the endoplasmic reticulum unfolded protein response. *Nat. Rev. Mol. Cell Biol.* **8**, 519–29

8. Cao, S. S., and Kaufman, R. J. (2012) Unfolded protein response. *Curr. Biol.* **22**, R622–R626

9. Moore, K., and Hollien, J. (2012) The unfolded protein response in secretory cell function. *Annu. Rev. Genet.* **46**, 165–83

10. Sriburi, R., Jackowski, S., Mori, K., and Brewer, J. W. (2004) XBP1: a link between the unfolded protein response, lipid biosynthesis, and biogenesis of the endoplasmic reticulum. *J. Cell Biol.* **167**, 35–41

11. Sriburi, R., Bommiasamy, H., Buldak, G. L., Robbins, G. R., Frank, M., Jackowski, S., and Brewer, J. W. (2007) Coordinate regulation of phospholipid biosynthesis and secretory pathway gene expression in XBP-1(S)-induced endoplasmic reticulum biogenesis. *J. Biol. Chem.* **282**, 7024–34

12. Iwakoshi, N. N., Lee, A.-H., Vallabhajosyula, P., Otipoby, K. L., Rajewsky, K., and Glimcher, L. H. (2003) Plasma cell differentiation and the unfolded protein response intersect at the transcription factor XBP-1. *Nat. Immunol.* **4**, 321–9

13. Lee, A.-H., Chu, G. C., Iwakoshi, N. N., and Glimcher, L. H. (2005) XBP-1 is required for biogenesis of cellular secretory machinery of exocrine glands. *EMBO J.* **24**, 4368–80

14. Walter, P., and Ron, D. (2011) The unfolded protein response: from stress pathway to homeostatic regulation. *Science* **334**, 1081–6

15. Calfon, M., Zeng, H., Urano, F., Till, J. H., Hubbard, S. R., Harding, H. P., Clark, S. G., and Ron, D. (2002) IRE1 couples endoplasmic reticulum load to secretory capacity by processing the XBP-1 mRNA. *Nature* **415**, 92–6

16. Lee, K., Tirasophon, W., Shen, X., Michalak, M., Prywes, R., Okada, T., Yoshida, H., Mori, K., and Kaufman, R. J. (2002) IRE1-mediated unconventional mRNA splicing and S2P-mediated ATF6 cleavage merge to regulate XBP1 in signaling the unfolded protein response. *Genes Dev.* **16**, 452–66

17. Yoshida, H., Matsui, T., Yamamoto, A., Okada, T., and Mori, K. (2001) XBP1 mRNA is induced by ATF6 and spliced by IRE1 in response to ER stress to produce a highly active transcription factor. *Cell* **107**, 881–91

18. Lee, A.-H., Scapa, E. F., Cohen, D. E., and Glimcher, L. H. (2008) Regulation of hepatic lipogenesis by the transcription factor XBP1. *Science* **320**, 1492–6

19. Wang, S., Chen, Z., Lam, V., Han, J., Hassler, J., Finck, B. N., Davidson, N. O., and Kaufman, R. J. (2012) IRE1α-XBP1s Induces PDI Expression to Increase MTP Activity for Hepatic VLDL Assembly and Lipid Homeostasis. *Cell Metab.* **16**, 473–86

20. Gregor, M. F., Misch, E. S., Yang, L., Hummasti, S., Inouye, K. E., Lee, A.-H., Bierie, B., and Hotamisligil, G. S. (2013) The Role of Adipocyte XBP1 in Metabolic Regulation during Lactation. *Cell Rep.* **3**, 1430–9

21. Hetz, C., Lee, A.-H., Gonzalez-Romero, D., Thielen, P., Castilla, J., Soto, C., and Glimcher, L. H. (2008) Unfolded protein response transcription factor XBP-1 does not influence prion replication or pathogenesis. *Proc. Natl. Acad. Sci. U. S. A.* **105**, 757–62

22. Yazinski, S. A., Westcott, P. M. K., Ong, K., Pinkas, J., Peters, R. M., and Weiss, R. S. (2009) Dual inactivation of Hus1 and p53 in the mouse mammary gland results in accumulation of damaged cells and impaired tissue regeneration. *Proc. Natl. Acad. Sci. U. S. A.* **106**, 21282–7

23. Selbert, S., Bentley, D. J., Melton, D. W., Rannie, D., Lourenço, P., Watson, C. J., and Clarke, A. R. (1998) Efficient BLG-Cre mediated gene deletion in the mammary gland. *Transgenic Res.* **7**, 387–96

24. Boumahrou, N., Andrei, S., Miranda, G., Henry, C., Panthier, J. J., Martin, P., and Bellier, S. (2009) The major protein fraction of mouse milk revisited using proven proteomic tools. *J. Physiol. Pharmacol.* **60**, 113–1118

25. Hussein, M., Harvatine, K. J., Boisclair, Y. R., and Bauman, D. E. (2013) Supplementation with fish oil as a source of n-3 fatty acids does not downregulate mammary lipogenesis in lactating mice. *J. Nutr.* **143**, 1913–9

26. Perfield, J. W., Delmonte, P., Lock, A. L., Yurawecz, M. P., and Bauman, D. E. (2006) Trans-10, trans-12 conjugated linoleic acid does not affect milk fat yield but reduces delta9-desaturase index in dairy cows. *J. Dairy Sci.* **89**, 2559–2566

27. Rudolph, M. C., Wellberg, E. A., and Anderson, S. M. (2009) Adipose-depleted mammary epithelial cells and organoids. *J. Mammary Gland Biol. Neoplasia* **14**, 381–6

28. Thorn, S. R., Giesy, S. L., Myers, M. G., and Boisclair, Y. R. (2010) Mammary ductal growth is impaired in mice lacking leptin-dependent signal transducer and activator of transcription 3 signaling. *Endocrinology* **151**, 3985–95

29. Cui, Y., Giesy, S. L., Hassan, M., Davis, K., Zhao, S., and Boisclair, Y. R. (2014) Hepatic FGF21 production is increased in late pregnancy in the mouse. *Am. J. Physiol. Regul. Integr. Comp. Physiol.* **307**, R290–8

30. Hess, D. A., Humphrey, S. E., Ishibashi, J., Damsz, B., Lee, A.-H., Glimcher, L. H., and Konieczny, S. F. (2011) Extensive pancreas regeneration following acinar-specific disruption of Xbp1 in mice. *Gastroenterology* **141**, 1463–72

31. Todd, D. J., McHeyzer-Williams, L. J., Kowal, C., Lee, A.-H., Volpe, B. T., Diamond, B., McHeyzer-Williams, M. G., and Glimcher, L. H. (2009) XBP1 governs late events in plasma cell differentiation and is not required for antigen-specific memory B cell development. *J. Exp. Med.* **206**, 2151–9

32. Kaser, A., Lee, A.-H., Franke, A., Glickman, J. N., Zeissig, S., Tilg, H., Nieuwenhuis, E. E. S., Higgins, D. E., Schreiber, S., Glimcher, L. H., and Blumberg, R. S. (2008) XBP1 links ER stress to intestinal inflammation and confers genetic risk for human inflammatory bowel disease. *Cell* **134**, 743–56

33. Lykidis, A., and Jackowski, S. (2001) Regulation of Mammalian Cell Membrane Biosynthesis. *Prog. Nucleic Acid Res. Mol. Biol.* **65**, 361–393

34. Neville, M. C. (1990) The physiological basis of milk secretion. *Ann. N. Y. Acad. Sci.* **586**, 1–11

35. Hennighausen, L., and Robinson, G. W. (2005) Information networks in the mammary gland. *Nat. Rev. Mol. Cell Biol.* **6**, 715–25

36. Rudolph, M. C., Russell, T. D., Webb, P., Neville, M. C., and Anderson, S. M. (2011) Prolactin-mediated regulation of lipid biosynthesis genes in vivo in the lactating mammary epithelial cell. *AM J Physiol Endocrinol Metab.* **300**, 1059–1068

37. Chen, C.-C., Stairs, D. B., Boxer, R. B., Belka, G. K., Horseman, N. D., Alvarez, J. V, and Chodosh, L. a (2012) Autocrine prolactin induced by the Pten-Akt pathway is required for lactation initiation and provides a direct link between the Akt and Stat5 pathways. *Genes Dev.* **26**, 2154–68

38. Shaffer, A. L., Shapiro-Shelef, M., Iwakoshi, N. N., Lee, A.-H., Qian, S.-B., Zhao, H., Yu, X., Yang, L., Tan, B. K., Rosenwald, A., Hurt, E. M., Petroulakis, E., Sonenberg, N., Yewdell, J. W., Calame, K., Glimcher, L.

H., and Staudt, L. M. (2004) XBP1, downstream of Blimp-1, expands the secretory apparatus and other organelles, and increases protein synthesis in plasma cell differentiation. *Immunity* **21**, 81–93

39. Hu, C.-C. A., Dougan, S. K., McGehee, A. M., Love, J. C., and Ploegh, H. L. (2009) XBP-1 regulates signal transduction, transcription factors and bone marrow colonization in B cells. *EMBO J.* **28**, 1624–36

40. Deng, Y., Wang, Z. V, Tao, C., Gao, N., Holland, W. L., Ferdous, A., Repa, J. J., Liang, G., Ye, J., Lehrman, M. A., Hill, J. A., Horton, J. D., and Scherer, P. E. (2013) The Xbp1s / GalE axis links ER stress to postprandial hepatic metabolism. *J. Clin. Invest.* **123**, 455–468

41. Prestoz, L. L., Daude, N., Cournu, I., Shin, Y. S., and Petry, K. G. (1998) Differential UDP-galactose-4'-epimerase (GALE) enzymatic activity and mRNA expression in the rat mammary gland during lactation. *FEBS Lett.* **431**, 391–4

42. Ning, J., Hong, T., Ward, A., Pi, J., Liu, Z., Liu, H.-Y., and Cao, W. (2011) Constitutive role for IRE1α-XBP1 signaling pathway in the insulin-mediated hepatic lipogenic program. *Endocrinology* **152**, 2247–55

43. Sundaram, M., and Yao, Z. (2010) Recent progress in understanding protein and lipid factors affecting hepatic VLDL assembly and secretion. *Nutr. Metab. (Lond).* **7**, 1–17

44. Ogg, S. L., Weldon, A. K., Dobbie, L., Smith, A. J. H., and Mather, I. H. (2004) Expression of butyrophilin (Btn1a1) in lactating mammary gland is essential for the regulated secretion of milk-lipid droplets. *Proc. Natl. Acad. Sci. U. S. A.* **101**, 10084–9

45. McManaman, J. L., Palmer, C. A., Wright, R. M., and Neville, M. C. (2002) Functional regulation of xanthine oxidoreductase expression and localization in the mouse mammary gland: evidence of a role in lipid secretion. *J. Physiol.* **545**, 567–579

46. Wang, W., Lv, N., Zhang, S., Shui, G., Qian, H., Zhang, J., Chen, Y., Ye, J., Xie, Y., Shen, Y., Wenk, M. R., and Li, P. (2012) Cidea is an essential transcriptional coactivator regulating mammary gland secretion of milk lipids. *Nat. Med.* **18**, 235–244

47. Lagace, T. A., and Ridgway, N. D. (2013) The role of phospholipids in the biological activity and structure of the endoplasmic reticulum. *Biochim. Biophys. Acta* **1833**, 2499–510

48. Gomez, B. P., Riggins, R. B., Shajahan, A. N., Klimach, U., Wang, A., Crawford, A. C., Zhu, Y., Zwart, A., Wang, M., and Clarke, R. (2007) Human X-box binding protein-1 confers both estrogen independence and antiestrogen resistance in breast cancer cell lines. *FASEB J.* **21**, 4013–27

49. Wang, G., Liu, G., Wang, X., Sethi, S., Ali-Fehmi, R., Abrams, J., Zheng, Z., Zhang, K., Ethier, S., and Yang, Z.-Q. (2012) ERLIN2 promotes breast cancer cell survival by modulating endoplasmic reticulum stress pathways. *BMC Cancer* **12**, 225

50. Andres, S. A., and Wittliff, J. L. (2011) Relationships of ESR1 and XBP1 expression in human breast carcinoma and stromal cells isolated by laser capture microdissection compared to intact breast cancer tissue. *Endocrine* **40**, 212–21

51. Lee, A.-H., Heidtman, K., Hotamisligil, G. S., and Glimcher, L. H. (2011) Dual and opposing roles of the unfolded protein response regulated by IRE1alpha and XBP1 in proinsulin processing and insulin secretion. *Proc. Natl. Acad. Sci. U. S. A.* **108**, 8885–90

52. Chapman, R. S., Lourenco, P. C., Tonner, E., Flint, D. J., Selbert, S., Takeda, K., Akira, S., Clarke, A. R., and Watson, C. J. (1999) Suppression of epithelial apoptosis and delayed mammary gland involution in mice with a conditional knockout of Stat3. **6**, 2604–2616

CHAPTER 4

EFFECT OF SEL1L MAMMARY EPITHELIAL CELL ABLATION ON MILK COMPOSITION, MAMMARY GLAND DEVELOPMENT, AND ENDOPLASMIC RETICULUM MORPHOLOGY[2]

The ER is the site of synthesis for secreted and membrane bound proteins, thus the maintenance of ER function is integral for secretory cells. Perturbations in ER luminal environment, such as accumulation of misfolded proteins, can disrupt ER function. Accordingly, ERAD restores ER homeostasis by eliminating misfolded protein aggregates from the ER lumen and targets them for degradation in the cytosol. Sel1L is an ER embedded protein that nucleates the most well characterized ERAD complex. Previous work has shown that Sel1L facilitates recognition of ERAD substrates and recruits other proteins to the ERAD complex. At the onset of lactation, the synthesis of all organic milk components increases dramatically. However it is unknown whether lactational demand alters ER homeostasis. More specifically, no research has investigated the role of Sel1L in the mammary gland during lactation. To this end, we generated an experimental model whereby Sel1L is specifically ablated in MEC during lactation. The absence of

[2] Davis, K. R., Giesy, S. L., Krumm, C., Long, Q., Harvatine, K. J., and Boisclair, Y. R. (2015) Sel1L is dispensable for initiating and sustaining lactation. *In preparation.*

Sel1L in the MEC caused a modest 10% pup growth deficit. Whole mount and histology analysis revealed Sel1L ablation did not affect mammary glands morphology. Lower lactose milk content suggests that a reduction in milk volume could contribute to the modest attenuation of pup growth. Abnormal ER morphology and increased indices of ER stress were evident in the absence of Sel1L. Overall, despite these obvious defects, the attenuation of lactation was very modest and appeared to relate to a reduction in milk volume.

Introduction

The ER is the site of synthesis for secreted and membrane bound proteins (1). The ER is the site where 75% of all proteins are synthesized (2). Perturbations in ER luminal environment can disrupt ER function. A variety of cellular conditions such as calcium depletion, hypoxia, oxidative stress and accumulation of misfolded proteins can disrupt ER homeostasis (3). As a result, periods of heightened protein synthesis in secretory cells can lead to accumulated misfolded proteins. The cell has adapted by developing regulatory systems devoted to maintaining homeostasis such as the ERAD. ERAD restores ER homeostasis by eliminating misfolded protein aggregates from the ER lumen and targets them for degradation in the cytosol. ERAD involves ER transmembrane complexes capable of recognition, delivery, and transfer of misfolded proteins to cytosolic proteasomes. Different ERAD systems have been described according to the type of ER proteins targeted (4, 5). The most well characterized ERAD pathway is known as ERAD-L and degrades misfolded luminal proteins (5, 6). ERAD-L contains an ER embedded E3 ubiquitin ligase, HRD1, which is nucleated with Sel1L. Sel1L is an ER embedded protein that facilitates recognition of ERAD substrates and controls HRD1 stability (4, 5). Furthermore, Sel1L recruits other proteins that assist in recognizing misfolded protein aggregates, such as EDEM1 (7–9). Thus, ablation of Sel1L has been used to investigate ERAD-L function. To date, the vast majority of what is known about Sel1L comes from yeast and

mammalian cell culture studies. The importance of Sel1L has recently been confirmed by gene knockout studies in the mouse (10–12). Nevertheless, very little is known about the *in vivo* function of Sel1L and targets of Sel1L/HRD1 ERAD complex.

The mammary gland is unique in its ability to dynamically secrete a complex fluid consisting of not only milk proteins but also lipids and carbohydrates. At the onset of lactation, the synthesis of all organic milk components increases dramatically. However it is unknown whether lactational demands alter ER homeostasis and whether a functional ERAD system is required in MEC. More specifically, to date, no research has investigated the role Sel1L in the mammary gland during lactation.

To this end, we generated an experimental model whereby Sel1L is specifically ablated in MEC during lactation. Unexpectedly, lactation was largely unaffected even though Sel1L absence disrupted ER morphology and increased indices of ER stress.

Materials and Methods

Animals and experiments

All procedures were approved by the Cornell Institutional Animal Care and Use Committee. Sel1L$^{f/f}$ mice with loxP sites on either side of exon 6 in the Sel1L gene were obtained from Dr. Qiaoming Long. Sel1L$^{f/f}$ mice were maintained on a mixed C57BL/6 background. BLG-Cre mice expressing a copy of the Cre recombinase under the control of the ovine β-lactoglobulin promoter were previously described (13). BLG-Cre mice were maintained on a mixed background. Experimental animals were generated by intercrossing Sel1L$^{f/f}$ females with Sel1L$^{f/f}$ males carrying one copy of the BLG-Cre transgene. Offspring retained for studies were either Sel1L$^{f/f}$ (designated WT) or Sel1L$^{f/f}$ carrying the BLG-Cre transgene (designated ΔSel1L^{MEC}). Litters were weaned and genotyped at 3 weeks of age.

All animals were housed in an environment with a constant ambient temperature (22°C) and photoperiod (lights on between 0600 and 1800 hours). Throughout the experiments, mice were fed *ab libitum* levels of a standard rodent chow diet containing 5% fat and 19% protein (Harlan Tekland 7912, Madison, WI). All terminal procedures involved euthanasia by CO_2 asphyxiation.

Reciprocal mating crosses was performed at 9-12 weeks of age (WT females x ΔSel1L^{MEC} males; ΔSel1L^{MEC} females x WT males). Parturition was

considered lactation day 0 (L0). These WT and ΔSel1L^{MEC} dams were used in three lactation experiments. The first experiment assessed lactational ability under standard conditions. WT or ΔSel1L^{MEC} mice (n=6-7 dams per genotype) were assigned to nurse litters of 9 pups starting on L1. Litter weight was recorded daily until L14. On L14, pups were removed from the dam for two hours to allow for mammary gland filling. Dams were anesthetized by IP injection with Avertin (Sigma-Aldrich, St. Louis, MO) followed immediately by administration of oxytocin (4 IU IP). Each mammary gland was milked for 10-15 minutes. The milking procedure involved massage of the gland combined with collection of milk droplet appearing at the tip of the nipple with a pipetteman. The milk yield ranged from 50 to 360 µl**.** Milk was diluted 1:1 with phosphate buffered saline (PBS) to reduce viscosity, sonicated to ensure homogeneity, and frozen until analyzed. Dams were then euthanized and individual mammary glands were dissected and processed for whole mount (gland #4), H&E analysis (gland #3), isolation of total RNA (gland #4), and preparation of total protein extracts (gland #5). Liver and gonadal adipose tissues were also collected for preparation of total RNA and protein extracts.

A second group of lactating WT and ΔSel1L^{MEC} dams (n=3-4 dams per genotype) was used to study impact of increased lactational demand. On day 1 of lactation, litters were standardized to 15 pups and litter weight recorded daily until L15. Finally, a third experiment was conducted to assess impact of Sel1L absence on involution. WT and ΔSel1L^{MEC} dams were assigned to

nurse litters of 7-9 pups. At L10, pups were removed and subgroups of dams were sacrificed immediately, or 3 and 6 days later (n=2-4 dams per genotype and developmental stage). Individual mammary glands were dissected and processed for whole mount (gland #4) and H&E analysis (gland #3).

Milk analysis

Lactose concentration in milk was determined by the Galactose and Lactose Colormetric Assay kit (Sigma-Aldrich). Milk protein content was measured by the Bradford assay using reconstituted milk powder as a standard. To visualize individual milk proteins, diluted milk (10 µl) was separated on 13% SDS-polyacrylamide gels and stained with Coomassie Blue (14). Milk samples were analyzed for fat content and fatty acid profile as described in (15). Briefly, approximately 60 mg of diluted whole milk were weighed into a glass extraction tube followed by the addition of dual internal standards (17:0 triglycerides and 19:0 methyl esters). Milk lipids were extracted by hexane:isopropanol extraction and methylated overnight (40°C) in 1% methanolic sulfuric acid. Gas chromatography was used to quantify methyl esters as previously described (16). Milk fat concentration was assessed based on the dilution of the internal standards.

Isolation of mammary epithelial cells

WT female mice were mated and evaluated daily for the presence of a copulatory plug (designated pregnancy day 0). Subsets of females were euthanized at P14, P18, L0, and L5 (n=5-8 dams for each mammary gland stage). Mammary epithelial cells (MEC) were isolated according to a recently validated procedure (17). In brief, the two abdominal mammary glands were dissected and the individual lymph nodes were removed. A small portion of each gland was dissected and snap frozen in liquid nitrogen. The remaining abdominal mammary glands were transferred to a glass plate on ice and minced to a paste consistency for approximately 4 minutes. Glands were incubated in a 50 mL conical tube with 5 mL of digestion buffer (DMEM containing 1 mg/mL trypsin, 2 mg/mL collagenase A, 50 mM sodium fluoride, and 1 mM sodium orthovanadate) for 30 minutes in a shaking water bath (37°C, 200 rpm). After incubation, the digestion reaction was quenched with 1 mL of fetal bovine serum. The digested mammary gland was transferred to a 15 mL conical tube containing 14 mL of wash buffer (1xPBS, 50 mM sodium fluoride, 1 mM sodium orthovanadate, 2 mM phenylmethanesulfonyl fluoride). MEC were pelleted by centrifugation (9300g for 10 min at 4°C) and the supernatant was discarded. The pellet was resuspended in wash buffer and the washing procedure was repeated two more times. After discarding the last supernatant, the MEC pellet was frozen at -80°C until isolation of total RNA.

Analysis of mammary development

Dissected abdominal mammary glands were spread onto individual glass plates for whole mount analysis (18). In brief, spread glands were fixed overnight in Carnoy's solution (60% ethanol, 30% chloroform, 10% acetic acid). After overnight fixation, glands were postfixed in 70% ethanol, rehydrated in decreasing concentrations of ethanol, and stained in carmine-alum. When uniformly stained, glands were dehydrated in increasing ethanol concentrations, cleared in xylene overnight, and secured with coverslips using Permount. Whole mounts were photographed using a digital camera attached to a dissecting microscope. For H&E analysis, the right thoracic mammary gland was fixed overnight in 10% buffered formalin and postfixed in 70% ethanol. Glands were embedded in paraffin and stained in hematoxylin and eosin. H&E histological sections were photographed using an Axiovert 40 microscope (Zeiss) bright light microscopy at 10X and 40X magnifications as previously described (18).

Total RNA isolation and analysis of gene expression

Snap frozen tissues (mammary gland, liver, gonadal adipose) collected were lyzed with Qiazol (Qiagen, Valencia, CA). Total RNA was isolated and purified using RNeasy Mini columns and on-column RNase-free DNase treatment (Qiagen). Quantity and integrity of total RNA were determined using the RNA Nano Lab Chip Kit and Bioanalyzer (Agilent, Palto Alto, CA).

Reverse transcription reactions were performed with 1 µg of RNA and 1 µl of 10X random primers in a total 10 µl volume with the high-capacity cDNA reverse transcription kit and RNase Inhibitor (Applied Biosystems, Foster City, CA). Gene expression was analyzed with quantitative real-time PCR assays using Power SYBR Green Mix (Applied Biosystems). Real-time PCR assays were performed in duplicate with a total 25 µl reaction volume containing 500 nM concentration of each primer and reverse transcribed RNA (25 ng except 2.5 ng for the internal standard gene 18S). The sequence of all primers used is given in Appendix I. mRNA data were analyzed using a relative standard curve of pooled cDNA from either mammary gland (MG), MEC, liver, or adipose, as indicated in figure legends. mRNA data was normalized to *18S* expression. The standard curve for each assay was a seven serial 2-fold dilution. Unknown samples expression levels were calculated from the standard curve.

Transmission Electron Microscopy

The right thoracic mammary gland was dissected from subsets of WT and ΔSel1L^{MEC} mice at L14 (n=2-3 for each genotype). Tissue cubes (1 mm^3) were prepared from each gland and immersed into Karnovsky's Fixative (16% paraformaldehyde, 50% glutaraldehyde, 0.2M sodium phosphate buffer, pH 7.2; Electron Microscopy Sciences, Hatfield, PA). Fixation was for 1 hour on ice followed by overnight at 4°C. Samples were then washed with 0.1M

sodium phosphate buffer three times for 10 minutes. Samples were embedded in EMbed 812 (Electron Microscopy Sciences) and then processed into 65 nm sections with a Leica Ultracut Ultramicrotome system. Images were captured using the JEM-1400 TEM. Embedding, processing and imaging were on a fee-for-service basis at the Electron Microscopy and Histology Core Facility at Weill Cornell Medical College.

Western Blotting

Tissues (mammary gland, liver, adipose tissue) were homogenized in 50 µl RIPA buffer (10 mM tris-HCl (pH 7.4), 150 mM sodium chloride, 1% nonidet P-40, 1 mM phenylmethylsulfonyl fluoride, 1 mM ethylenediaminetetraacetic acid (EDTA), 1 mM sodium flouride, 0.25% sodium deoxycholate, and 10% glycerol), supplemented with protease and phosphatase inhibitors (Halt TM phosphatase inhibitor mixture EDTA-free, Thermo Scientific, Waltham, MA). Protein concentrations were determined using the BCA protein assay (Thermo Scientific). Fixed protein amounts (60 ug) were separated on 7-10% SDS-PAGE gels. Separated proteins were then transferred onto nitrocellulose membranes (Protran, Schleicher & Schuell Bioscience, Keene, NH) and blocked for 1 hour at room temperature in tris-buffered saline with tween-20 (TBS-T) (0.05M tris-HCl (pH 7.4), 0.2M sodium chloride and 0.1% Tween-20) supplemented with 5% wt/vol nonfat dried skim milk. Membranes were then incubated overnight at 4^0C with specific primary

antibodies: Sel1L (Abcam, Cambridge, MA), HRD1 (Novus Biologicals, Littleton, CO), HSP90 (Cell Signaling), β-Actin (Cell Signaling), IRE1-α (Cell Signaling, Danvers, MA), and BiP (Cell Signaling). Primary antibodies were diluted 1:1000 in blocking solution except HRD1 which was diluted 1:2000. For direct quantitative analysis, membranes were incubated with 1:20,000 dilution of IRDye 800 anti-rabbit secondary antibody (LI-COR Biotechnology, Lincoln, NE) and then visualized using the LI-COR Odyssey infrared imaging system.

Statistical Analysis

Analyses were performed using the fit model procedure of JMP Pro 11.0 statistical software (SAS Institute, Cary, NC). Mammary mRNA abundance of Sel1L and other ERAD component in late pregnancy and early lactation was analyzed by a model accounting for the fixed effect of development (P14, P18, L0 and L5). Variation accounted by development was partitioned into 3 preplanned orthogonal contrasts: development (Dev, pregnancy vs lactation), stage of pregnancy (Preg, P14 vs P18), and stage of lactation (Lact, L0 vs L5). Pup growth data were analyzed by a model accounting for the fixed effect of genotype, day of lactation, and their interaction. All other variables were analyzed by a model accounting for the fixed effect of genotype (WT or $\Delta Sel1L^{MEC}$). Liver, mammary, adipose, and muscle protein abundance of Sel1L and HRD1 was compared by pairwise comparisons with Tukey adjustment. Statistical significance was set at $P<0.05$.

Results

Sel1L is expressed in the mammary epithelial cell compartment

Tissue-specific ablation of Sel1L has revealed the importance of ERAD in various professional secretory cells (10, 11). Lactation represents a period of copious secretion of milk proteins however it is unknown whether Sel1L and other ERAD components are expressed in mammary epithelial cells. Therefore, we initially assayed the transcript abundance of Sel1L, HRD1, and EDEM1 on pregnancy day 14 (P14), P18, lactation day 0 (L0), and L5. This analysis was performed in purified mammary epithelial cells in order to avoid contamination by adipocyte where Sel1L and other ERAD components are expressed (10, 11). Expression was consistently higher during pregnancy than lactation for Sel1L, HRD1, and EDEM1 (Figure 4.1; Dev, $P < 0.01$ and lower). Stage of pregnancy or lactation did not significantly affect the expression of these genes, with the exception that HRD1 expression was lower at L5 than at L0 (Lact, $P < 0.03$).

To corroborate meaningful mammary expression of ERAD components, protein extracts were prepared and analyzed by Western blotting for Sel1L and HRD1 abundance. This analysis included tissues with high and low Sel1L expression (liver, adipose, and muscle) and was conducted on day 14 of lactation when the mammary gland consists of an epithelial compartment devoid of visible adipocytes (19). Sel1L and HRD1 proteins were higher in liver

Figure 4.1 Mammary expression of SEL1L and other components of the ERAD system in late pregnancy and lactation.

Mammary epithelial cells (MEC) were isolated from mammary glands of WT mice on either pregnancy day 14 (P14), pregnancy day 18 (P18), lactation day 0 (L0), or lactation day 5 (L5). Total RNA was isolated and analyzed by quantitative RT-PCR for suppressor enhancer Lin12 1-like *(Sel1L)*, synovial apoptosis inhibitor 1 *(HRD1)*, and ER degradation enhancer mannosidase α-like 1 *(EDEM1)* mRNA abundance. At each stage of development, expression is relative to P14 and each bar represents the mean ± SE of the indicated mRNA abundance (n=5-8 for each development stage). Each variable was analyzed by contrasts accounting for the effect of mammary development (Dev, pregnancy vs lactation), stage of pregnancy (Preg, P14 vs P18) or stage of lactation (Lact, L0 vs L5). The P-values of these contrasts are given when $P < 0.10$.

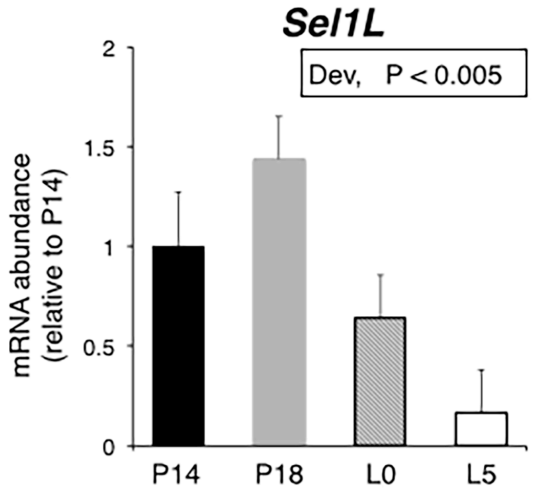
Sel1L
Dev, P < 0.005
mRNA abundance
(relative to P14)
2
1.5
1
0.5
0
P14
P18
L0
L5

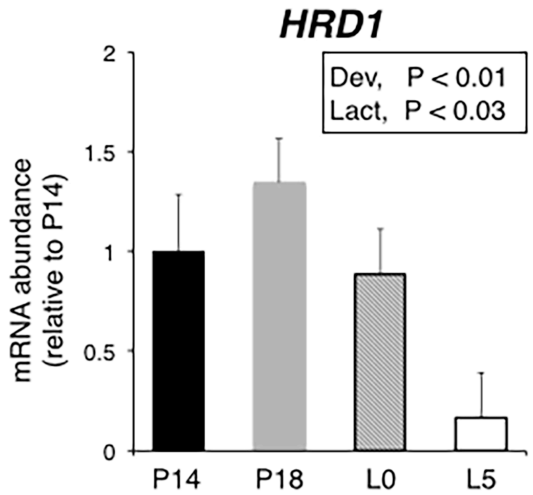
HRD1
Dev, P < 0.01
Lact, P < 0.03
mRNA abundance
(relative to P14)
2
1.5
1
0.5
0
P14
P18
L0
L5

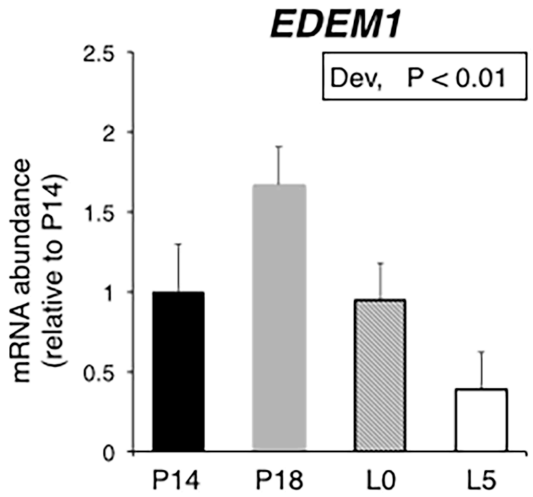
EDEM1
Dev, P < 0.01
mRNA abundance
(relative to P14)
2.5
2
1.5
1
0.5
0
P14
P18
L0
L5

than gonadal adipose tissue and absent in skeletal muscle (Figure 4.2). Notably, Sel1L and HRD1 protein abundance in the mammary gland did not differ from either liver or gonadal adipose tissue. Collectively, the mRNA and protein expression data demonstrate meaningful expression of Sel1L and other ERAD components in the mammary epithelial compartment during late pregnancy and lactation.

BLG-Cre mediated recombination of Sel1L transcripts in the mammary epithelial cells

To examine the role of Sel1L in mammary epithelium during lactation, we generated experimental female mice carrying floxed Sel1L alleles in absence or presence of one copy of the BLG-Cre transgene (respectively referred to in the following text as WT and ΔSel1L^{MEC}). WT and ΔSel1L^{MEC} dams were mated and then studied over the first 14 days of lactation. Sel1L loxP sites are positioned in the introns flanking exon 6 thus resulting in the removal of exon 6 upon Cre-mediated recombination. Accordingly, we measured BLG-Cre mediated recombination of Sel1L utilizing a quantitative RT-PCR assay with forward and reverse primers located in exon 5 and exon 6. Furthermore, we collected the mammary gland, gonadal adipose, and liver tissues from both WT and ΔSel1L^{MEC} mice at L14 to determine the specificity of the BLG-Cre mediated recombination. Exon-6 containing *Sel1L* transcripts were reduced by over 80% in mammary glands collected from ΔSel1L^{MEC} mice

Figure 4.2 Protein abundance of SEL1L and other components of the ERAD system in selected tissues of lactating mice.

Protein extracts were prepared from liver, the fifth mammary gland, gonadal adipose tissue, and skeletal muscle collected from wild type (WT) mice on lactation day 14 (L14). **(A)** Protein extracts were analyzed by western immunoblotting using antibodies specific for Sel1L, HRD1, and the ubiquitous protein HSP90. All samples were run on the same blot. Two representative samples are shown for each tissue. **(B)** Each bar represents the mean ± SE of indicated protein abundance (n=3-4 dams for each tissue). Bars with different letters are significantly different ($P<0.05$ or less).

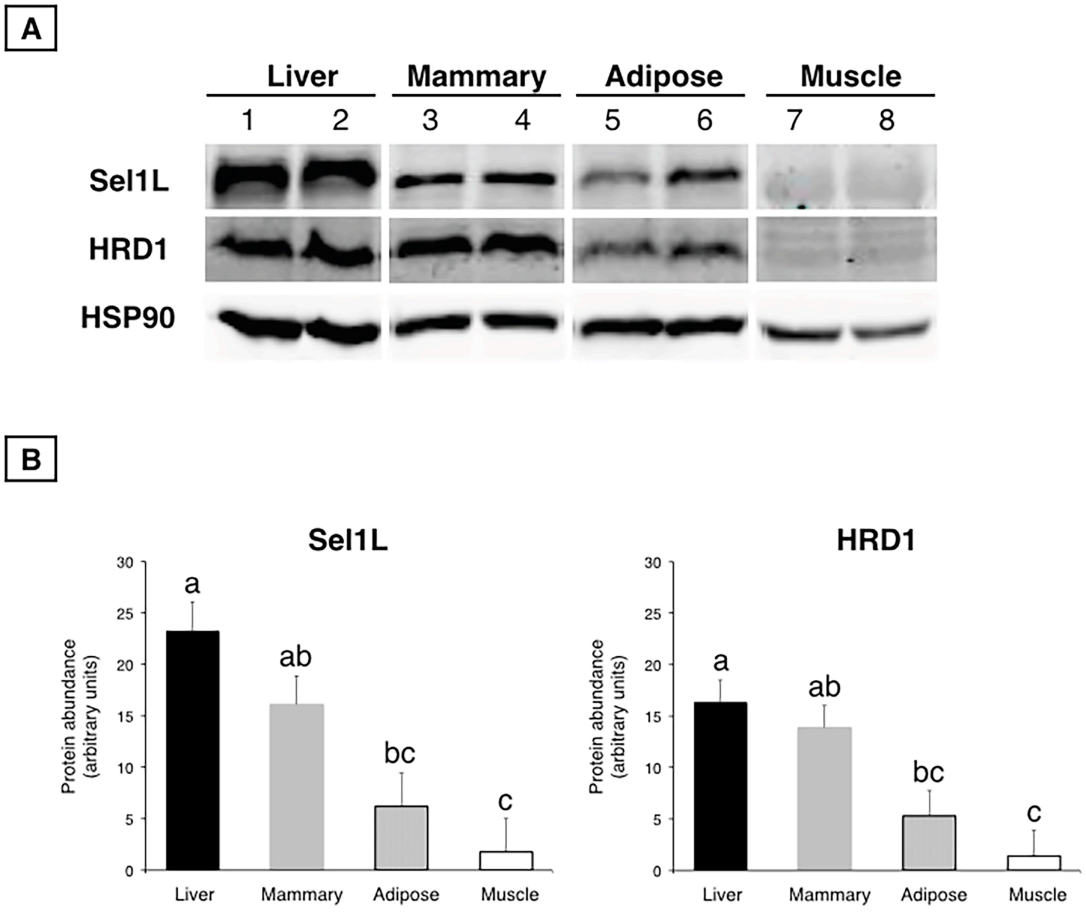
A
Liver
Mammary
Adipose
Muscle
1
2
3
4
5
6
7
8
Sel1L
HRD1
HSP90
B
Sel1L
HRD1
Protein abundance (arbitrary units)
30
25
20
15
10
5
0
a
ab
bc
c
Liver
Mammary
Adipose
Muscle

(Figure 4.3A, $P < 0.001$) but were not affected by genotype in adipose tissue or liver. In addition, we measured effects of BLG-Cre mediated recombination of Sel1L on *HRD1* and *EDEM1* mRNA abundance. *HRD1* transcript abundance was elevated by 41% in the mammary gland collected from $\Delta Sel1L^{MEC}$ mice (Figure 4.3B, $P < 0.01$) and again unaffected by genotype in other tissues. In contrast, *EDEM1* transcript abundance did not differ by genotype in any tissue (Figure 4.3C).

To substantiate these results, adipose and mammary tissues collected at L14 were analyzed by Western blotting (Figure 4.4). Sel1L was easily detected in WT mammary tissue and nearly absent in $\Delta Sel1L^{MEC}$ mammary tissue (Figure 4.4B, $P < 0.01$). HRD1 protein abundance was also lower in $\Delta Sel1L^{MEC}$ than in WT mammary glands (Figure 4.4C, $P < 0.03$). In contrast, Sel1L and HRD1 protein abundance did not differ in adipose and liver (Figure 4.4B and C, and results not shown). Collectively, these findings indicate that BLG-Cre mediated recombination of Sel1L was efficient and occurred only in the mammary gland.

Sel1L ablation attenuates lactation

To assess the effect of Sel1L ablation in MEC, we measured pup growth over the first 14 days of lactation. We employed a reciprocal mating strategy to eliminate any potential effect of pup genotype (i.e. WT dam x floxed male carrying BLG-Cre; $\Delta Sel1L^{MEC}$ dam x floxed male) and litters were

Figure 4.3 Effect of BLG-Cre mediated recombination on Sel1L transcript abundance.

Mice harboring floxed Sel1L alleles in absence (WT) or presence of the β-lactoglobulin transgene (ΔSel1L^{MEC}) were studied on lactation day 14 (L14). Total RNA was isolated from the fourth mammary gland, adipose tissue, and liver and analyzed by quantitative RT-PCR for the mRNA abundance of **(A)** *Sel1L*, **(B)** *HRD1*, and **(C)** *EDEM1*. For each gene, expression is relative to WT mRNA and each bar represents the mean ± SE of the indicated mRNA abundance (n=5 mice for each genotype and tissue). ^{a,b} $P<0.001$. ^{c,d} $P<0.01$.

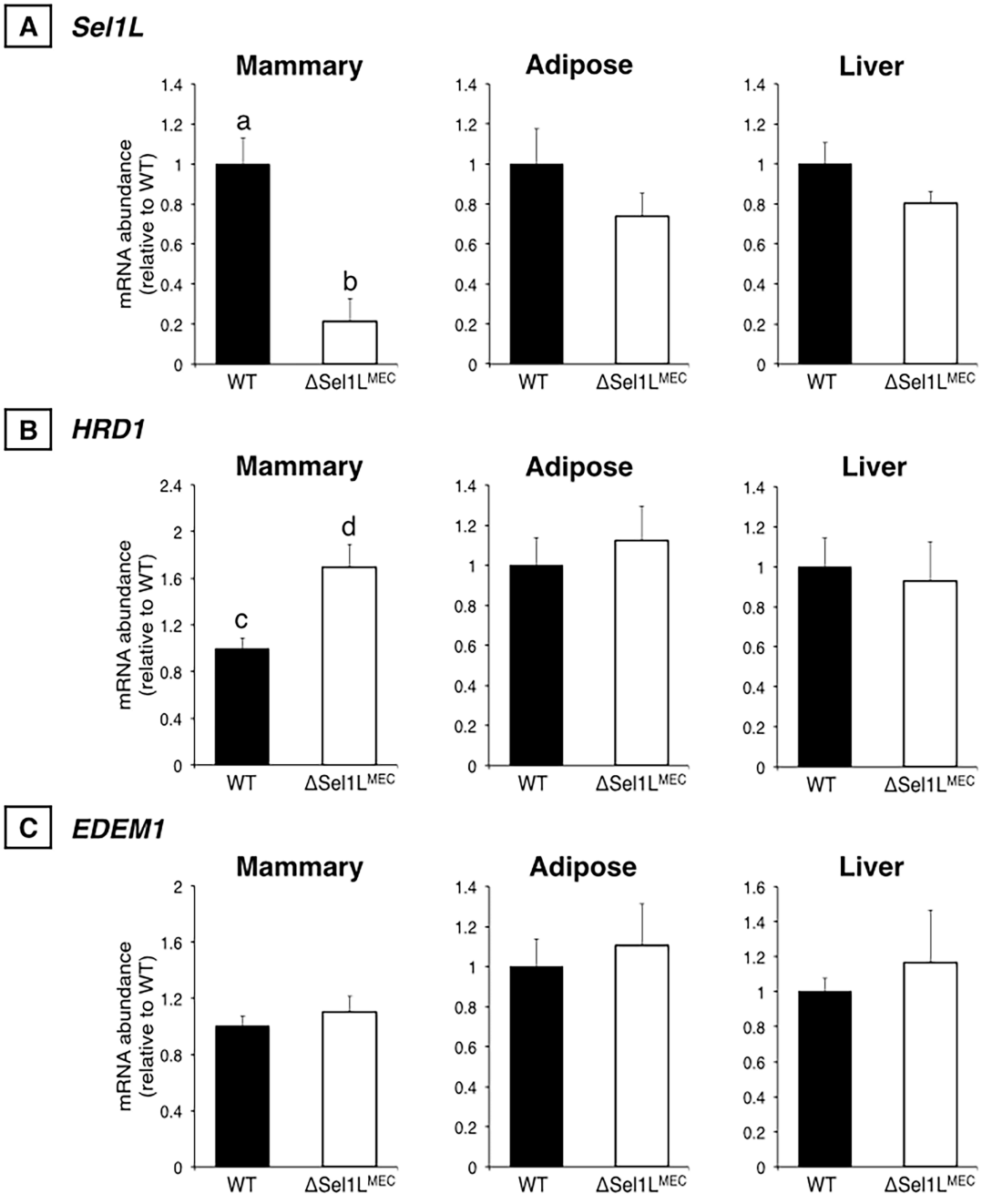
A
Sel1L
Mammary
Adipose
Liver
mRNA abundance (relative to WT)
a
b
WT
ΔSel1L^MEC
B
HRD1
c
d
C
EDEM1

Figure 4.4 Effect of BLG-Cre mediated recombination on Sel1L protein abundance.

Mice harboring floxed Sel1L alleles in absence (WT) or presence of the β-lactoglobulin transgene ($\Delta Sel1L^{MEC}$) were studied on lactation day 14 (L14). **(A)** Total cellular extracts were prepared from adipose tissue and the fifth mammary gland and analyzed by western immunoblotting using antibodies specific for Sel1L and HRD1. All samples were run on the same blot. Two representative samples are shown for each genotype and tissue. **(B)** Sel1L and **(C)** HRD1 signal was normalized to actin signal. For each protein, expression is relative to WT and each bar represents mean ± SE of indicated protein abundance (n=3-4 mice for each genotype and tissue). ^{a,b} $P<0.01$. ^{c,d} $P<0.03$.

A

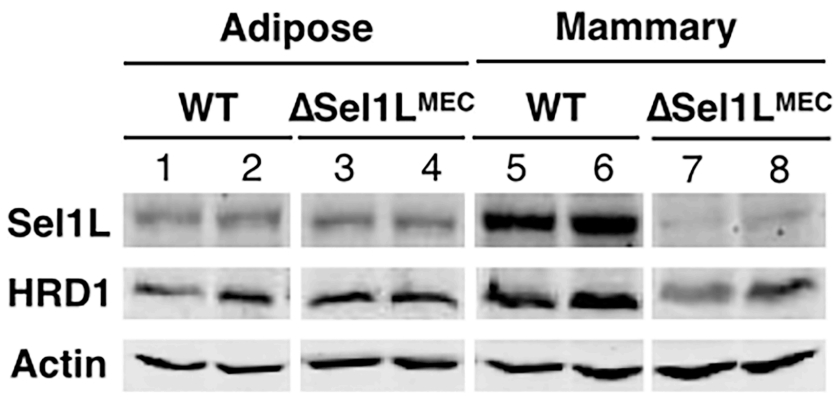

B Sel1L

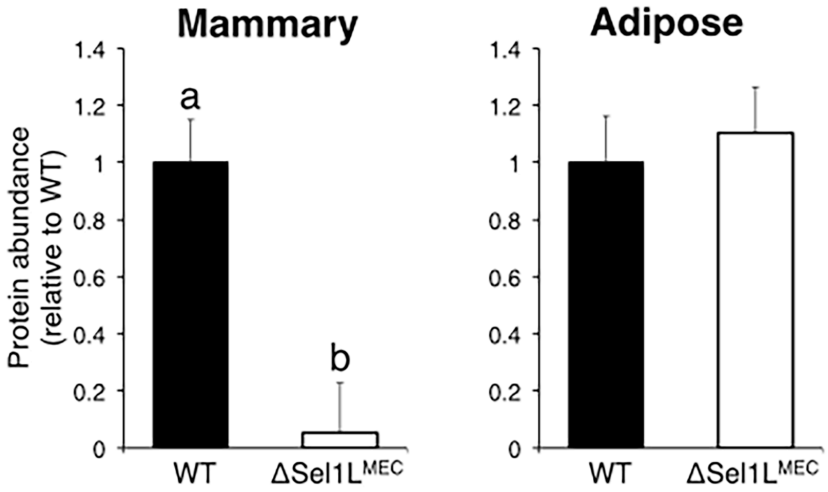

C HRD1

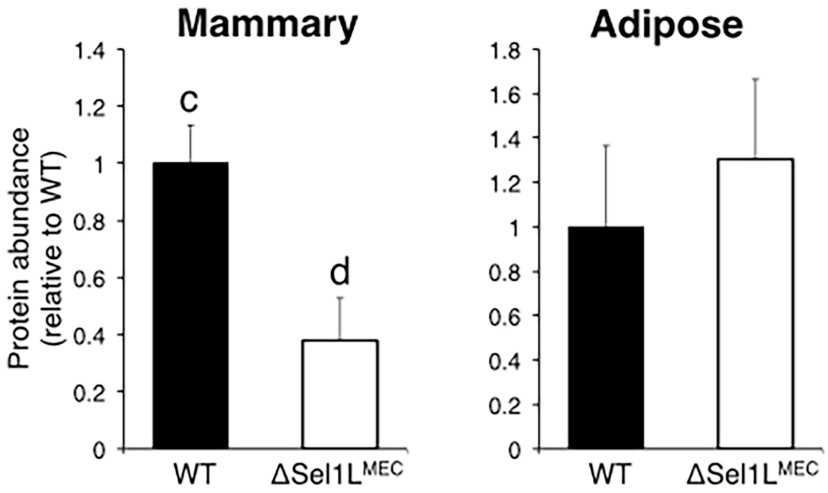

standardized to 9 pups/dam. Maternal genotype had no effect on pup weight on day 1 of lactation. More importantly, over the course of lactation, a growth difference was observed such that the average pup weight nursing from ΔSel1L^{MEC} dams was 10% less than that of pups nursing from WT dams on L14 (Figure 4.5, Genotype $P < 0.0001$). To further understand the lactation attenuation observed in ΔSel1L^{MEC} dams, we examined mammary gland morphology at L14 by whole mount and H&E staining (Figure 4.6). Whole mount analyses did not reveal any difference between WT and ΔSel1L^{MEC} dams in terms of ductal branching and alveolar density (Figure 4.6A). Likewise, alveolar structure and size were unaffected by genotype (Figure 4.6B). These results show that the absence of Sel1L had no obvious impact on the mammary epithelial compartment but nevertheless results in a slight impairment of MEC lactational ability.

To determine whether absence of Sel1L altered milk composition, milk was collected from WT and ΔSel1L^{MEC} female mice at L14. The content of the major osmotic regulator of milk, lactose, tended to be reduced by 17% in milk collected from ΔSel1L^{MEC} female mice (Figure 4.7A, $P < 0.08$), suggesting the possibility of a reduction in milk volume. In contrast, milk protein and fat contents were unaltered. Further analysis of milk by SDS-PAGE and gas chromatography, did not reveal genotype effects on individual proteins or fatty acids (Figure 4.7B and results not shown). With respect to fatty acids, the lack of a genotype effect was also evident when they were grouped according to

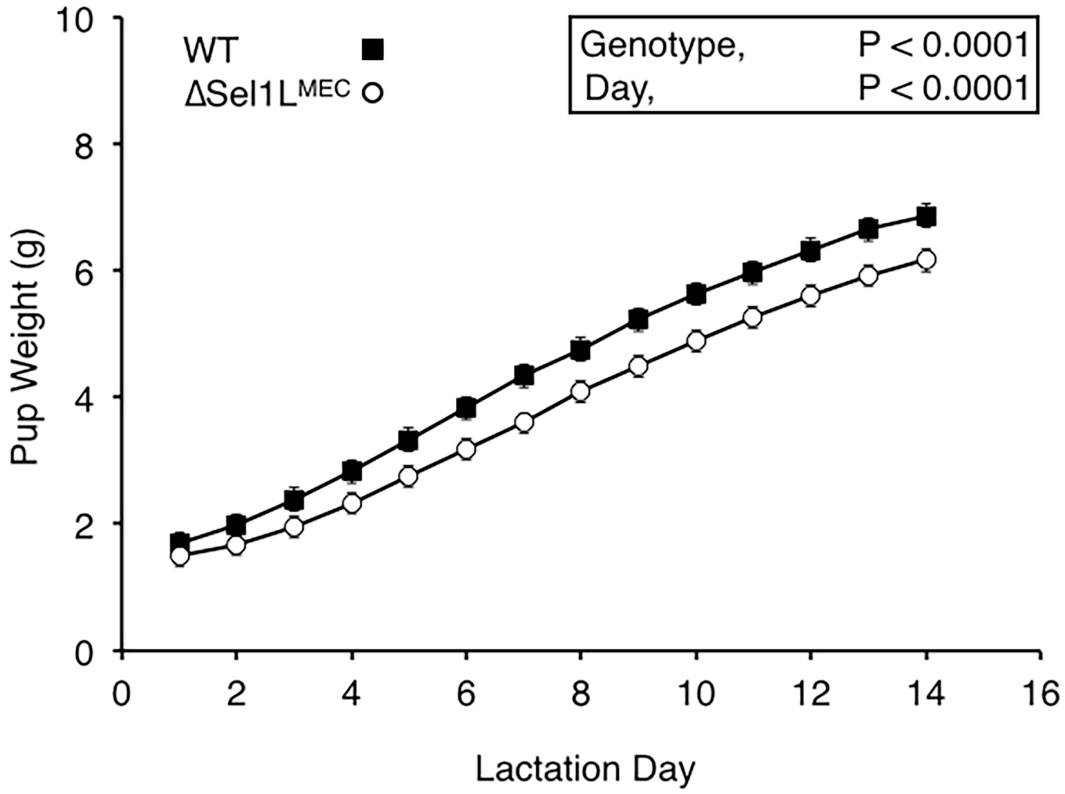

Figure 4.5 Effect of mammary specific ablation of Sel1L on pup growth.

Mice harboring wild type Sel1L (WT) or null Sel1L in mammary epithelial cells ($\Delta Sel1L^{MEC}$) were studied between day 1 and 14 of lactation (n=6-7 dams for each genotype). Litters were standardized to 9 pups and weighed each day. Each curve represents the average weight of individual pups nursing from either WT dams or $\Delta Sel1L^{MEC}$ dams. The significant effects of genotype and day are reported.

Figure 4.6 Effect of mammary specific ablation of Sel1L on mammary gland morphology.

Mice harboring wild type Sel1L (WT) or null Sel1L in mammary epithelial cells ($\Delta Sel1L^{MEC}$) were sacrificed on lactation day 14 (n=6-8 dams for each genotype). The fourth mammary gland was collected for analysis. **(A)** Glands were analyzed by whole mount and photographed at low magnification. A single representative photograph is shown for each genotype. **(B)** Hematoxylin and eosin (H&E) stained mammary gland sections were photographed at 10X magnification (all images) and 40X magnification (bottom right hand corner). A single representative photograph is shown for each genotype.

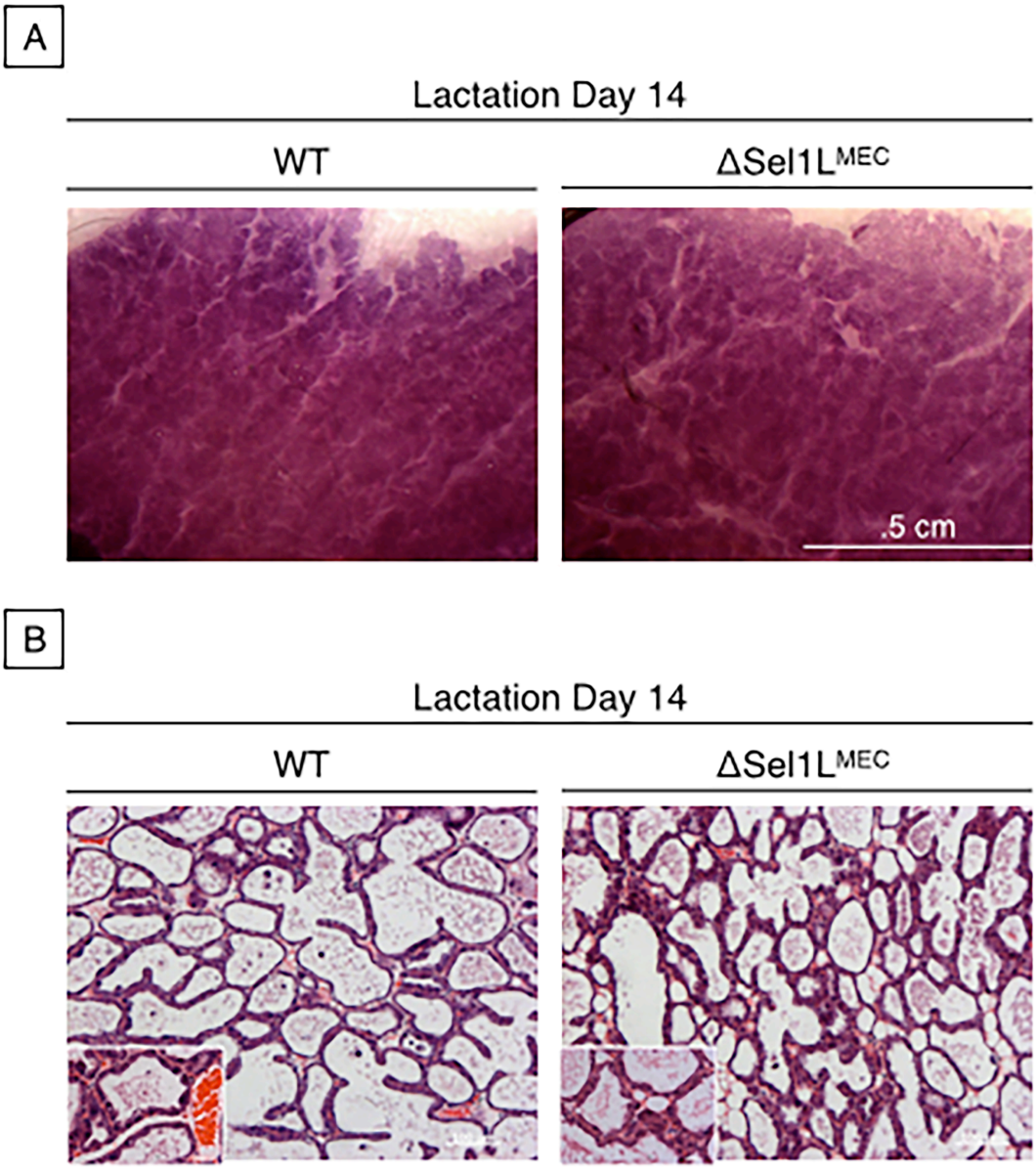
A
Lactation Day 14
WT
ΔSel1L^MEC
.5 cm
B
Lactation Day 14
WT
ΔSel1L^MEC

Figure 4.7 Effect of mammary specific ablation of Sel1L on milk composition.

Mice harboring wild type Sel1L (WT) or null Sel1L in mammary epithelial cells ($\Delta Sel1L^{MEC}$) were studied on day 14 of lactation. **(A)** Milk was collected from WT or $\Delta Sel1L^{MEC}$ dams and analyzed for lactose, protein, and fat content. Bars represent the mean ± SE of the indicated milk component (n=4-7 dams per genotype). [a,b] $P<0.08$. **(B)** Milk was analyzed by SDS-PAGE and Coomassie blue staining (n=5 per genotype). Two representative samples are shown for each genotype. Position of the molecular weight markers are shown on the left whereas identity of milk proteins is given on the right (Lf: lactoferrin, SA: serum albumin, α-CSN: α-casein, β-CSN: β-casein, γ-CSN: γ-casein, ε-CSN: ε-casein, WAP: whey acidic protein). **(C)** The fatty acid profile of milk was analyzed by gas chromatography (n=6-7 dams for each genotype). Fatty acids were grouped by categories reflecting their chain length [less than 16 carbons (C<16), exactly 16 carbons (C=16), or more than 16 carbons (C>16)] and each category was expressed as a % of total fatty acids.

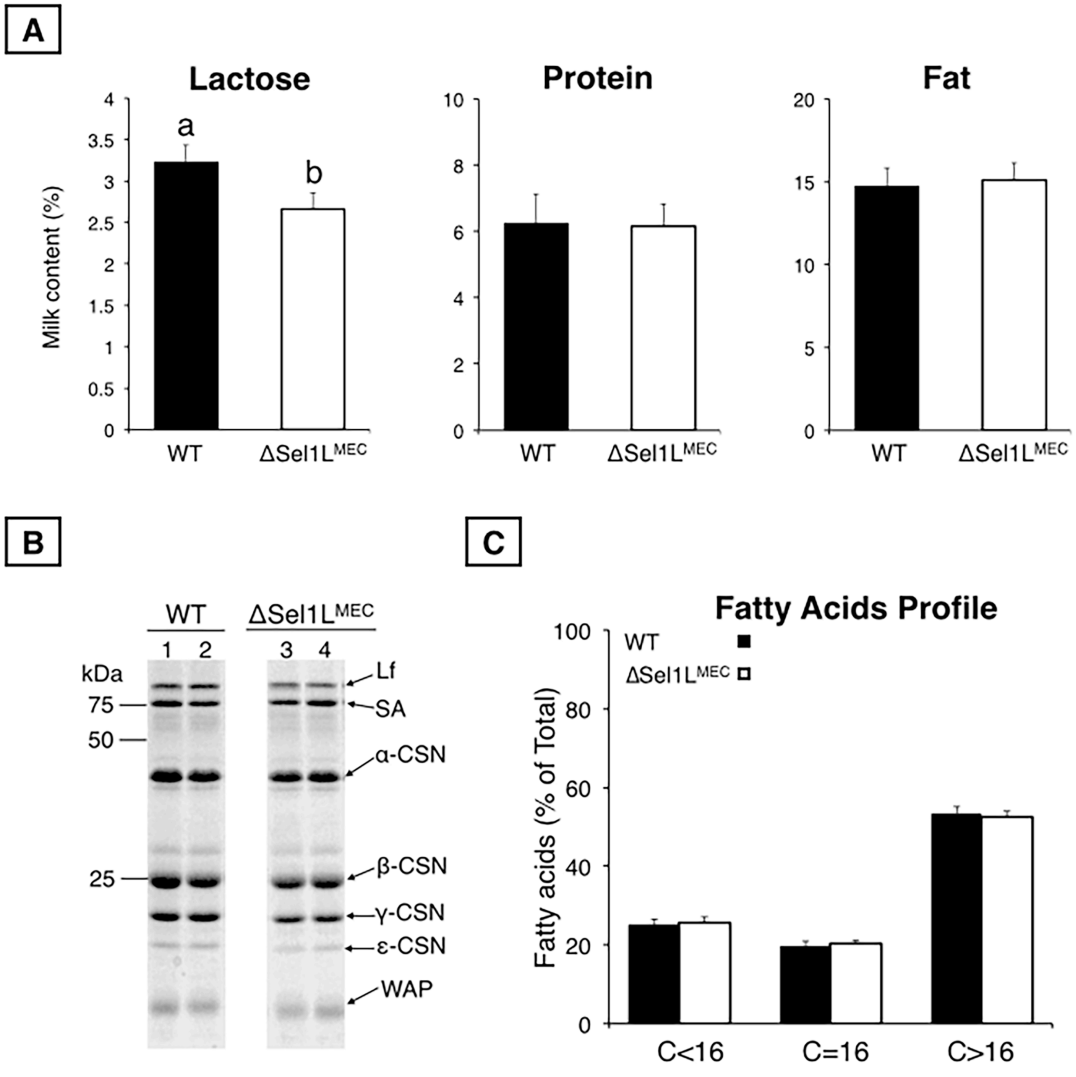
A
Lactose
Protein
Fat
Milk content (%)
a
b
WT
ΔSel1L^MEC
B
C
WT
ΔSel1L^MEC
1 2
3 4
kDa
75
50
25
Lf
SA
α-CSN
β-CSN
γ-CSN
ε-CSN
WAP
Fatty Acids Profile
Fatty acids (% of Total)
C<16
C=16
C>16

their origin (mammary origin, C<16; mammary and non-mammary origin, C=16; non-mammary origin, C>16) (Figure 4.7C). Lower lactose in absence of changes in milk protein and fat raise the possibility that a reduction in milk volume could contribute to the attenuation of pup growth.

Finally, we investigated whether Sel1L ablation in MEC influenced expression of genes related to milk synthesis. Expression of the gene encoding the glucose acceptor protein of the lactose synthase complex (*α-lalba*) was not affected by genotype (Figure 4.8A). Expression of the mammary specific proteins β casein (β-*Csn)* and whey acidic protein (*WAP*) were significantly reduced in ΔSel1L^{MEC} mammary glands compared to WT glands by 27% and 37% respectively (Figure 4.8A, $P < 0.05$). Sel1L ablation also decreased expression of two genes involved in fatty acid synthesis (Figure 4.8B, *Fasn,* $P < 0.095$*; Scd1,* $P < 0.05$*)* but had no effect on two other genes involved in this pathway (*Dgat1, LPL*). Taken together, milk volume reduction combined with lower expression of genes involved in protein and fatty acid synthesis may explain the absence of a genotype effect on milk protein and fat content.

Sel1L ablation induces markers of ER stress and abnormal ER morphology

Absence of Sel1L in hepatocytes and pancreatic acinar cells resulted in dilated ER morphology (10, 20). To assess whether Sel1L ablation influenced

Figure 4.8 Effect of mammary specific ablation of Sel1L on expression of genes engaged in the synthesis of organic milk components.

Mammary glands (MG) were collected on day 14 of lactation from dams harboring wild type (WT) or null Sel1L in mammary epithelial cells ($\Delta Sel1L^{MEC}$). Total RNA was isolated and analyzed by quantitative RT-PCR for expression of genes involved in **A:** synthesis of milk proteins [α-lactalbumin (*α-lalba*), β-casein (*β-Csn*), and whey acidic protein (*WAP*)], **B:** synthesis of milk lipids [fatty acid synthase (*Fasn*), stearoyl-Coenzyme A desaturase 1 (*SCD1*), diacylglycerol O-acyltransferase 1 (*Dgat1*), and lipoprotein lipase (*LPL*)]. For each gene, expression is relative to WT mRNA with bars representing the mean ± SE of indicated mRNA abundance (n=6-8 dams for each genotype). ^{a,b} $P<0.05$. ^{c,d} $P<0.095$.

A **Synthesis of lactose and milk proteins**

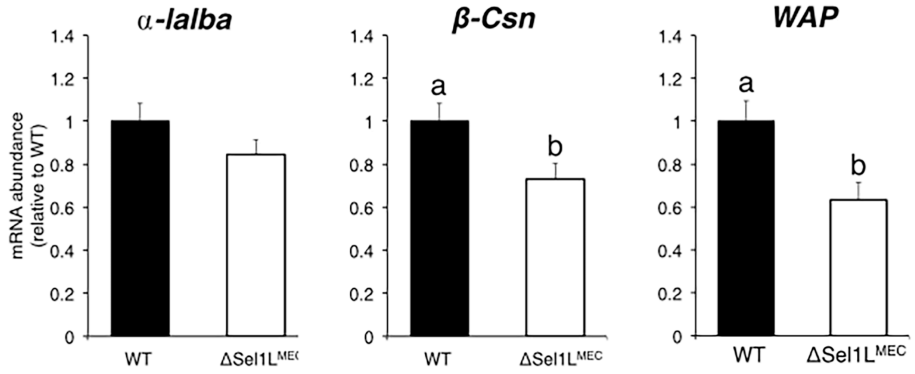

B **Synthesis of milk lipids**

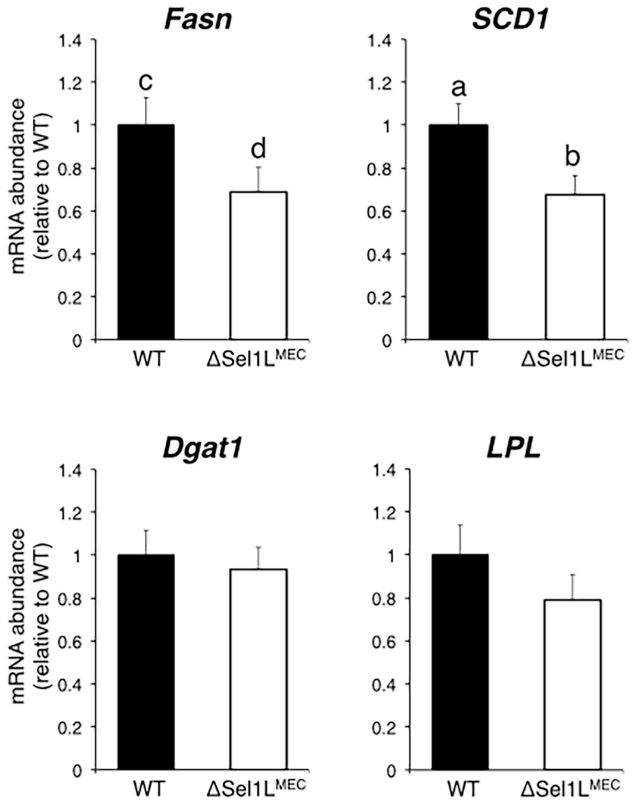

ER morphology in MEC, transmission electron microscopy (TEM) analysis was performed on L14 mammary glands. In WT MEC, a dense network of ER ribbons was evident throughout the cellular space (Figure 4.9). ΔSel1L^{MEC} MEC also displayed a prominent ER compartment but it appears as a collection of dilated structures rather than stacks of ribbons.

The abnormal ER morphology seen in other cell types after Sel1L ablation is associated with an ER stress response (10, 20). Accordingly, we evaluated mammary transcript abundance of markers of ER stress response in WT and ΔSel1L^{MEC} mammary glands at L14. Spliced *XBP1* and *Bip* mRNA abundance were elevated 50% and 55%, respectively, in ΔSel1L^{MEC} mammary glands (Figure 4.10A; $P < 0.05$ or less). Furthermore, absence of Sel1L resulted in upregulation of *CHOP* mRNA transcripts in ΔSel1L^{MEC} mammary glands compared to WT glands (Figure 4.10A, $P < 0.05$). To confirm these results, mammary tissues collected at L14 were also analyzed by Western blotting (Figure 4.10B). Similar to Bip transcripts, Bip protein abundance was elevated 67% in ΔSel1L^{MEC} mammary glands compared to WT mammary glands (Figure 4.10B, $P < 0.005$). Furthermore, IREα protein abundance tended to be increased in ΔSel1L^{MEC} mammary glands (Figure 4.10B, $P < 0.09$). Taken together, these results indicate that absence of Sel1L triggered an ER stress response.

Mammary response to physiological stress in absence of Sel1L

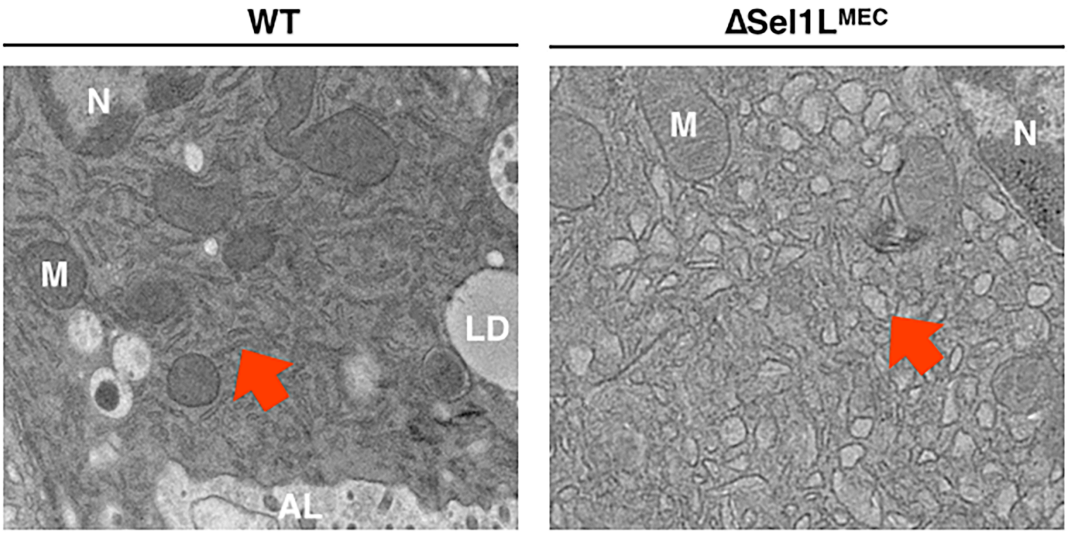

Figure 4.9 Effect of mammary specific ablation of Sel1L on ER morphology.

Mice harboring wild type Sel1L (WT) or null Sel1L in mammary epithelial cells (ΔSel1L^{MEC}) were sacrificed on lactation day 14. The third mammary gland was collected and analyzed by transmission electron microscopy (n=2-3 dams per genotype). A representative image is shown for each genotype. Nucleus (N), lipid droplet (LD), mitochondria (M), and alveolar lumen (AL) are labeled. ER structures are shown by red arrows.

Figure 4.10 Effect of mammary specific ablation of Sel1L on markers of ER stress response.

Dams harboring wild type Sel1L (WT) or null Sel1L in mammary epithelial cells ($\Delta Sel1L^{MEC}$) were studied on day 14 of lactation. **(A)** Total RNA was isolated from the fourth mammary glands and analyzed by quantitative RT-PCR for expression of genes indicative of ER stress [spliced X-box binding protein (*spliced XBP1),* heat shock protein 5 (*Bip*), DNA-damage inducible transcript 3 (*CHOP*)]. For each gene, expression is relative to WT mRNA, with bars representing mean ± SE of the indicated mRNA abundance (n=6-8 dams per genotype). ^{a,b} $P<0.005$. ^{c,d} $P<0.05$. **(B)** Mammary gland protein extracts were prepared from the fifth mammary glands and analyzed by western immunoblotting using antibodies specific for IRE1α and Bip. IRE1α and Bip signal was normalized to the actin signal. All samples were run on the same blot. Three representative samples are shown for each genotype. For each protein, expression is relative to WT and each bar represents mean ± SE of indicated protein abundance (n=6 dams per genotype). ^{a,b} $P<0.005$. ^{c,d} $P<0.09$.

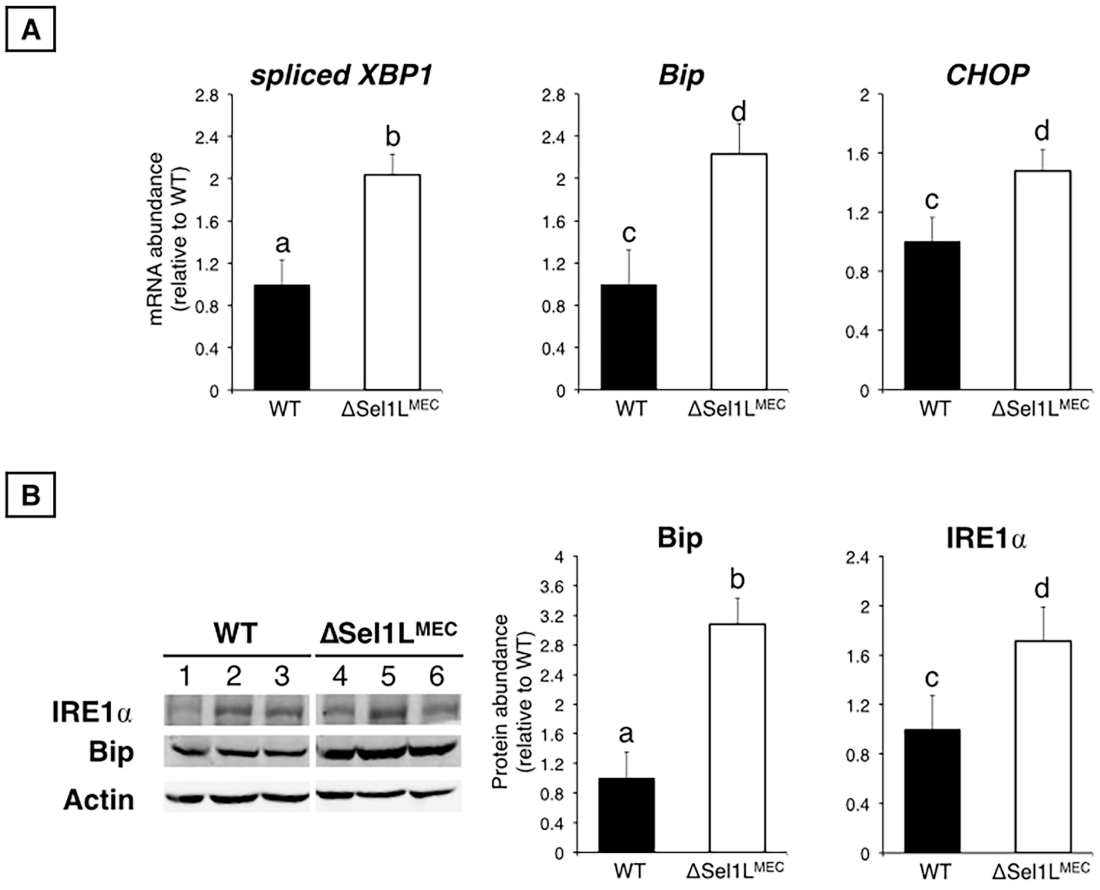
A
spliced XBP1
Bip
CHOP
mRNA abundance (relative to WT)
a
b
c
d
WT
ΔSel1L^MEC
B
WT
ΔSel1L^MEC
1 2 3 4 5 6
IRE1α
Bip
Actin
Bip
IRE1α
Protein abundance (relative to WT)

Finally, we asked whether ablating Sel1L would impair MEC ability to respond to physiological stresses. In a second experiment, litter size was increased to 15 pups to exacerbate the lactational demand (21). Consistent with the results of the first lactation experiment, lack of Sel1L in MEC had no effect on pup weight on the first few days of lactation, but led to a growth deficit over time (Figure 4.11; Genotype, $P < 0.0001$). The growth deficit was only 9% by L15 and thus was not larger than the deficit reported with normal litters (see Figure 4.5). These data indicate that absence of Sel1L did not impair the ability of the mammary gland to meet increased lactational demand.

Given increased expression of the pro-apoptotic signal CHOP in $\Delta Sel1L^{MEC}$ mammary glands (Figure 4.10A), we asked whether absence of Sel1L would accelerate mammary epithelial cell involution upon pup withdrawal. Accordingly, we removed nursing pups at day 10 of lactation (Involution day 0) from WT and $\Delta Sel1L^{MEC}$ dams. Mammary gland morphology was analyzed by whole mount and H&E staining in subsets of mice at day 0, 3, and 6 of involution. Consistent with results at L14 (Figure 4.6), alveolar density and expansion was not impacted by maternal genotype on day 10 of lactation (Involution day 0) (Figures 4.12A and 4.12B). On day 3 of involution, WT glands were characterized by the near absence of expanded alveolar structures and the reappearance of the adipocyte compartment. By day 6 of involution, the alveolar structures were completely collapsed and the adipocyte compartment was predominant. These hallmarks of involution appeared to the

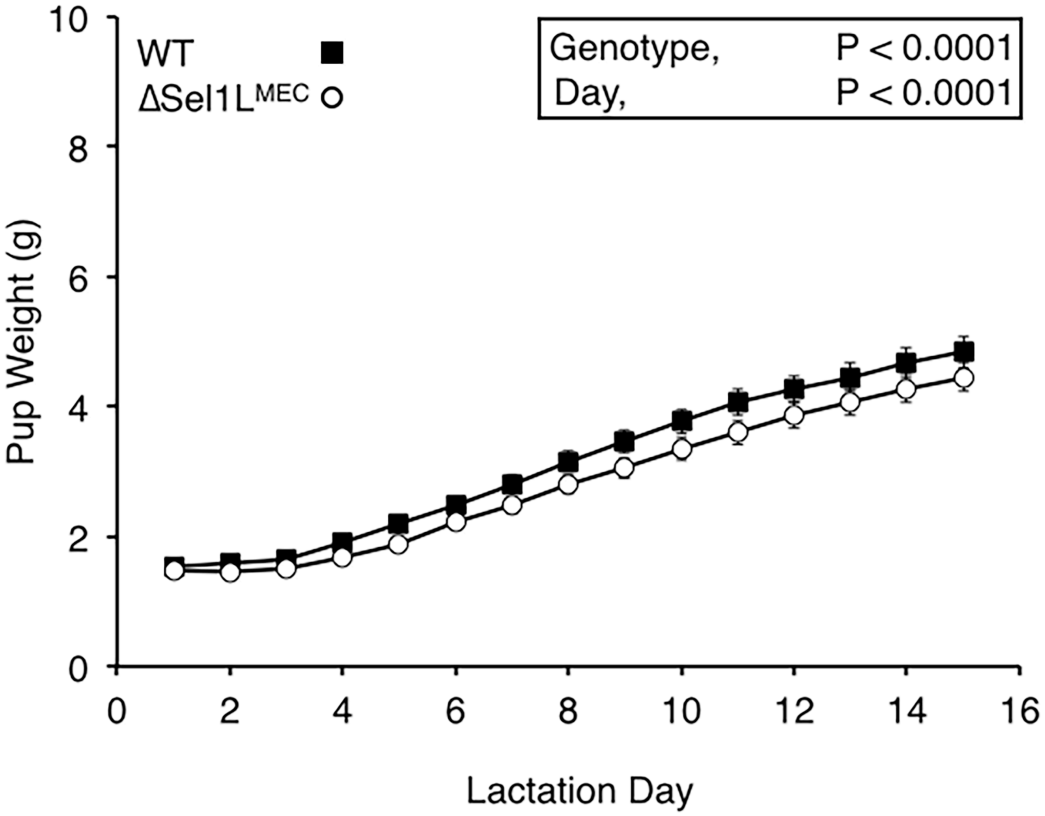

Figure 4.11 Effect of mammary specific ablation of Sel1L on the ability to nurse large litters.

Dams harboring a wild type Sel1L (WT) or null Sel1L in mammary epithelial cells ($\Delta Sel1L^{MEC}$) were studied between day 1 and 15 of lactation (n=3-4 dams for each genotype). Litters were standardized to 15 pups and weighed each day. Each curve represents the average weight of individual pups nursing from either WT dams or $\Delta Sel1L^{MEC}$ dams. The significant effects of genotype and day are reported.

Figure 4.12 Effect of mammary specific ablation of Sel1L on mammary gland involution.

Mice harboring a wild type Sel1L (WT) or null Sel1L in mammary epithelial cells ($\Delta Sel1L^{MEC}$) were studied on day 10 of lactation when pups were removed (involution day 0) and 3 and 6 days laters (involution day 3 and 6). At each time, the fourth mammary gland was collected for analysis (n=2-4 dams for each genotype and involution day). **(A)** Glands were analyzed by the whole mount procedure and photographed at low magnification. A single representative photograph is shown for each combination of genotype and time. **(B)** Hematoxylin and eosin (H&E) stained mammary gland sections were photographed at 10X magnification (all images) and 40X magnification (bottom right hand corner). A single representative photograph is shown for each combination of genotype and time.

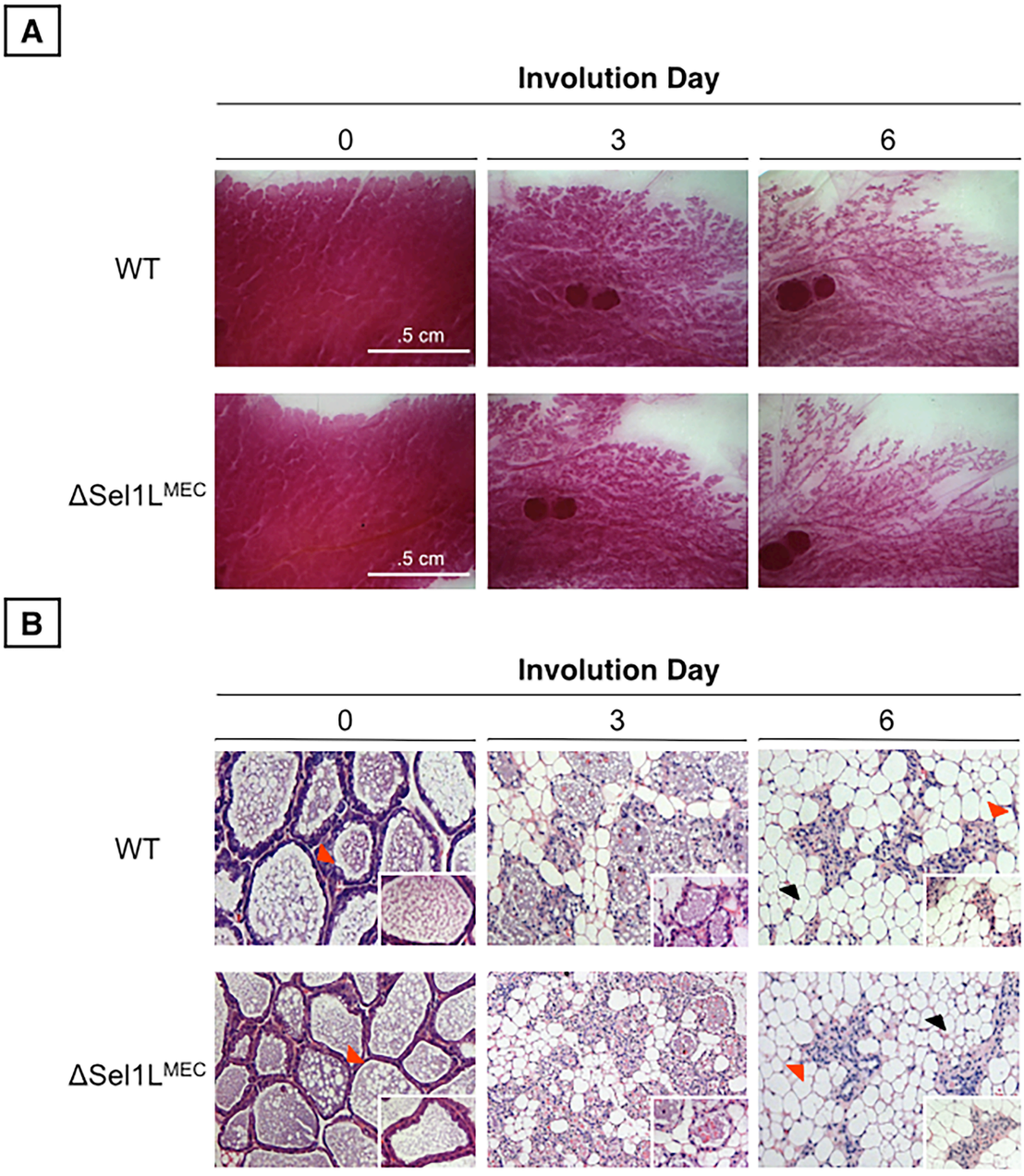
A
Involution Day
0
3
6
WT
.5 cm
ΔSel1L^MEC
.5 cm
B
Involution Day
0
3
6
WT
ΔSel1L^MEC

same extent and time in ΔSel1L^{MEC} mammary glands. Taken together, these data suggest that absence of Sel1L does not increase MEC susceptibility to naturally occurring apoptotic signals.

Discussion

The mouse mammary gland has an exceptional capacity to secrete proteins. This can be illustrated by considering the first two weeks of lactation when milk is the sole source of nutrition for the growing pups (22). During this period, we estimated a protein output of 6.9 grams using litter weight gain (5.15 g) and protein content (13.5%) and efficiency of protein utilization in rodent pups (91%) (21). In other protein secretory cells, the ERAD system plays a critical role in eliminating misfolded and/or improperly modified proteins associated with high protein production (5). For example, ablation of the essential ERAD component Sel1L in the exocrine pancreas reduced production of digestive enzymes, impaired food digestion and absorption, and caused death within 2-3 weeks of ablation (10). As an initial step to determine whether ERAD plays a role in lactation, we asked whether its key components Sel1L, HRD1, and EDEM1 were expressed in MEC during late pregnancy and lactation. Surprisingly, expression levels of all three components peaked during late pregnancy and progressively declined during lactation. Nevertheless, when investigated in the mammary gland on lactation day 14 Sel1L and HRD1 protein abundance was comparable to those seen in liver and gonadal adipose, two tissues recently shown to express high levels of these ERAD components (10). Taken together, the mRNA and protein expression data are consistent with a role for Sel1L and ERAD in the mammary epithelial compartment.

In order to investigate the role of Sel1L in the mammary gland, we generated dams carrying floxed Sel1L alleles in presence of the BLG-Cre transgene, which specifically directs Cre expression to the MEC (23). We assessed the efficiency of BLG-Cre mediated recombination of Sel1L in the mammary gland at both mRNA and protein levels. Both variables confirmed efficient mammary ablation of Sel1L in the mammary gland, but not in liver or adipose on day 14 of lactation. We found that mammary ablation of Sel1L increased HRD1 mRNA but had the opposite effect on HRD1 protein. Similar reciprocal changes were previously reported after Sel1L ablation in the exocrine pancreas and supports the notion that Sel1L stabilizes HRD1 (10).

We previously showed that BLG-Cre mediated recombination is efficient as early as P14 in the MEC (see Chapter 3, Figure 3.3), consistent with BLG-Cre transgene activity as early as P5 in pregnancy (24). Accordingly, it is likely that a substantial degree of ablation was already present in late pregnancy and early lactation. Nevertheless, pup growth over the first two days of lactation was indistinguishable between genotypes. This suggests that Sel1L ablation had no effect on mammary developmental events occurring during late pregnancy, such as expansion of the epithelial compartment and alveolar formation. Analysis of mammary gland morphology during late pregnancy and early lactation would be needed to confirm this inference but we note that no defects in mammary morphology were visible later (L10 or L14).

Over the course of lactation, a modest 10% growth deficit developed in pups nursed by ΔSel1L^{MEC} dams. It is important to note that this deficit was not exacerbated by increasing the litter size from 9 to 15 pups. Analysis of milk organic components along with gene expression alluded to the possibility that a reduction in milk volume contributed to the growth deficit. Specifically, lactose was reduced by 17% in milk collected from ΔSel1L^{MEC} dams. Lactose is the major regulator of osmolarity in most milk, including mouse milk. It does so by driving an influx of water into the golgi. As a result, the rate of lactose synthesis regulates water flux into milk and ultimately determines milk volume (25, 26). Accordingly, a reduction in milk lactose content could lead to a reduction in volume. Moreover, we found reduced expression of genes involved in the synthesis of milk proteins and fatty acids in ΔSel1L^{MEC} mammary glands. Unchanged milk protein and lipid content in ΔSel1L^{MEC} milk could relate to the combination of these two effects (reduced volume and lower synthesis rate of proteins and lipids). The exact mechanism whereby Sel1L depletion could alter milk lactose content is unclear and warrants further investigation.

A recent report identified a functional role for Sel1L in LPL secretion (11). Specifically mice lacking Sel1L in adipose tissue had increased serum TAG levels and liver fat and were protected from obesity when fed a high fat diet. The inability to partition lipids to adipose tissue was traced to defective LPL secretion. Sel1L was shown to physically interact with the LPL maturation

factor. In absence of Sel1L, LPL fails to undergo final maturation and is retained in the ER (11). Intriguingly, LPL is extremely abundant in the lactating mammary gland but whether it is synthesized in MEC or by another cell type remains uncertain (27–29). Irrespective of its origin, mammary LPL is required for mammary extraction of preformed fatty acids present in lipoproteins. These preformed fatty acids account for 50% of C16 fatty acids and all of C>16 fatty acids (25, 28). The proportion of these fatty acids were unaltered in $\Delta Sel1L^{MEC}$ milk, suggesting that LPL is unaffected by Sel1L ablation in MEC.

Absence of Sel1L in MEC was associated with severe disruptions in ER morphology. ER structures appeared as densely packed ribbons in WT MEC whereas a dilated ER morphology was evident in the absence of Sel1L. Similarly fragmented, dilated ER structures were also reported in hepatocytes, adipocytes, and pancreatic acinar cells lacking Sel1L (10, 11, 20). Interestingly, ER dilation in absence of Sel1L causes an ER stress response but is not always associated with an overt phenotype. For example, deleting Sel1L in adipocytes resulted in apparent ER dilation but did not elicit inflammatory or apoptotic responses (11). Collectively, these studies illustrate the commonality that abnormal ER morphology is associated with an ER stress response although the severity of the phenotype differed. Consistent with previous findings, we observed changes of gene expression suggestive of ER stress in $\Delta Sel1L^{MEC}$ mammary glands but no overt negative consequences on lactation or mammary gland morphology. One possible explanation could

relate to the structure of milk proteins. Caseins are mammary specific proteins and constitute the majority of proteins secreted into milk. Some casein proteins are post-translationally modified by phosphorylation or glycosylation (30). However, caseins have very little secondary structure and are secreted loosely folded in a macromolecular complex (30, 31). Thus, even though demands for copious milk protein synthesis and secretion at the onset of lactation could disrupt ER homeostasis in the absence of Sel1L, it is possible that the mammary gland depends primarily on a protein quality control system independent of Sel1L, such as other ERAD complexes or autophagy.

Our gene expression analysis revealed increased *CHOP* mRNA abundance in absence of Sel1L. In other cell types, unmitigated ER stress can trigger apoptotic pathway by promoting the CHOP transcription factor (3, 32). These results suggested the possibility that absence of Sel1L increases susceptibility to apoptosis. MEC apoptosis is the primary mechanism accounting for mammary gland remodeling during involution (19, 33, 34). Involution is characterized by the collapse of alveolar structures and the reappearance of adipocytes (19, 33, 35). To determine whether Sel1L ablation promotes apoptosis, we provoked involution by removing pups during establish lactation. Involuting mammary gland morpholgy was similar regardless of presence or absence of Sel1L.

In summary, our results show that absence of Sel1L in MEC disrupts ER morphology and elicits ER stress. Despite these obvious defects, the

attenuation of lactation was very modest and appeared to relate to a reduction in milk volume.

References

1. Fagone, P., and Jackowski, S. (2009) Membrane phospholipid synthesis and endoplasmic reticulum function. *J. Lipid Res.* **50 Suppl**, S311–6

2. Fu, S., Watkins, S. M., and Hotamisligil, G. S. (2012) The role of endoplasmic reticulum in hepatic lipid homeostasis and stress signaling. *Cell Metab.* **15**, 623–34

3. Cao, S. S., and Kaufman, R. J. (2012) Unfolded protein response. *Curr. Biol.* **22**, R622–R626

4. Smith, M. H., Ploegh, H. L., and Weissman, J. S. (2011) Road to ruin: targeting proteins for degradation in the endoplasmic reticulum. *Science* **334**, 1086–90

5. Olzmann, J. A., Kopito, R. R., and Christianson, J. C. (2013) The Mammalian Endoplasmic Reticulum-Associated Degradation System. *Cold Spring Harb. Perspect. Biol.* **5**, 1–17

6. Carvalho, P., Goder, V., and Rapoport, T. A. (2006) Distinct ubiquitin-ligase complexes define convergent pathways for the degradation of ER proteins. *Cell* **126**, 361–73

7. Bernasconi, R., Galli, C., Calanca, V., Nakajima, T., and Molinari, M. (2010) Stringent requirement for HRD1, SEL1L, and OS-9/XTP3-B for disposal of ERAD-LS substrates. *J. Cell Biol.* **188**, 223–35

8. Cormier, J. H., Tamura, T., Sunryd, J. C., and Hebert, D. N. (2009) EDEM1 recognition and delivery of misfolded proteins to the SEL1L-containing ERAD complex. *Mol. Cell* **34**, 627–633

9. Mueller, B., Klemm, E. J., Spooner, E., Claessen, J. H., and Ploegh, H. L. (2008) SEL1L nucleates a protein complex required for dislocation of misfolded glycoproteins. *Proc. Natl. Acad. Sci.* **105**, 12325–12330

10. Sun, S., Shi, G., Han, X., Francisco, A. B., Ji, Y., Mendonça, N., Liu, X., Locasale, J. W., Simpson, K. W., Duhamel, G. E., Kersten, S., Iii, J. R. Y., Long, Q., and Qi, L. (2014) Sel1L is indispensable for mammalian endoplasmic reticulum-associated degradation, endoplasmic reticulum homeostasis, and survival. *Proc. Natl. Acad. Sci. U. S. A.* **111**, 6115

11. Sha, H., Sun, S., Francisco, A. B., Ehrhardt, N., Xue, Z., Liu, L., Lawrence, P., Mattijssen, F., Guber, R. D., Panhwar, M. S., Brenna, J. T., Shi, H., Xue, B., Kersten, S., Bensadoun, A., Péterfy, M., Long, Q., and Qi, L. (2014) The ER-associated degradation adaptor protein Sel1L regulates LPL secretion and lipid metabolism. *Cell Metab.* **20**, 458–70

12. Francisco, A. B., Singh, R., Sha, H., Yan, X., Qi, L., Lei, X., and Long, Q. (2011) Haploid insufficiency of suppressor enhancer Lin12 1-like (SEL1L) protein predisposes mice to high fat diet-induced hyperglycemia. *J. Biol. Chem.* **286**, 22275–82

13. Yazinski, S. A., Westcott, P. M. K., Ong, K., Pinkas, J., Peters, R. M., and Weiss, R. S. (2009) Dual inactivation of Hus1 and p53 in the mouse mammary gland results in accumulation of damaged cells and impaired tissue regeneration. *Proc. Natl. Acad. Sci. U. S. A.* **106**, 21282–7

14. Boumahrou, N., Andrei, S., Miranda, G., Henry, C., Panthier, J. J., Martin, P., and Bellier, S. (2009) The major protein fraction of mouse milk revisited using proven proteomic tools. *J. Physiol. Pharmacol.* **60**, 113–1118

15. Hussein, M., Harvatine, K. J., Boisclair, Y. R., and Bauman, D. E. (2013) Supplementation with fish oil as a source of n-3 fatty acids does not downregulate mammary lipogenesis in lactating mice. *J. Nutr.* **143**, 1913–9

16. Perfield, J. W., Delmonte, P., Lock, A. L., Yurawecz, M. P., and Bauman, D. E. (2006) Trans-10, trans-12 conjugated linoleic acid does not affect milk fat yield but reduces delta9-desaturase index in dairy cows. *J. Dairy Sci.* **89**, 2559–2566

17. Rudolph, M. C., Wellberg, E. A., and Anderson, S. M. (2009) Adipose-depleted mammary epithelial cells and organoids. *J. Mammary Gland Biol. Neoplasia* **14**, 381–6

18. Thorn, S. R., Giesy, S. L., Myers, M. G., and Boisclair, Y. R. (2010) Mammary ductal growth is impaired in mice lacking leptin-dependent signal transducer and activator of transcription 3 signaling. *Endocrinology* **151**, 3985–95

19. Richert, M. M., Schwertfeger, K. L., Ryder, J. W., and Anderson, S. M. (2000) An atlas of mouse mammary gland development. *J. Mammary Gland Biol. Neoplasia* **5**, 227–41

20. Francisco, A. B., Singh, R., Li, S., Vani, A. K., Yang, L., Munroe, R. J., Diaferia, G., Cardano, M., Biunno, I., Qi, L., Schimenti, J. C., and Long, Q. (2010) Deficiency of suppressor enhancer Lin12 1 like (SEL1L) in mice leads to systemic endoplasmic reticulum stress and embryonic lethality. *J. Biol. Chem.* **285**, 13694–703

21. Fiorotto, M. L., Burrin, D. G., Perez, M., and Reeds, P. J. (1991) Intake and use of milk nutrients by rat pups suckled in small, medium, or large litters. *Am. J. Physiol.* **260**, R1104–R1113

22. Anderson, S. M., Rudolph, M. C., McManaman, J. L., and Neville, M. C. (2007) Secretory activation in the mammary gland: it's not just about milk protein synthesis! *Breast Cancer Res.* **9**, 204

23. Selbert, S., Bentley, D. J., Melton, D. W., Rannie, D., Lourenço, P., Watson, C. J., and Clarke, A. R. (1998) Efficient BLG-Cre mediated gene deletion in the mammary gland. *Transgenic Res.* **7**, 387–96

24. Neville, M. C., Webb, P., Ramanathan, P., Mannino, M. P., Pecorini, C., Monks, J., Anderson, S. M., and MacLean, P. (2013) The insulin receptor plays an important role in secretory differentiation in the mammary gland. *Am. J. Physiol. Endocrinol. Metab.* **305**, E1103–14

25. Neville, M. C. (1990) The physiological basis of milk secretion. *Ann. N. Y. Acad. Sci.* **586**, 1–11

26. McManaman, J. L., Reyland, M. E., and Thrower, E. C. (2006) Secretion and Fluid Transport Mechanisms in the Mammary Gland: Comparisons with the Exocrine Pancreas and the Salivary Gland. *J. Mammary Gland Biol. Neoplasia* **11**, 249–268

27. Wang, Y., Tong, J., Li, S., Zhang, R., Chen, L., Wang, Y., Zheng, M., Wang, M., Liu, G., Dai, Y., Zhao, Y., and Li, N. (2011) Over-expression of human lipoprotein lipase in mouse mammary glands leads to reduction of milk triglyceride and delayed growth of suckling pups. *PLoS One* **6**, e20895

28. Neville, M. C., and Picciano, M. F. (1997) Regulation of Milk Lipid Secretion and Composition. *Annu. Rev. Nutr.* **17**, 159–184

29. Jensen, D. R., Gavigan, S., Sawicki, V., Witsell, D. L., Eckel, R. H., and Neville, M. C. (1994) Regulation of lipoprotein lipase activity and mRNA in the mammary gland of the lactating mouse. *Biochem. J.* **298**, 321–327

30. Ginger, M. R., and Grigor, M. R. (1999) Comparative aspects of milk caseins. *Comp. Biochem. Physiol. B. Biochem. Mol. Biol.* **124**, 133–45

31. Sakono, M., Motomura, K., Maruyama, T., Kamiya, N., and Goto, M. (2011) Alpha casein micelles show not only molecular chaperone-like aggregation inhibition properties but also protein refolding activity from the denatured state. *Biochem. Biophys. Res. Commun.* **404**, 494–7

32. Walter, P., and Ron, D. (2011) The unfolded protein response: from stress pathway to homeostatic regulation. *Science* **334**, 1081–6

33. Chapman, R. S., Lourenco, P. C., Tonner, E., Flint, D. J., Selbert, S., Takeda, K., Akira, S., Clarke, A. R., and Watson, C. J. (1999) Suppression of epithelial apoptosis and delayed mammary gland involution in mice with a conditional knockout of Stat3. **6**, 2604–2616

34. Ning, Y., Hoang, B., Schuller, A. G. P., Cominski, T. P., Hsu, M.-S., Wood, T. L., and Pintar, J. E. (2007) Delayed mammary gland involution in mice with mutation of the insulin-like growth factor binding protein 5 gene. *Endocrinology* **148**, 2138–47

35. Uejyo, T., Kuki, C., Oyama, S., Kumura, H., and Kobayashi, K. (2015) Early down-regulation of milk production after weaning by pup removal and prior to involution in mouse mammary glands. *Cell Tissue Res.* **359**, 643–653

CHAPTER 5

SUMMARY AND CONCLUSIONS

The mammary gland is an extraordinarily efficient organ in terms of synthesis and secretion of both proteins and lipids (1). The ER is intimately involved in the synthesis of these organic milk components, and yet little is known about the processes ensuring its biogenesis and homeostasis in the mammary gland. The maintenance of ER function is integral for secretory cells. In order to preserve ER homeostasis, the biosynthetic capacity of the ER must match its export demands. Imbalances in ER homeostasis are inevitable in secretory cells that undergo periods of heightened synthesis (2–4). Accordingly, cells rely on adaptive systems, such as UPR and ERAD, to restore ER homeostasis (5–7). Furthermore, recent evidence implicates XBP1 and Sel1L, two vital components of the UPR and ERAD homeostatic systems respectively in maintaining ER function in secretory cells (8–13).

In this work, we investigated whether these two homeostatic systems are essential for initiating and sustaining lactation. To this end, we generated experimental models whereby XBP1 and Sel1L were specifically ablated in the mouse mammary epithelium during lactation. Overall, our findings indicate that XBP1 and Sel1L expression is regulated in the MEC during pregnancy and lactation, with expression at the highest during late pregnancy and declining

during lactation. These findings demonstrate that XBP1 and Sel1L expression peaks when the MEC acquires the capability to secrete copious amounts of organic milk components.

In our first experiment, we examined whether XBP1 is required for the function of the MEC during lactation. Sudden and intense increase in milk synthesis could perturb the ER luminal environment and the UPR signaling cascade could be essential for restoring ER homeostasis in MEC during lactation. To date, the only UPR signaling component studied in the context of lactation was the ER transmembrane stress sensor, PERK (14). Specifically ablating PERK in the MEC resulted in decreased pup growth and unfilled alveolar structures, similar to our findings. Moreover, they reported that PERK was required for normal expression of lipogenic genes. However, it is important to note that analysis of mRNA in this study was conducted using the whole mammary gland tissue even though the adipose tissue compartment persisted in the mammary gland of dams lacking PERK. Finally, this group ablated PERK with the MMTV-Cre recombinase. One of the two existing MMTV-Cre lines was recently shown to impair lactation in absence of any other effects (15). It is unclear which of the two MMTV-Cre founding lines was used in the PERK study (14).

Our findings demonstrate that milk composition was slightly altered in the absence of XBP1, however, not to the extent needed to explain the 80% pup growth deficit. Notably, there was a substantial lack of organized ER

structures. The mammary epithelial compartment was reduced in the absence of XBP1, which corresponded to reciprocal changes in proliferation and apoptosis. Furthermore, XBP1 ablation resulted in a mammary gland morphology that resembled involuting mammary glands. This was supported by increased expression of signaling events associated with apoptosis (*CHOP)* and mammary involution (phosphorylated STAT3). Taken together, this experiment illustrates that XBP1 is indispensable for ER biogenesis and expansion event that occurs during lactation in MEC. Thus, the biosynthetic capacity of the ER was impaired in the absence of XBP1 and this led to a smaller mammary epithelial cell compartment and severely impaired lactation.

In our second experiment, we examined whether a functional ERAD system is necessary in MEC by specifically ablating Sel1L. Despite abnormal ER morphology and ER stress response, an overt negative consequence in lactational ability was not seen. In contrast to our findings with XBP1 ablation in the MEC, Sel1L ablation did not appear to affect mammary gland development. Milk composition together with gene expression analysis suggested the possibility that milk volume was reduced and accounted for the modest 10% pup growth deficit. Taken together, our findings indicate that Sel1L plays a dispensable role in MEC.

Although our experiment did not reveal an overt phenotype, it is possible that ERAD is not functionally required in the MEC. One way to determine whether a competent mammary ERAD system may be needed is to

exploit the biosynthetic capacity of the mammary gland to synthesize non-mammary proteins. For example, Sel1L is required for insulin secretion in pancreatic β-cells and transgenic mice overexpressing human proinsulin in the mammary gland were recently described (16, 17). In these transgenic mice, human proinsulin is secreted in milk. ΔSel1L^{MEC} mice overexpressing proinsulin could serve as an experimental model to determine the functionality of ERAD in the mammary gland. Lack of an apparent lactation defect in this experimental model would suggest that the mammary could depend on a protein quality control system independent of Sel1L, such as other ERAD complexes or autophagy.

Overall, these experiments contribute new knowledge to the mechanisms that initiate and sustain lactation as well as provide a more comprehensive view of the roles of XBP1 and Sel1L in sustaining MEC secretory activity.

References

1. Anderson, S. M., Rudolph, M. C., McManaman, J. L., and Neville, M. C. (2007) Secretory activation in the mammary gland: it's not just about milk protein synthesis! *Breast Cancer Res.* **9**, 204

2. Fagone, P., and Jackowski, S. (2009) Membrane phospholipid synthesis and endoplasmic reticulum function. *J. Lipid Res.* **50 Suppl**, S311–6

3. Fu, S., Watkins, S. M., and Hotamisligil, G. S. (2012) The role of endoplasmic reticulum in hepatic lipid homeostasis and stress signaling. *Cell Metab.* **15**, 623–34

4. Lagace, T. A., and Ridgway, N. D. (2013) The role of phospholipids in the biological activity and structure of the endoplasmic reticulum. *Biochim. Biophys. Acta* **1833**, 2499–510

5. Cao, S. S., and Kaufman, R. J. (2012) Unfolded protein response. *Curr. Biol.* **22**, R622–R626

6. Ron, D., and Walter, P. (2007) Signal integration in the endoplasmic reticulum unfolded protein response. *Nat. Rev. Mol. Cell Biol.* **8**, 519–29

7. Olzmann, J. A., Kopito, R. R., and Christianson, J. C. (2013) The Mammalian Endoplasmic Reticulum-Associated Degradation System. *Cold Spring Harb. Perspect. Biol.* **5**, 1–17

8. Moore, K., and Hollien, J. (2012) The unfolded protein response in secretory cell function. *Annu. Rev. Genet.* **46**, 165–83

9. Lee, A.-H., Scapa, E. F., Cohen, D. E., and Glimcher, L. H. (2008) Regulation of hepatic lipogenesis by the transcription factor XBP1. *Science* **320**, 1492–6

10. Gregor, M. F., Misch, E. S., Yang, L., Hummasti, S., Inouye, K. E., Lee, A.-H., Bierie, B., and Hotamisligil, G. S. (2013) The Role of Adipocyte XBP1 in Metabolic Regulation during Lactation. *Cell Rep.* **3**, 1430–9

11. Wang, S., Chen, Z., Lam, V., Han, J., Hassler, J., Finck, B. N., Davidson, N. O., and Kaufman, R. J. (2012) IRE1α-XBP1s Induces PDI

Expression to Increase MTP Activity for Hepatic VLDL Assembly and Lipid Homeostasis. *Cell Metab.* **16**, 473–86

12. Sha, H., Sun, S., Francisco, A. B., Ehrhardt, N., Xue, Z., Liu, L., Lawrence, P., Mattijssen, F., Guber, R. D., Panhwar, M. S., Brenna, J. T., Shi, H., Xue, B., Kersten, S., Bensadoun, A., Péterfy, M., Long, Q., and Qi, L. (2014) The ER-associated degradation adaptor protein Sel1L regulates LPL secretion and lipid metabolism. *Cell Metab.* **20**, 458–70

13. Sun, S., Shi, G., Han, X., Francisco, A. B., Ji, Y., Mendonça, N., Liu, X., Locasale, J. W., Simpson, K. W., Duhamel, G. E., Kersten, S., Iii, J. R. Y., Long, Q., and Qi, L. (2014) Sel1L is indispensable for mammalian endoplasmic reticulum-associated degradation, endoplasmic reticulum homeostasis, and survival. *Proc. Natl. Acad. Sci. U. S. A.* **111**, 6115

14. Bobrovnikova-Marjon, E., Hatzivassiliou, G., Grigoriadou, C., Romero, M., Cavener, D. R., Thompson, C. B., and Diehl, J. A. (2008) PERK-dependent regulation of lipogenesis during mouse mammary gland development and adipocyte differentiation. *Proc. Natl. Acad. Sci. U. S. A.* **105**, 16314–9

15. Yuan, T., Wang, Y., Pao, L., Anderson, S. M., and Gu, H. (2011) Lactation defect in a widely used MMTV-Cre transgenic line of mice. *PLoS One* **6**, e19233

16. Francisco, A. B., Singh, R., Sha, H., Yan, X., Qi, L., Lei, X., and Long, Q. (2011) Haploid insufficiency of suppressor enhancer Lin12 1-like (SEL1L) protein predisposes mice to high fat diet-induced hyperglycemia. *J. Biol. Chem.* **286**, 22275–82

17. Qian, X., Kraft, J., Ni, Y., and Zhao, F.-Q. (2014) Production of recombinant human proinsulin in the milk of transgenic mice. *Sci. Rep.* **4**, 1–8

APPENDIX

Appendix I *Murine primers used in real-time PCR analysis*

Gene	Primer[1]	Product (bp)	Accession No.
α-lact[2]			
F	GTCGGAGAACATCTGTGGCA	74	NM_010679.1
R	TGGCACACGCTATGTCATCA		
B2M[2]			
F	CATGGCTCGCTCGGTGACC	166	NM_009735
R	AATGTGAGGCGGGTGGAACTG		
Bgal			
F	CCCGGCTTGAAGAGCAACTT	110	NM_022305.4
R	ATCAGCATGGGGCCAACGAG		
Bip[3]			
F	CATCCCGTGGCATAAACC	133	NM_001163434
R	GGGACAAACATCAAGCAGTA		
Btn			
F	CTTACCAGCTCCCTTCGTGC	143	NM_013483.3
R	CCTTCTTCCGCAGACTGGAT		
Casein[4]			
F	TCACTCCAGCATCCAGTCACA	126	NM_009972
R	GGCCCAAGAGATGGCACCA		
CHOP[5]			
F	TTCACTACTCTTGACCCTGCGTC	176	NM_007837.3
R	CACTGACCACTCTGTTTCCGTTTC		
Cidea			
F	GGCCGTGTTAAGGAATCTGCT	150	NM_007702.2
R	ATGAACCAGCCTTTGGTGCT		
Dgat1			

F	TAGAAGAGGACGAGGTGCGA	104	NM_010046.2
R	GTCTTTGTCCCGGGTATGGG		
EDEM[3]			
F	CCTGATGTTCTCTTCTACCCT	116	NM_138677
R	AGACTCTGCAGAATGTCCATT		
Erdj3[3]			
F	CTTACGGTTCCGAATCAAA	112	NM_026400
R	CATCTCAAAGCCAACCAGA		
Fasn[2]			
F	AGAGATCCCGAGACGCTTCT	158	NM_007988
R	GCCTGGTAGGCATTCTGTAGT		
Gale[6]			
F	CCATAACGCCATTCGTGGAG	204	NM_178389.3
R	TCCAGAGGCTTCTGCACTGA		
HRD1			
F	GGTATTTGGCTTTGAGTACGCC	115	NM_001164709.1
R	TACAGCCTTGTTGTCCCAGG		
LPL			
F	TCGTCATCGAGAGGATCCGA	162	NM_008509.2
R	TGTTTGTCCAGTGTCAGCCA		
Pcyt1[7]			
F	GATGCACAGAGTTCAGCTAAAGT	129	NM_00116359.1
R	TGGCTGCCGTAAACCAACTG		
Pcyt2[7]			
F	TGTGTTCACGGCAATGACATC	189	NM_024229.2
R	TTCCCGGTACTCAGAGGACAT		
Pemt[7]			
F	TTGGGGATTCGTGTTTGTGCT	118	NM_008819.2
R	CACGCTGAAGGGAAATGTGG		
Perilipin			
F	AGTGTGGGGTCCTTGGGCGT	119	NM_175640.2

R	CCTGCTCAGGGAGGTCTCCATCC		
SCD1[8]			
F	AGATCTCCAGTTCTTACACGACCAC	108	NM_009127
R	GACGGATGTCTTCTTCCAGGTG		
Sel1L[3]			
F	GCCGGGATGAAGATACTGAAT	114	NM_001039089
R	GGACACTCTCTCCAGGGCTTT		
sXBP1[9]			
F	GGTCTGCTGAGTCCGCAGCAGG	311	NM_013842
R	AGGCTTGGTGTATACATGG		
uXBP1			
F	GCCAAGGGGAGTGGAGTAAG	73	NM_013842
R	GCAGAGGTGCACATAGTCTGA		
WAP[10]			
F	CCCGGTTCCTGTGGTAGGA	74	NM_011709.5
R	TTCCAAGGGCAGAAGCCA		
Wfs[11]			
F	CCATCAACATGCTCCCGTTC	64	NM_011716.2
R	GGGTAGGCCTCGCCATACA		
XBP1			
F	CGGAGGAGAAAGCGCTGCGG	89	NM_013842
R	CAGCTCGCTCATCCGGGCTT		
XO			
F	AGAGCGGACCTTGAGGGTAT	115	NM_011723.2
R	CCTTGGGCACCTCTTGGAAA		

[1]Sequence of forward (F) and reverse (R) primer is given in 5' to 3' orientation
[2]Primers reported by Kevin Harvatine Dissertation 2008
[3]Primers reported by Dr. Long's laboratory
[4]Primers reported by Baratta et al (2006)
[5]Primers reported by Laybutt et al (2012)
[6]Primers reported by Scherer et al (2013)
[7]Primers reported by Hotamisligil et al (2011)
[8]Primers reported by Glimcher et al (2008)

[9]Primers reported by Hotamisligil et al (2013)
[10]Primers reported by Rudolph et al (2011)
[11]Primers reported by Urano et al (2009)

Appendix II Efficient isolation of mammary epithelial cell after mammary specific ablation of XBP1.

Mammary epithelial cells (MEC) were isolated from mammary glands of mice harboring null XBP1 in mammary epithelial cells ($\Delta XBP1^{MEC}$) on either pregnancy day 14 (P14), pregnancy day 18 (P18), or lactation day 5 (L5). Total RNA was isolated and analyzed by quantitative RT-PCR for perilipin mRNA abundance in both MG and MEC. At each stage of development, expression is relative to MG mRNA and each bar represents the mean ± SE of perilipin mRNA abundance (n=5-11 for each tissue and development stage). $^{*}P<0.001$.

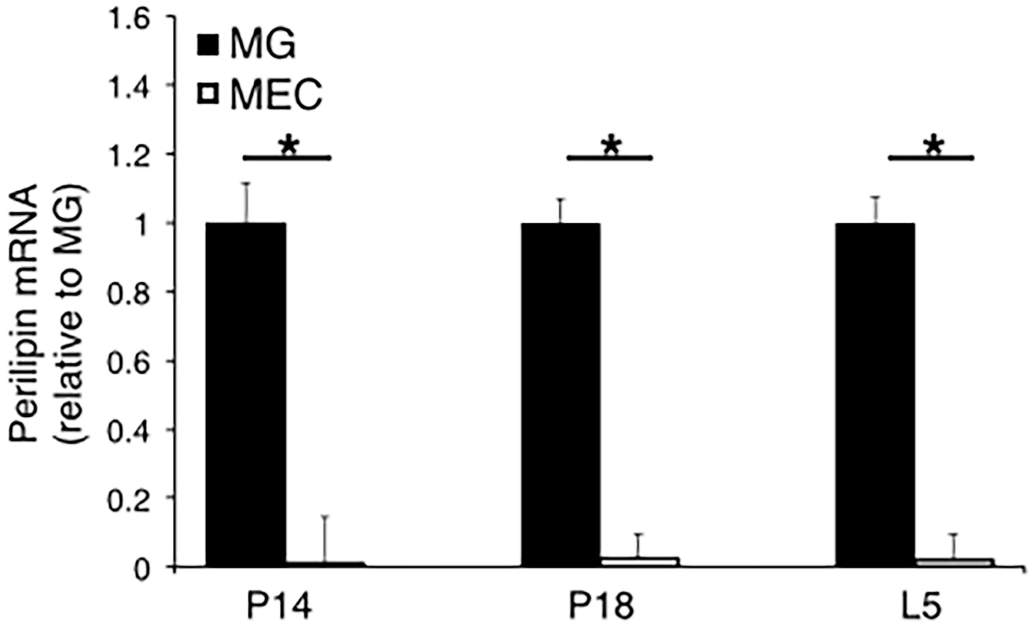
1.6
1.4
1.2
1
0.8
0.6
0.4
0.2
0
MG
MEC
Perilipin mRNA
(relative to MG)
*
*
*
P14
P18
L5

Appendix III Effect of presence of the β-Lactoglobulin transgene on pup growth.

Mice harboring one floxed XBP1 allele in presence of the β-lactoglobulin transgene ($\Delta XBP1^{+/-}$) were studied between day 1 and day 14 of lactation (n=2 dams). Litters were standardized to 8-9 pups and weighed each day. Growth curve of pups nursing from mice harboring wild type XBP1 (WT) or null XBP1 in mammary epithelial cells ($\Delta XBP1^{MEC}$) as shown in Figure 3.3 are displayed for comparison purposes. Each curve represents the average daily weight of individual pups.

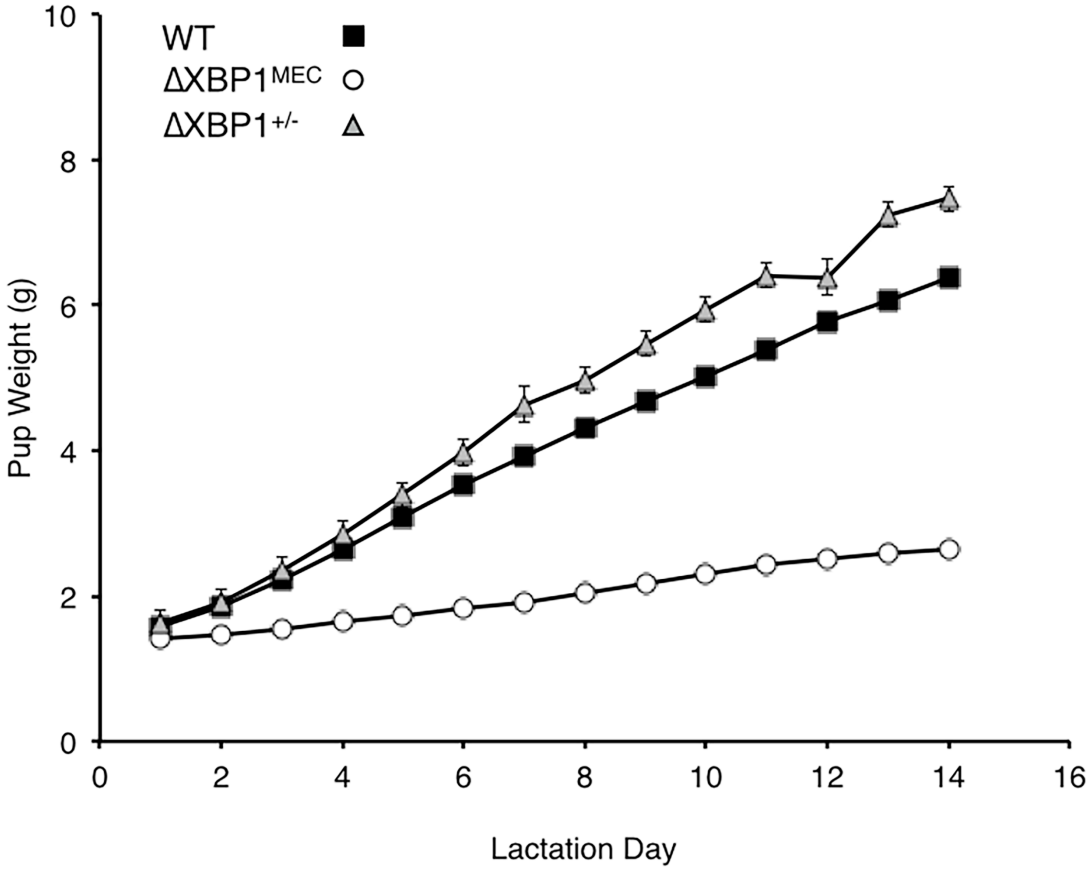
WT
ΔXBP1MEC
ΔXBP1+/-
Pup Weight (g)
Lactation Day
0
2
4
6
8
10
12
14
16